SAND2024-06536C

Sandia National Laboratories

Exceptional service in the national interest

Neutron Source Reconstruction from One-Dimensional Imager of Neutrons at the Z Facility

University of Michigan Seminar

Ozzy Ricketts[1,4]

Collaborators: M. A. Mangan[1], P. Volegov[2], D. N. Fittinghoff[3], M. L. Adams[4], J. E. Morel[4], [1]O. M. Mannion[1], W. E. Lewis[1], A. J. Harvey-Thompson[1], D. J. Ampleford[1]

[1]Sandia National Laboratories, Albuquerque, NM

[2]Los Alamos National Laboratory, Los Alamos, NM

[3]Lawrence Livermore National Laboratory, Livermore, CA

[4]Department of Nuclear Engineering, Texas A&M University, College Station, TX

Sandia National Laboratories is a multimission laboratory managed and operated by National Technology and Engineering Solutions of Sandia LLC, a wholly owned subsidiary of Honeywell International Inc. for the U.S. Department of Energy's National Nuclear Security Administration under contract DE-NA0003525.

U.S. DEPARTMENT OF ENERGY

NNSA

About Myself

- B.S. Physics from Oklahoma State University – 2017
- M.S. Nuclear Engineering from Texas A&M University – 2021
- Ph.D. Nuclear Engineering from Texas A&M University – 2024 (hopefully)

M.S. Research

- Originally wanted to study nuclear security and nonproliferation
- Instead did calibration and validation experiments for Texas A&M's parallel deterministic transport code PDT (now called OpenSn)
- Used a low-scatter HDPE "box" where experiments could be performed in a controlled environment

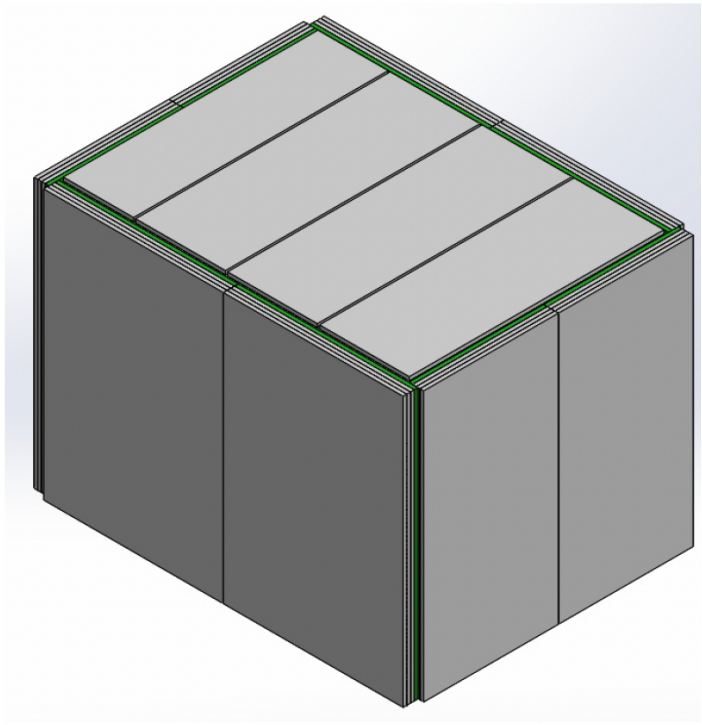

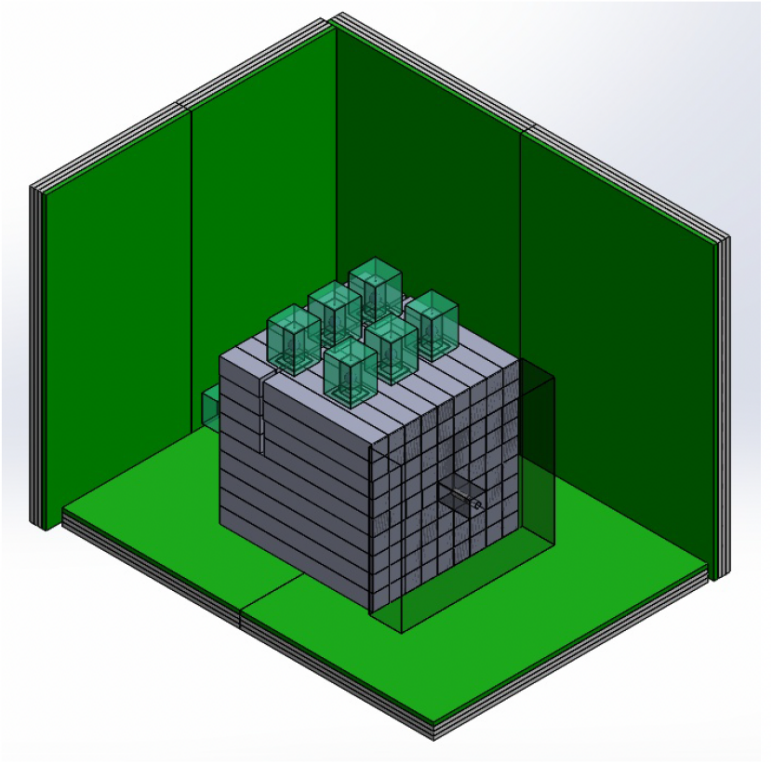

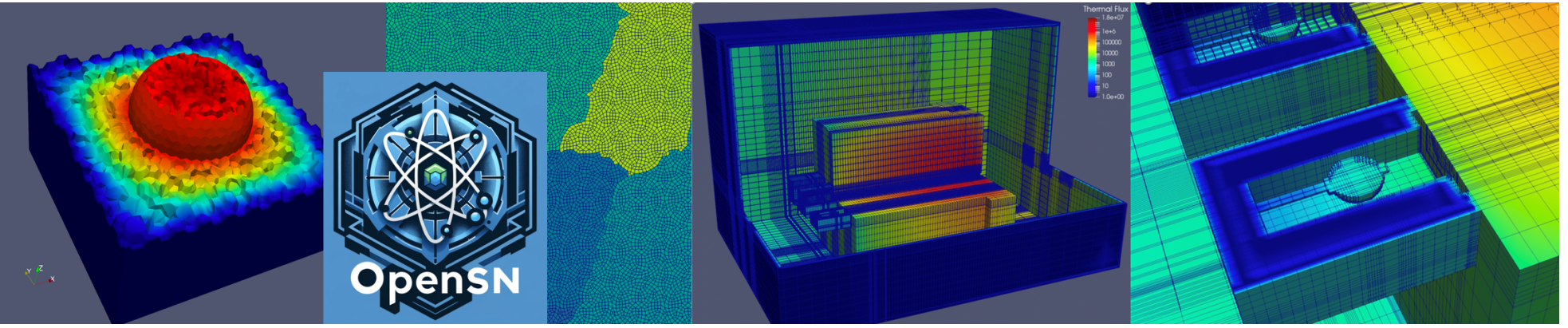

github.com/Open-Sn

M.S. Research

- Performed neutron measurements on graphite configurations with increasing complexity
- Verified results with MCNP simulations
- Conducted a sensitivity study to determine issues with cadmium lining in the detector shroud

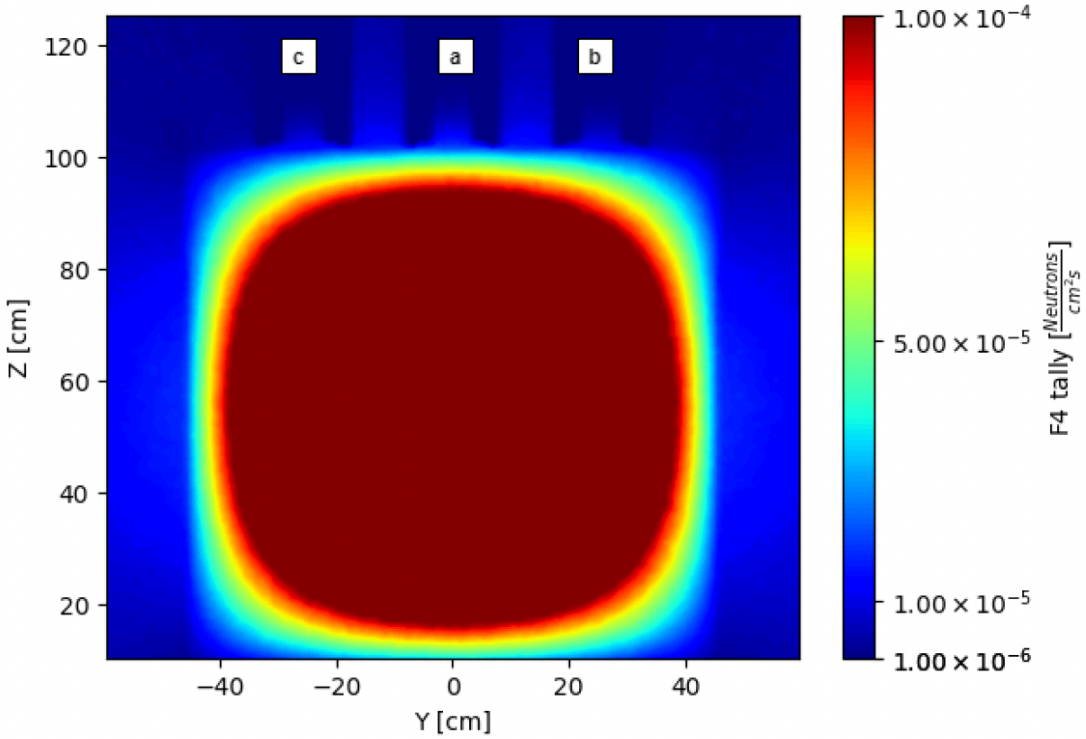

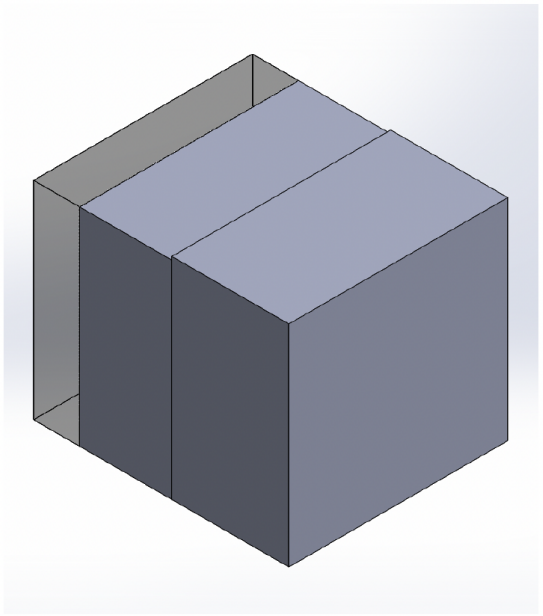

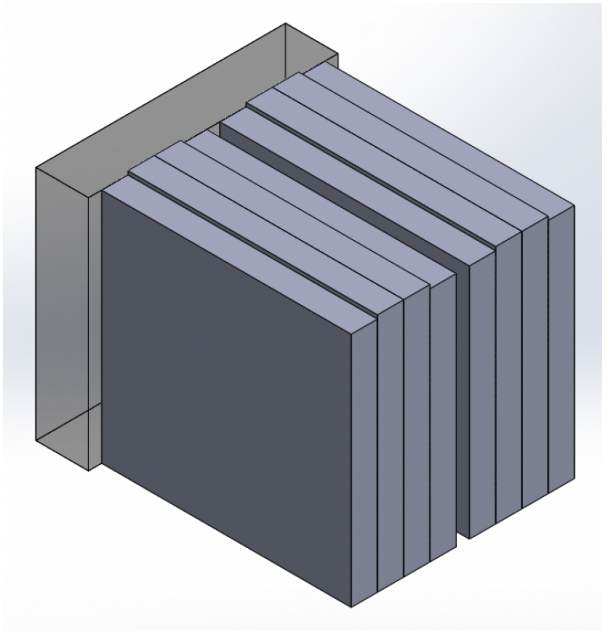

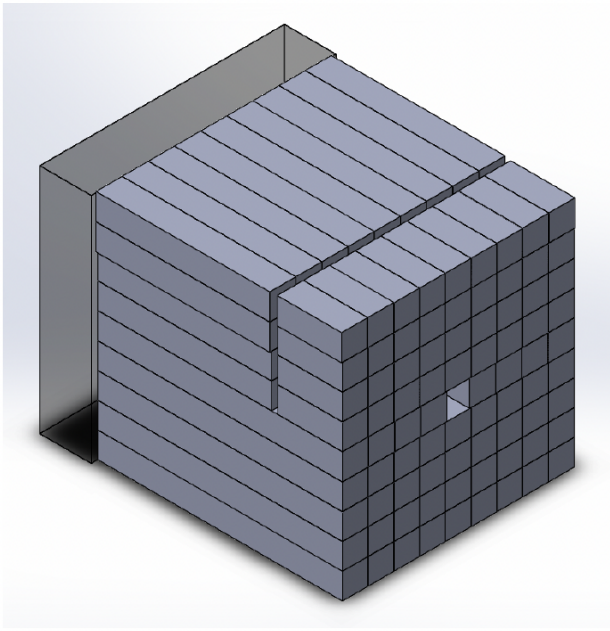

Sandia Internship and COVID-19

- One of the lucky few to intern remotely at Sandia National Laboratories with the Fusion Experiments group
- Developed python tools to accurately align and accumulate one-dimensional imager of neutron (ODIN) data for signal-to-noise (SNR) improvement
- First introduction to fusion research, continued with Sandia for my Ph.D. Research

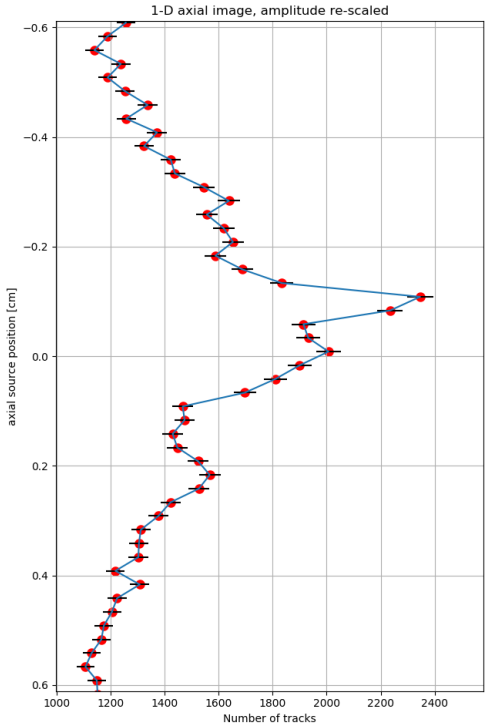

Single Front scan

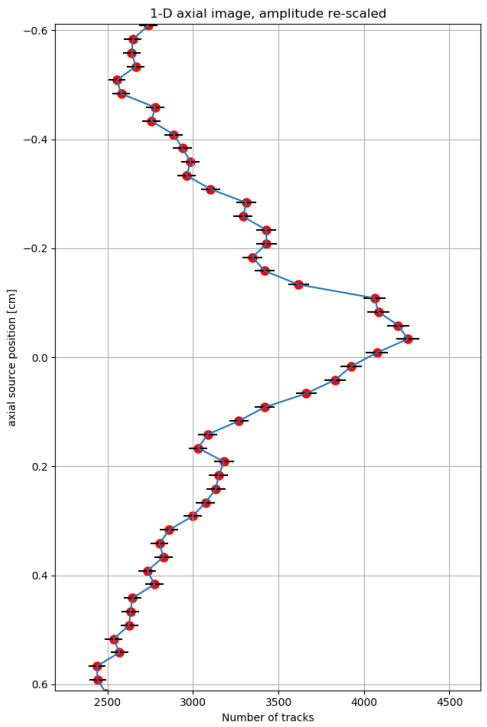

Front and Back scan incorrectly aligned

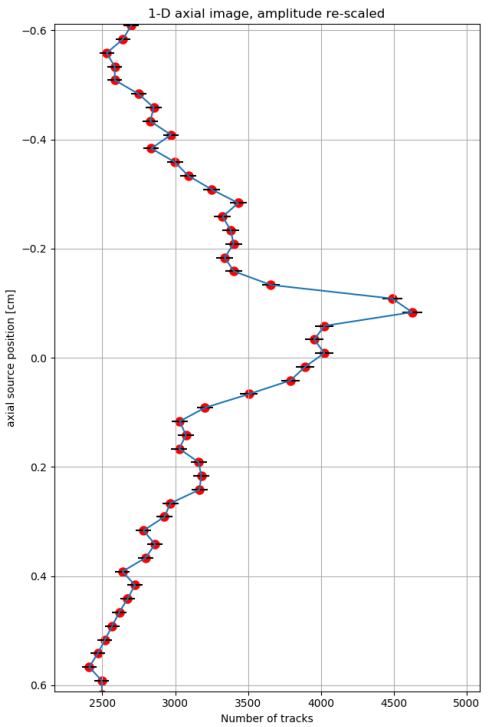

Front and Back scan correctly aligned

S. A. Ricketts, M. A. Mangan; Data processing to improving the signal of one-dimensional neutron images at Sandia's Z Pulsed Power Facility, APS Division of Plasma Physics Meeting 2021 (Poster)

Outline of Ph.D. Research

- Overview of Z machine and Magnetized Liner Inertial Fusion (MagLIF)
- One-Dimensional Imager of Neutrons (ODIN)
- ODIN Forward Model
- Image Reconstruction Methods
- ODIN forward Model and Sensitivity Analysis
- Source Reconstruction from ODIN Data
- Final Thoughts and Conclusions

Overview of Z Machine and MagLIF

Z Machine

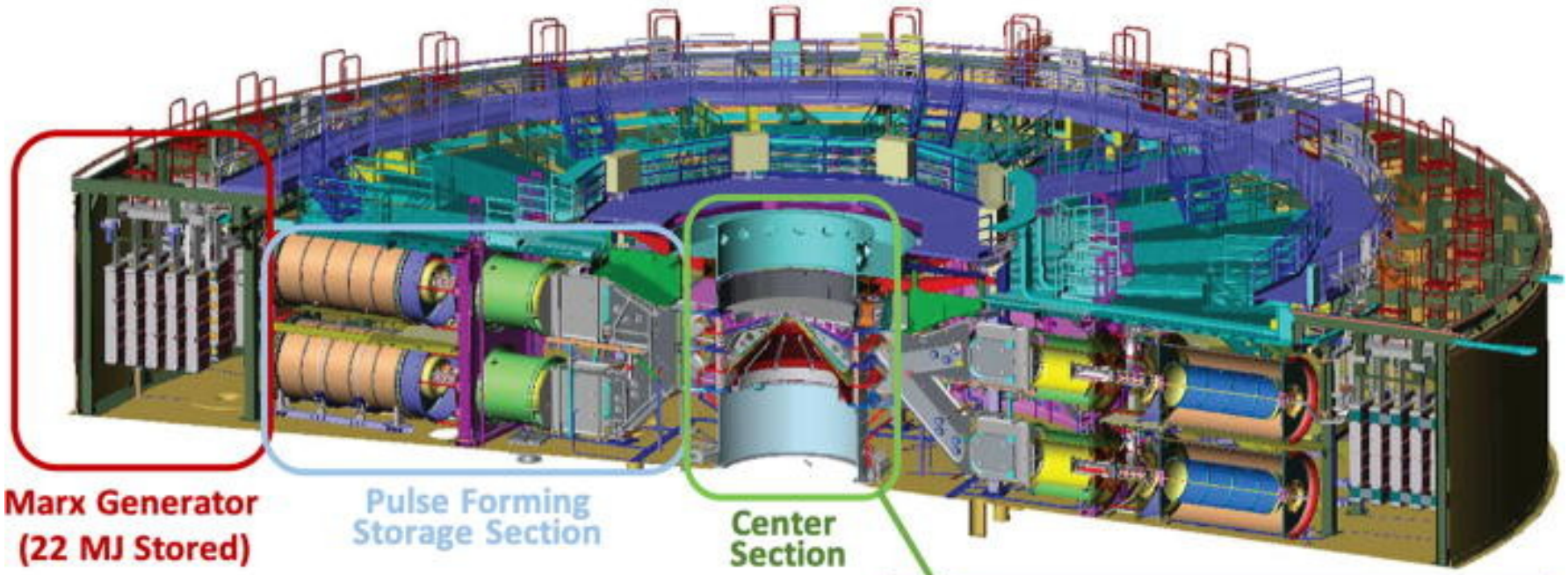

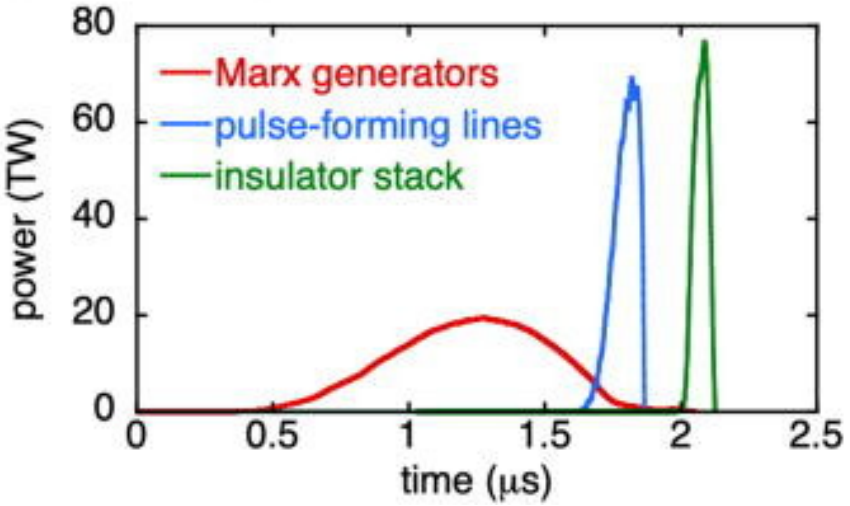

D. B. Sinars et al., "Review of pulsed power-driven high energy density physics research on z at sandia," Physics of Plasmas., vol. 27, no. 7, 2020.

Magnetized Liner Inertial Fusion (MagLIF)

- Magnetization stage applies a magnetic field around the target to reduce radial thermal conduction loss
- Laser Preheat stage raises the fuel temperature to reduce the required compression for fusion conditions
- Compression stage implodes the target from the magnetic field of the electrical pulse

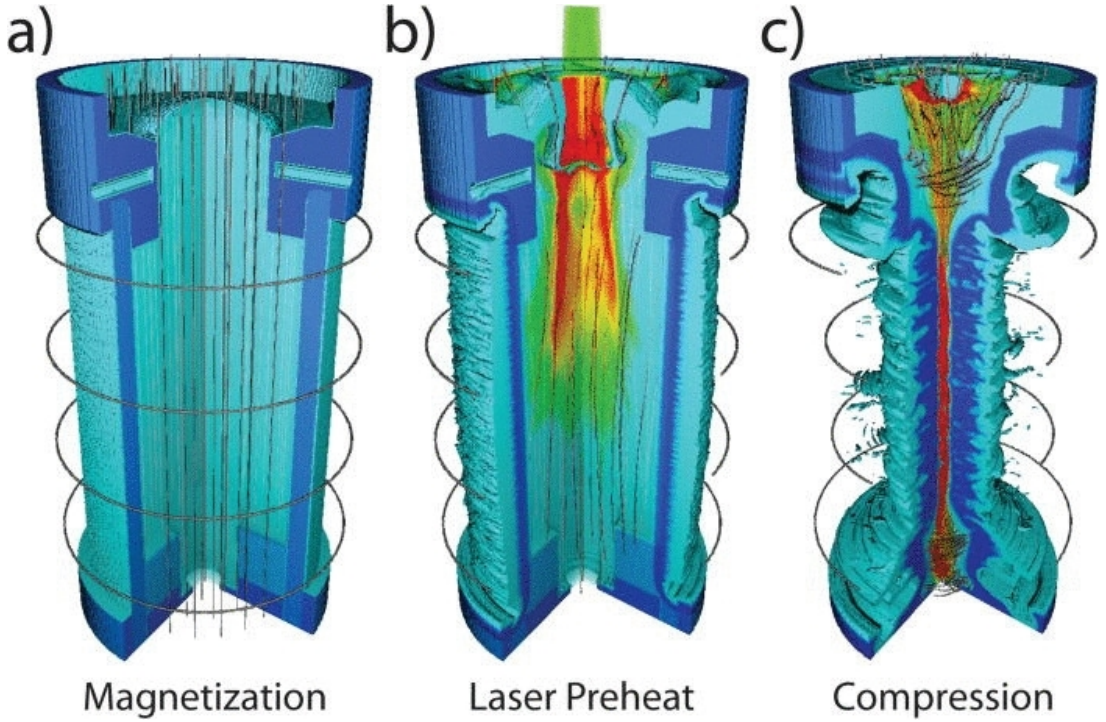

$$D + D \rightarrow {}^{3}He\ (0.8\ MeV) + n(2.45\ MeV)\ 50\%$$
$$\rightarrow p(3.02\ MeV) + T(1.01\ MeV)\ 50\%$$
$$D + T \rightarrow \alpha\ (3.6\ MeV) + n(14.1\ MeV)$$

P. F. Knapp et al., "Effects of magnetization on fusion product trapping and secondary neutron spectra," Physics of Plasmas., vol. 22, no. 5, 2015.

One-Dimensional Imager of Neutrons (ODIN)

One-Dimensional Imager of Neutrons (ODIN)

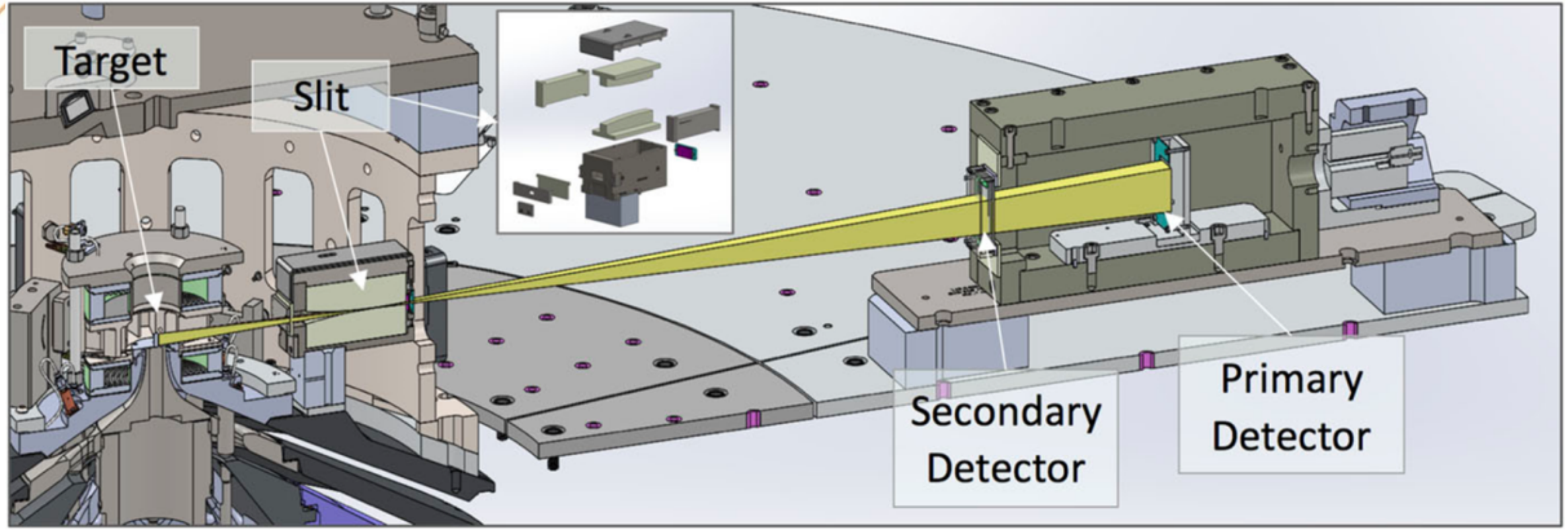

- Images neutrons emitted by MagLIF experiments on the Z facility
- Yields range from ~1X10^{12} to ~1X10^{13} from ~1cm tall target which are recorded as tracks on CR-39 pieces

David J. Ampleford, et al. "One dimensional imager of neutrons on the Z machine", Review of Scientific Instruments 89, 10I132 (2018)

Aperture

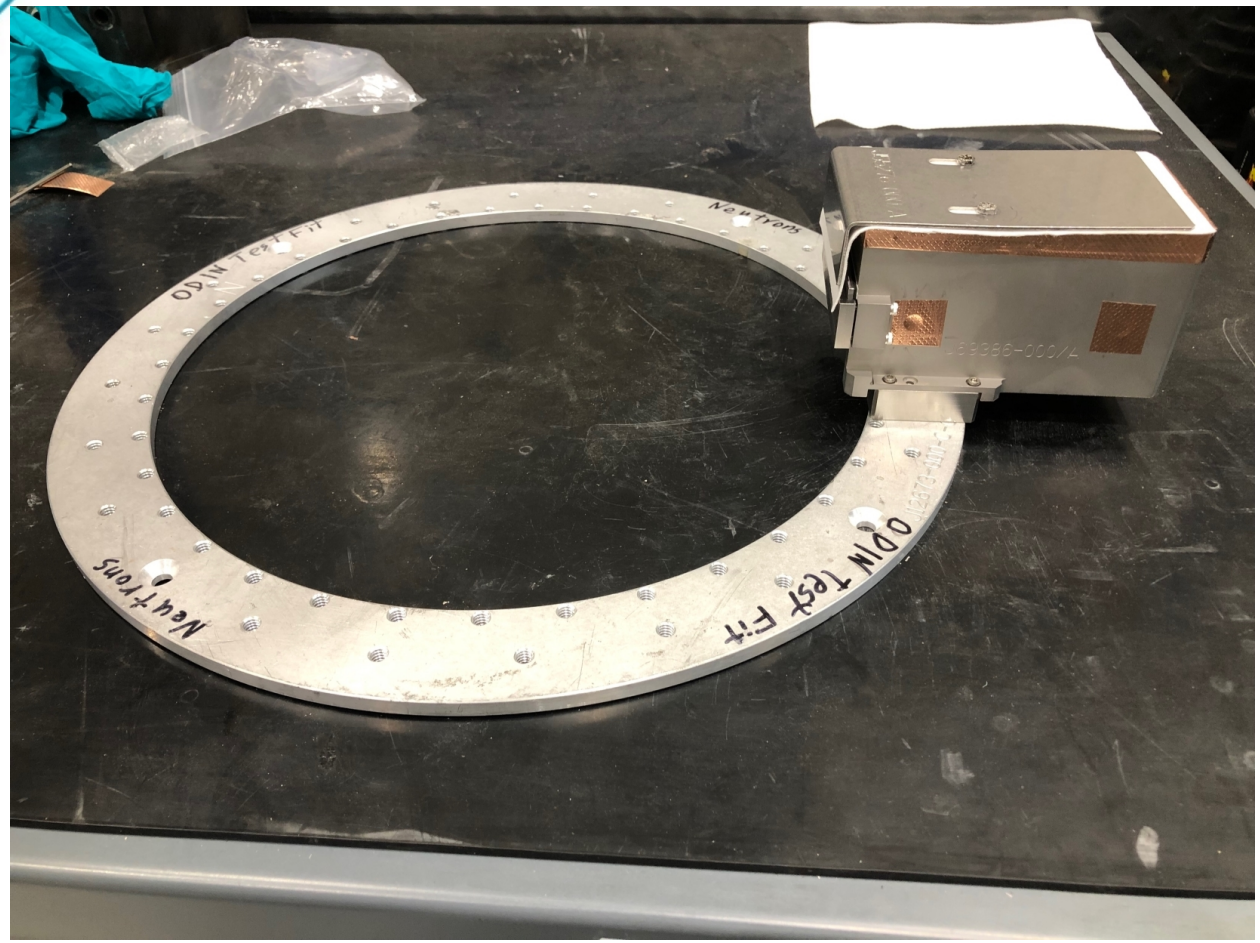

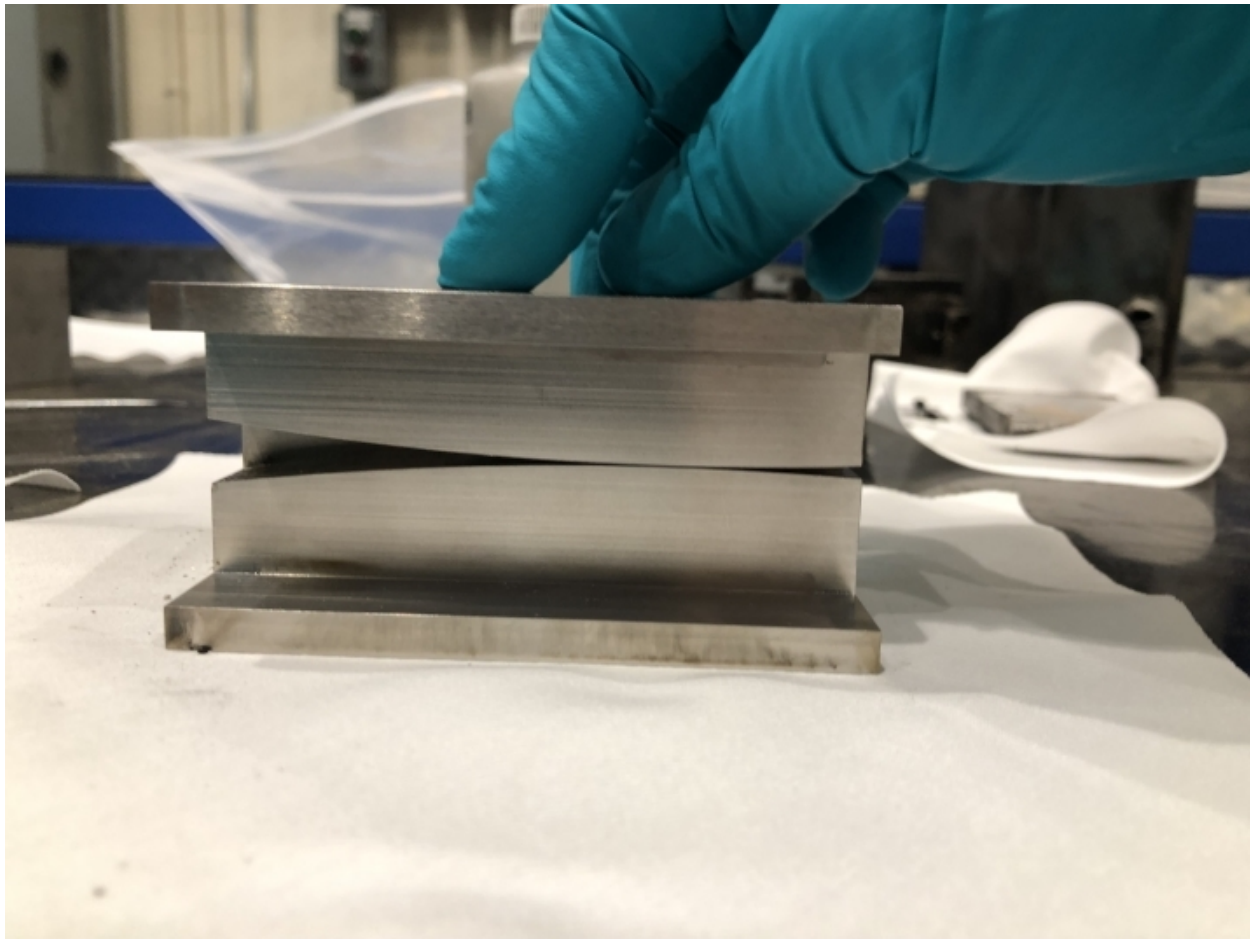

- The aperture is 10 cm long, with a nominal spacing of 250 μm

CR-39 Nuclear Track Detector

- DD Neutrons elastically scatter and produce recoil protons which leave destructive tracks
- High density polyethylene is placed in front of the CR-39 to increase the detection efficiency
- Microscope scans provide information on track location, diameter, contrast, and eccentricity

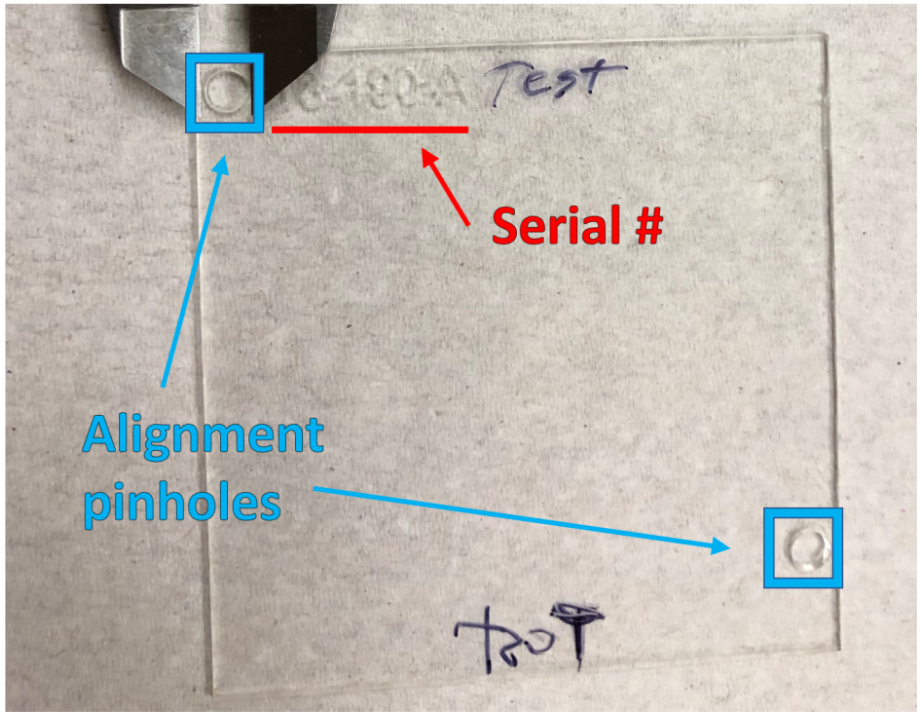

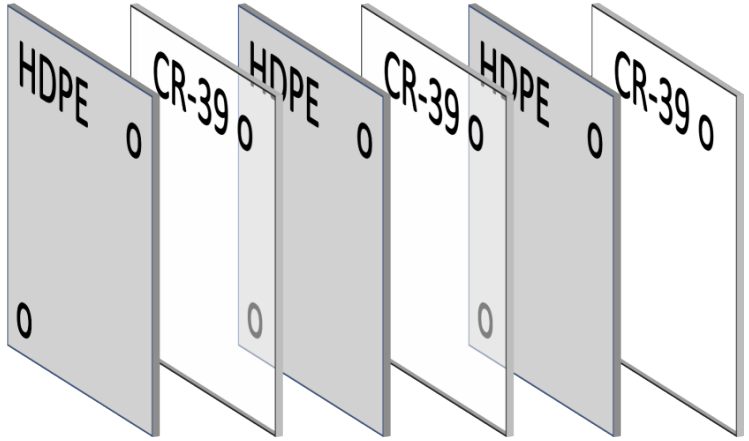

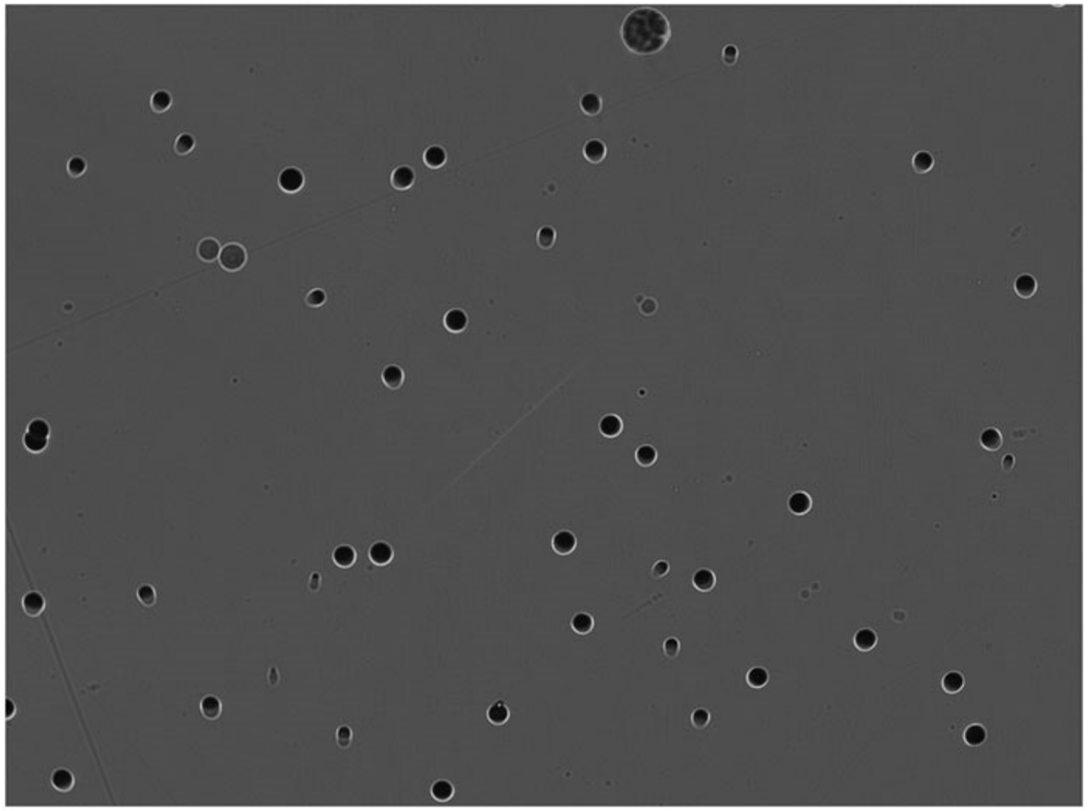

B. Lahmann et al. “CR-39 nuclear track detector response to inertial confinement fusion relevant ions,” Rev Sci Instrum 1 May 2020; 91 (5): 053502. https://doi.org/10.1063/5.0004129

Track Discrimination

- Track information is used to discriminate incident neutrons
- Diameter indicates the energy and type of charged particle
- Eccentricity (how circular the track is) indicates the angle of interaction
- Contrast indicates the depth of the track

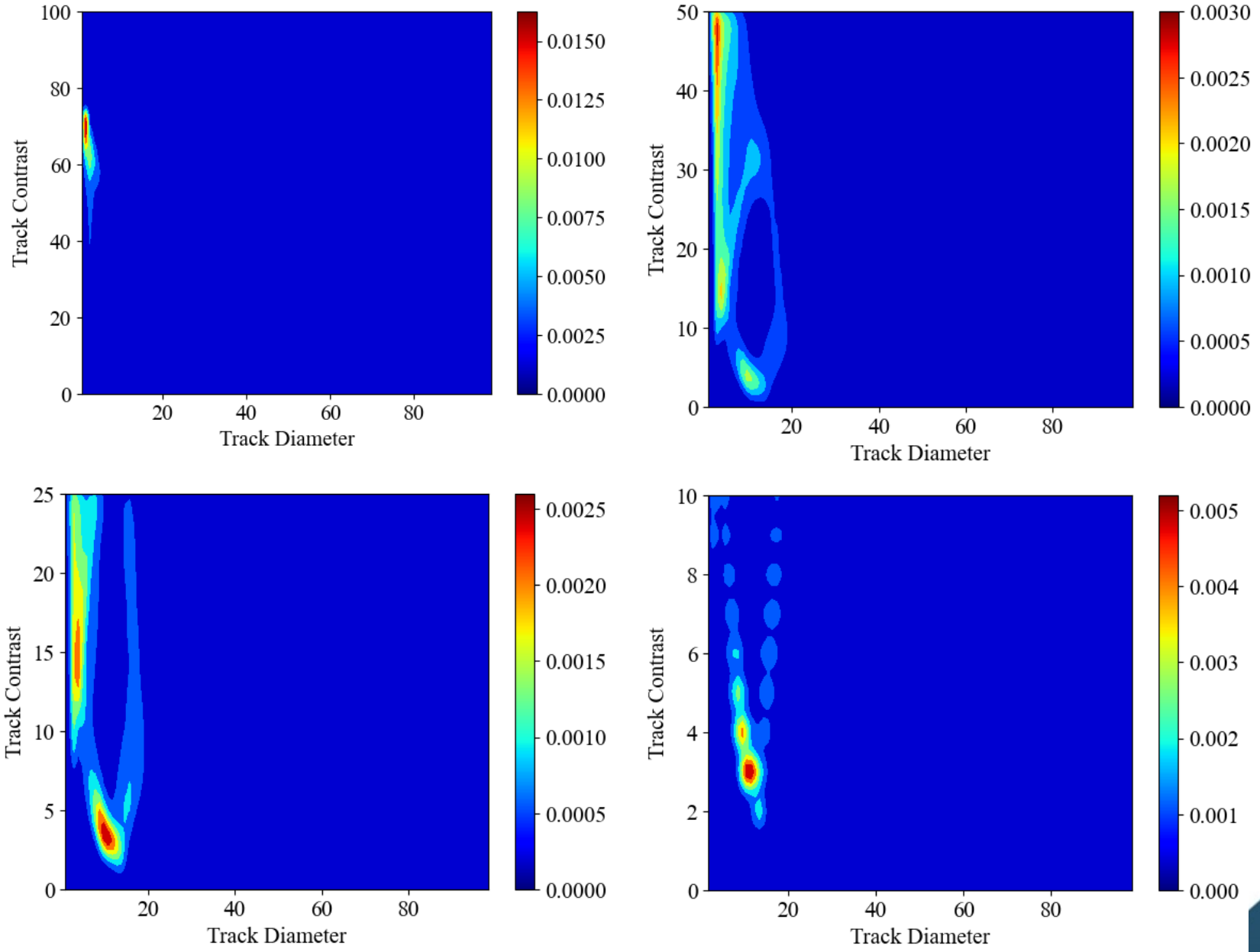

1D Data Generation

- Non-incident neutrons are filtered out, data rebinned to ODIN's resolution
- Data is integrated along the resolving axis to produce an axial detector measurement
- A subset of the data is used to remove the pinholes and tag number

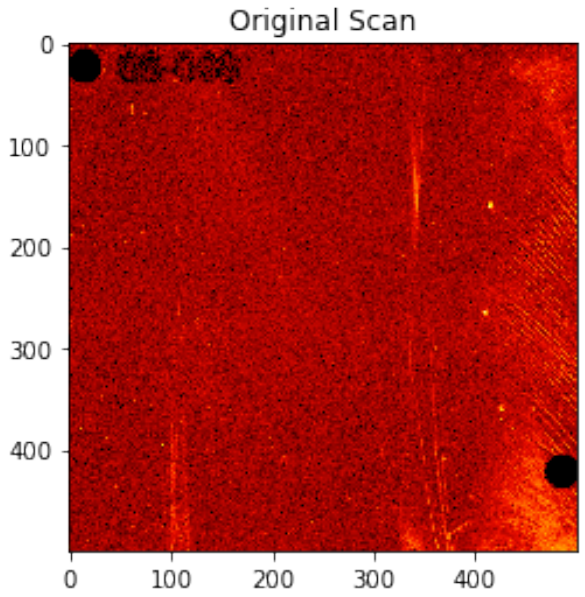

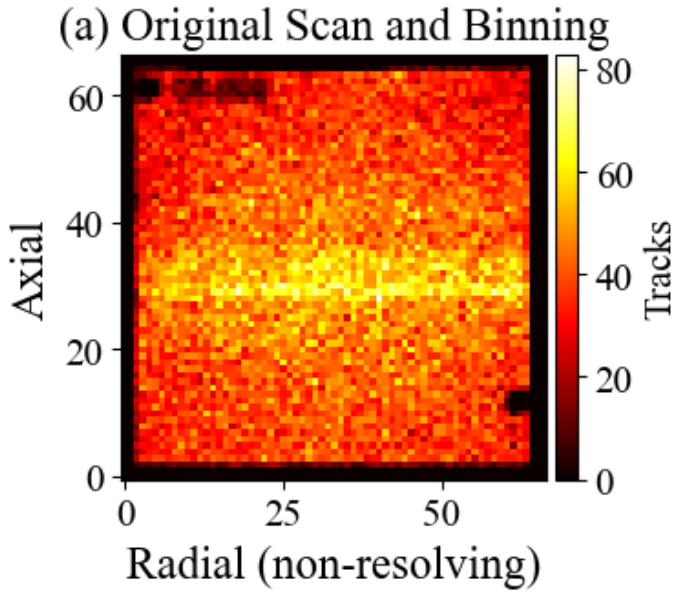

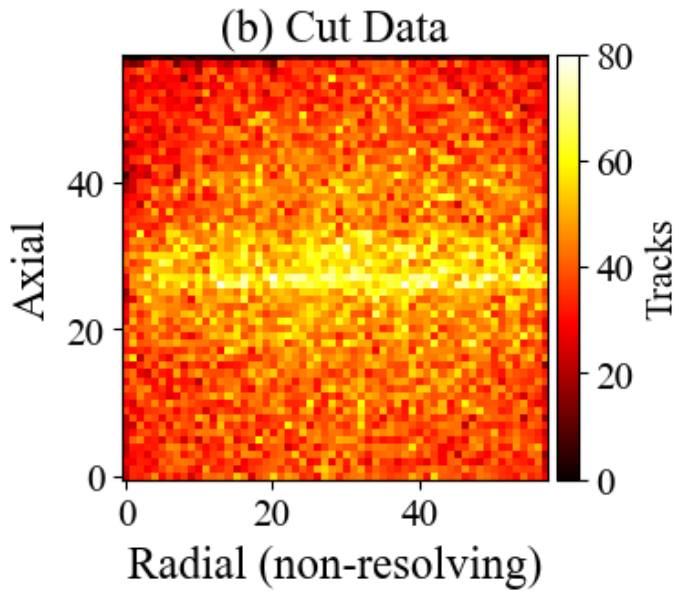

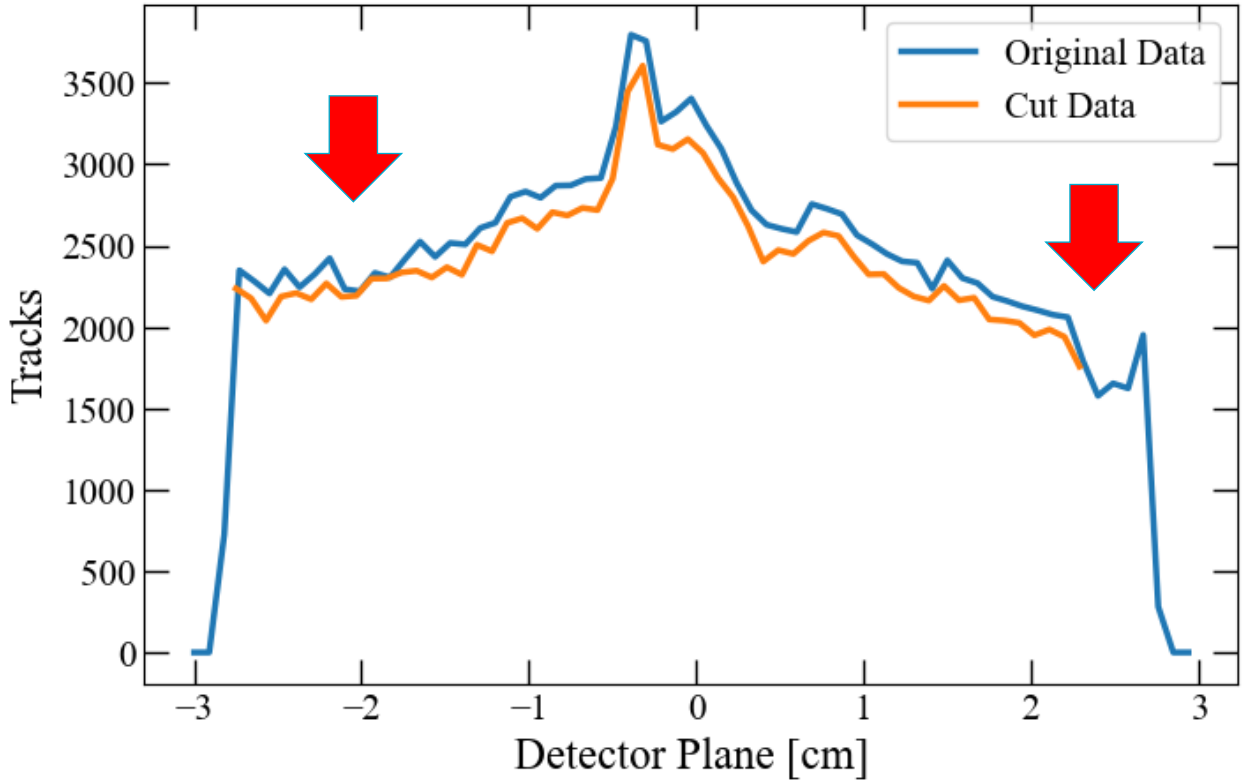

ODIN Previous Analysis

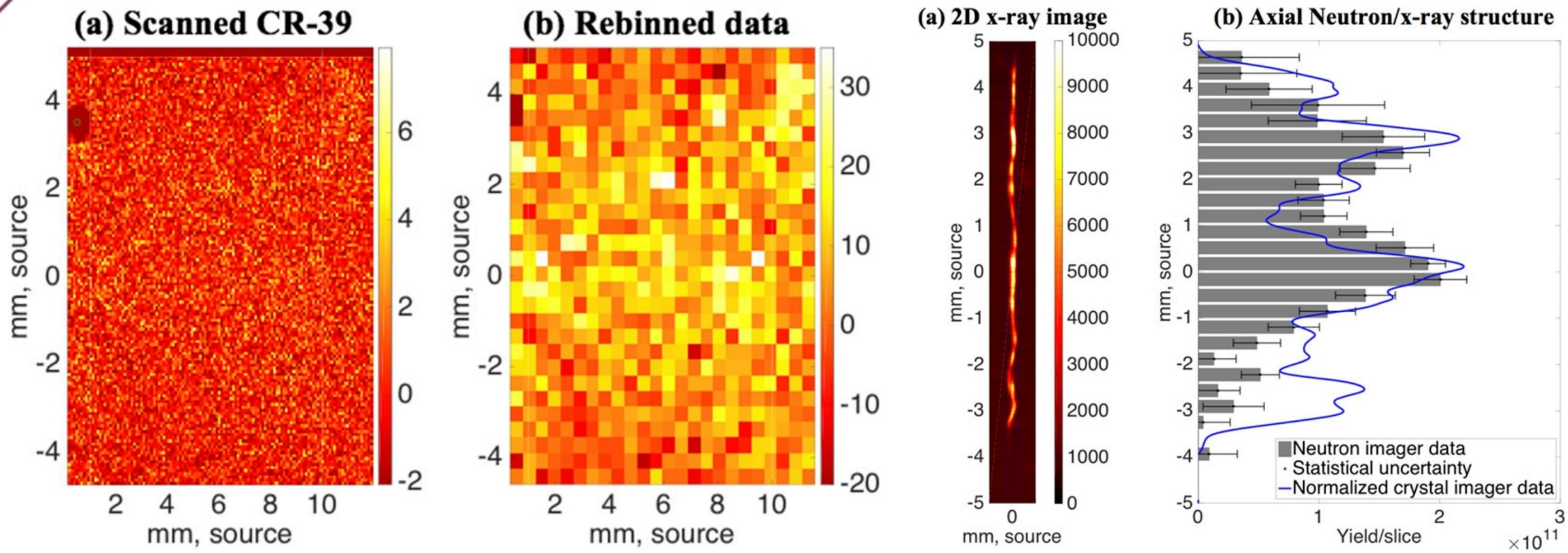

- No further reconstruction has been attempted

- **Objective: Use image reconstruction methods to improve imaging of the spatial distribution of neutron emissions from the stagnation column**

David J. Ampleford, et al. "One dimensional imager of neutrons on the Z machine", Review of Scientific Instruments 89, 10I132 (2018)

Image Reconstruction - Fredholm Integral Equation of the First Kind

$$\int_a^b P(x,y)G_0(y)dy = N_0(x), c \leq x \leq d$$

Kernel/ Instrument Response Function

Neutron Source

Neutron Image Data

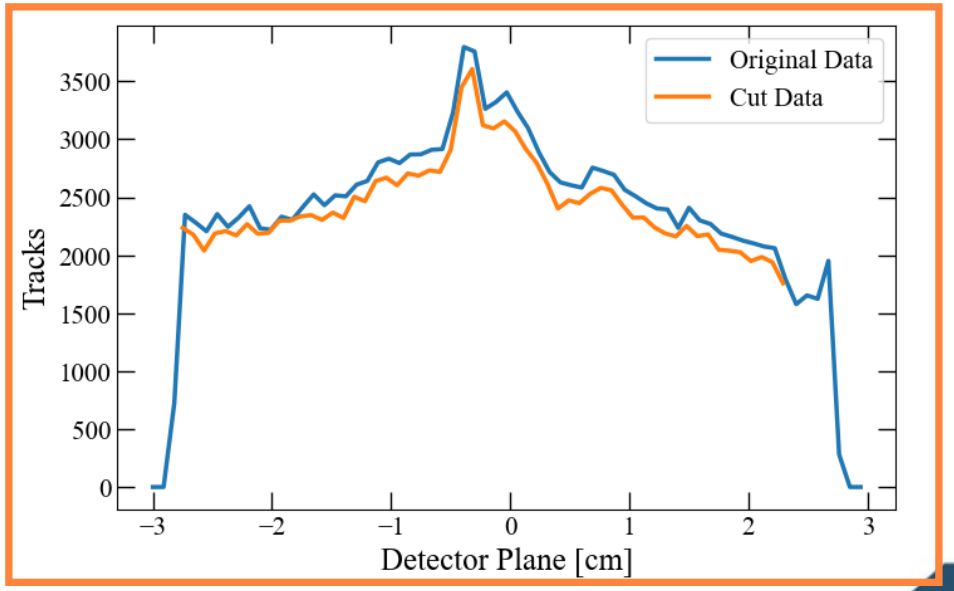

ODIN Forward Model

Analytical Forward Model

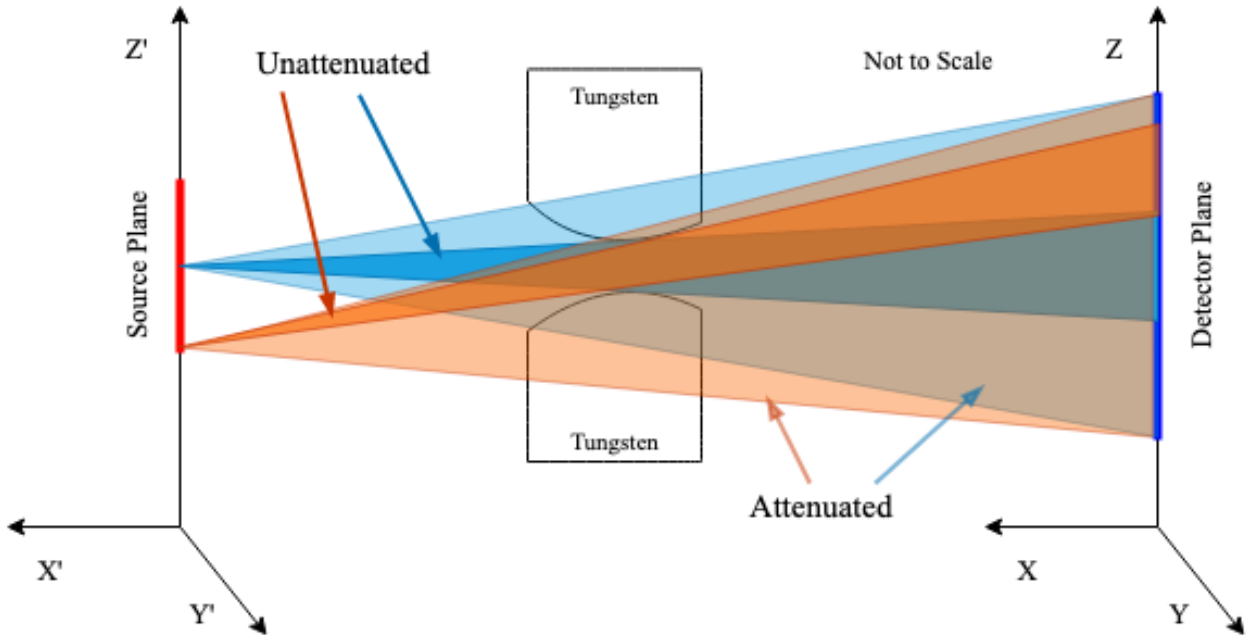

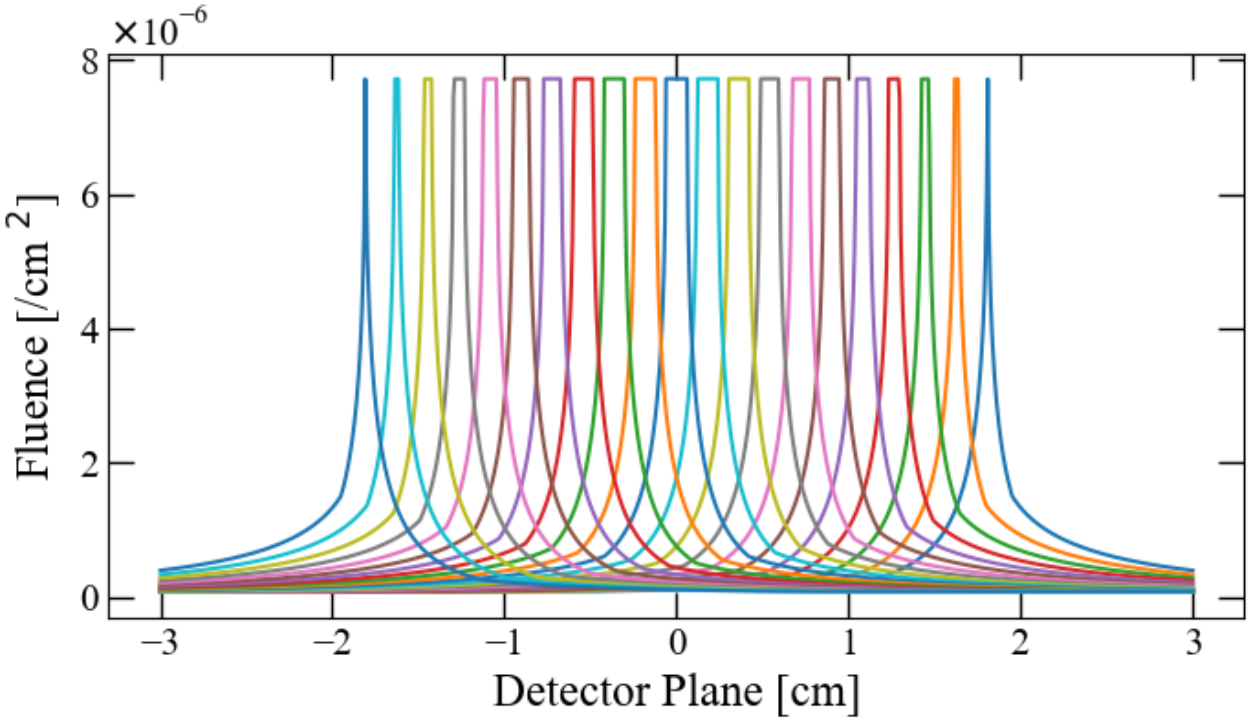

- Rays from source points are generated towards interaction points along the detector plane
- Neutrons can attenuate through the tungsten or pass freely through the aperture
- The flat tops of each function is proportional to the direct line of sight opening through the aperture

Analytical Forward Model Validation

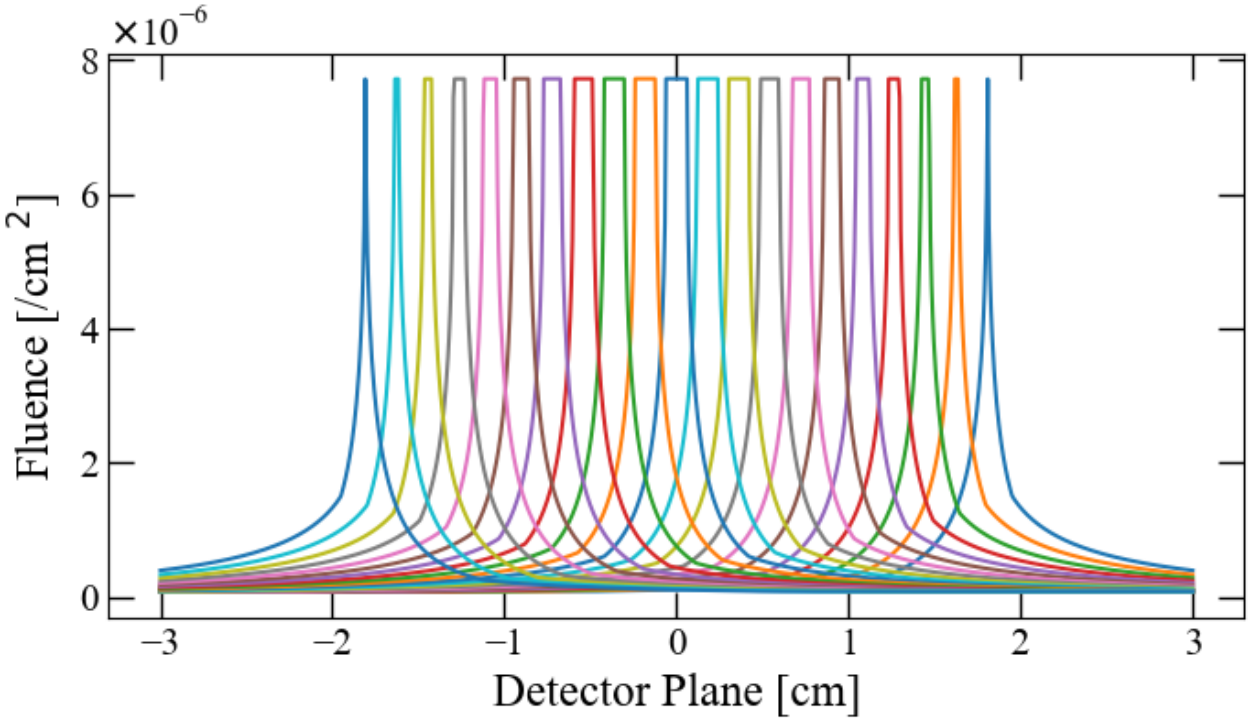

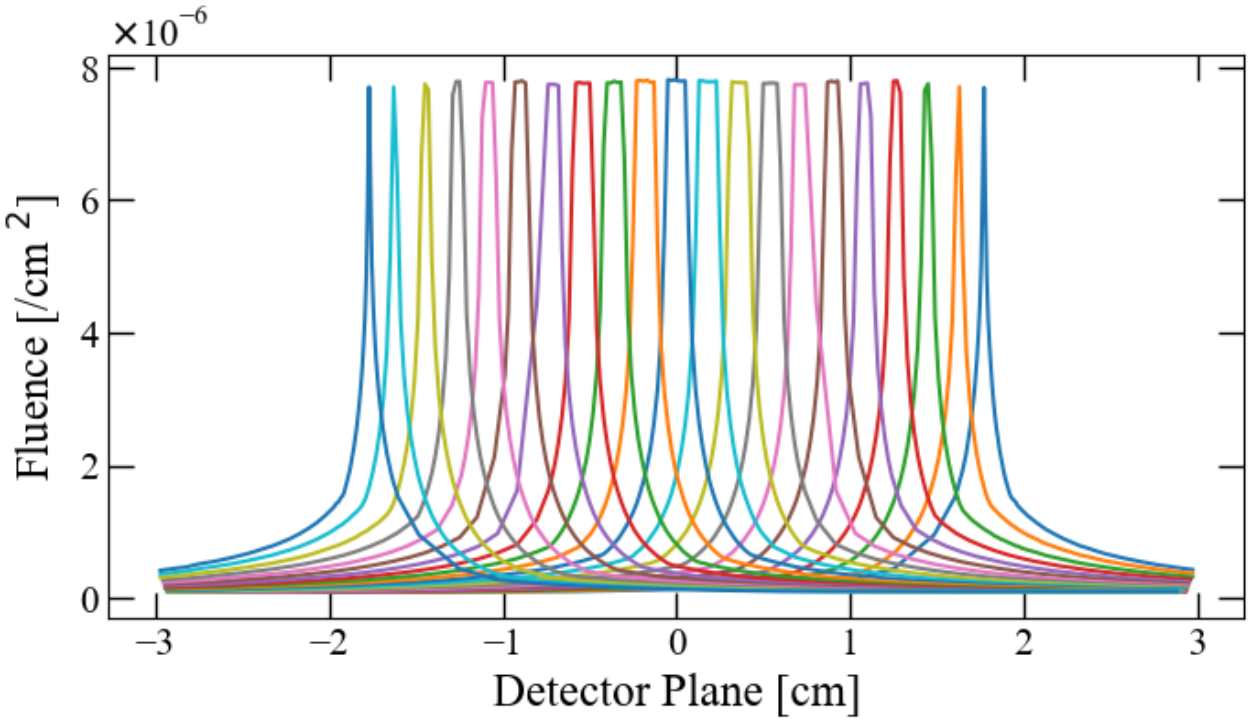

- Fluence amplitude is in agreement with Monte Carlo N-Particle Transport Code (MCNP) simulations (J. D. Vaughan et al.)
- For a uniform source, ~635 tracks/cm^2 (D. J. Ampleford et al. ~650 tracks/cm^2)

IRF Matrix Generation

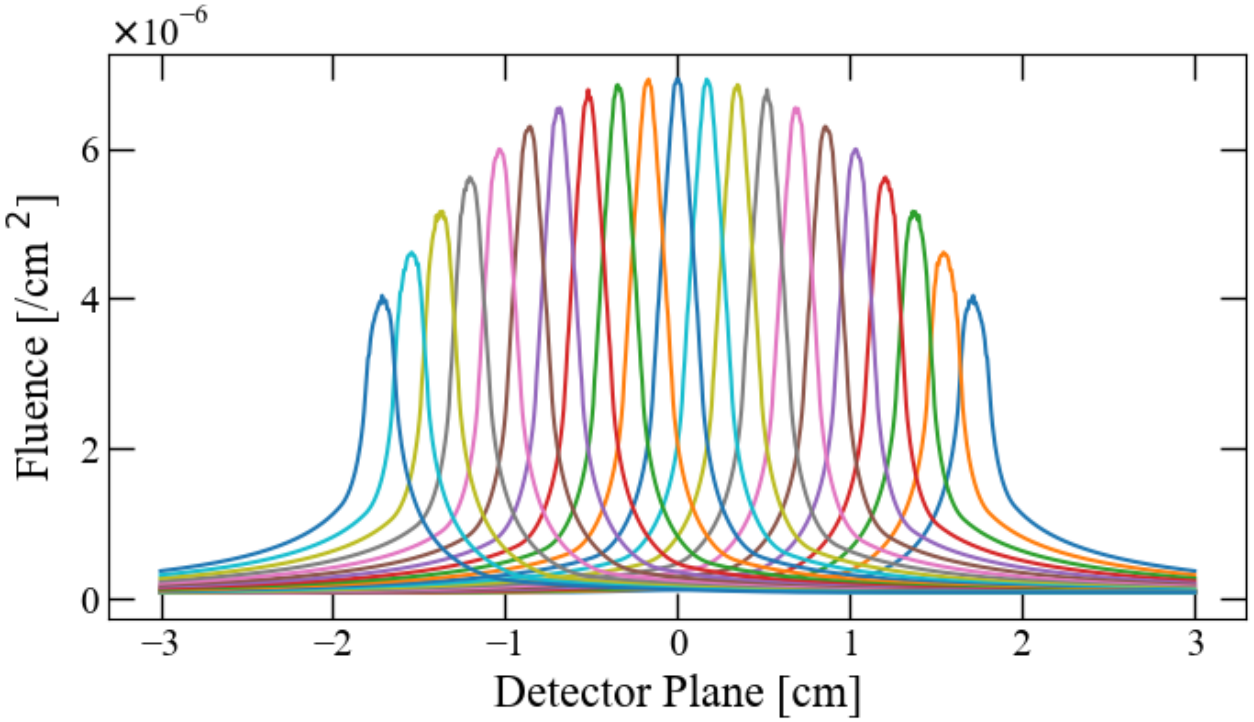

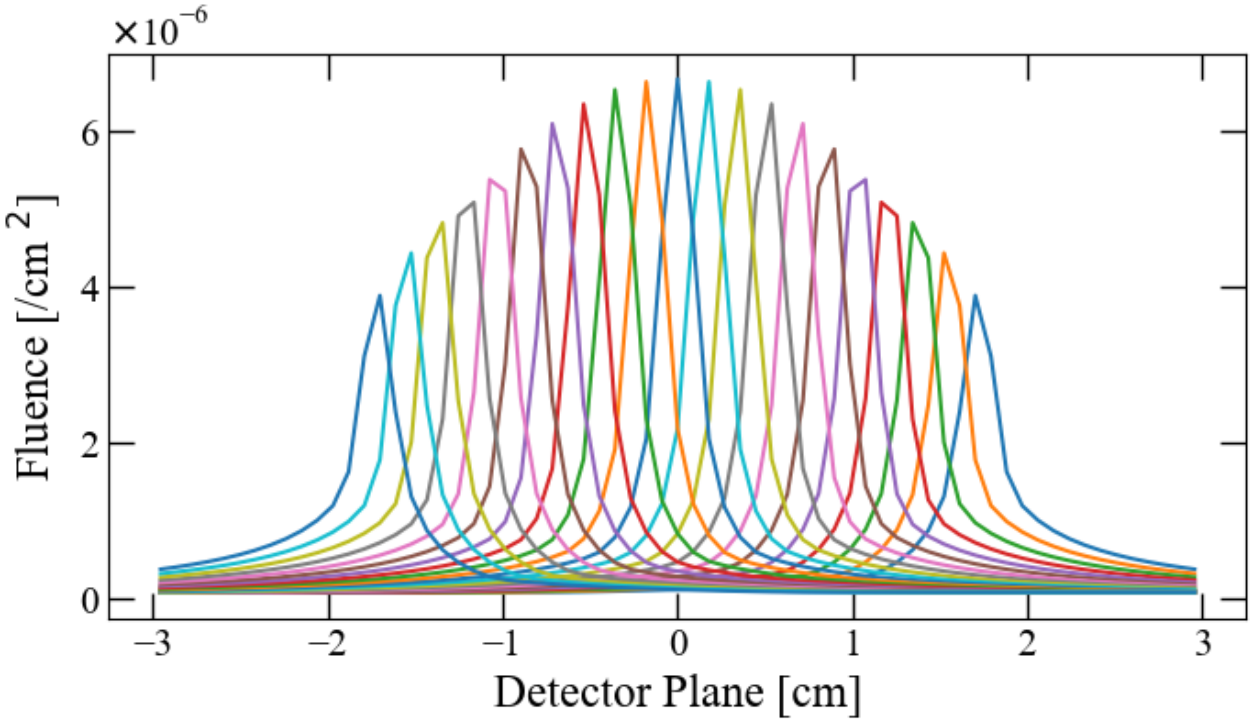

- To better approximate a line source, IRFs used in reconstructions are averaged over multiple points sources in each bin

Synthetic Data Generation

- **A**) Define a synthetic source profile
- **B**) Pass source profile through ODIN Forward Model
- **C**) Poisson sample Nominal Detector Response to generate 2D data set
- **D**) Integrate across non-resolving axis to generate 1D axial profile

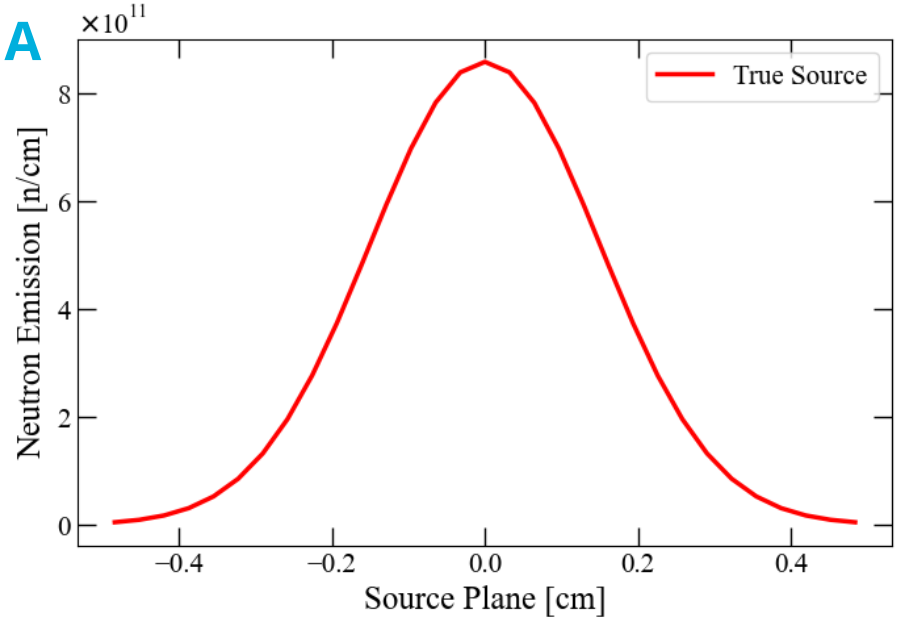

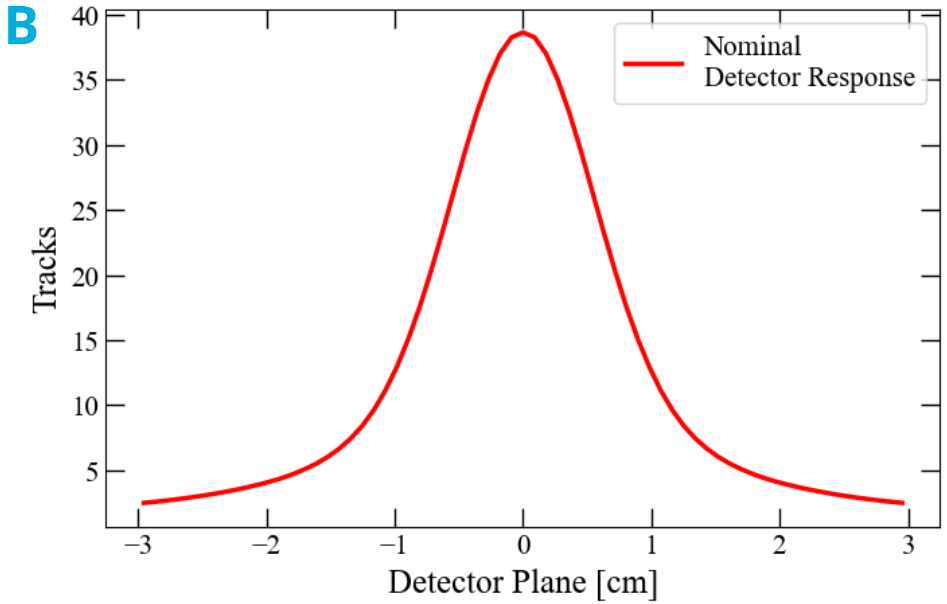

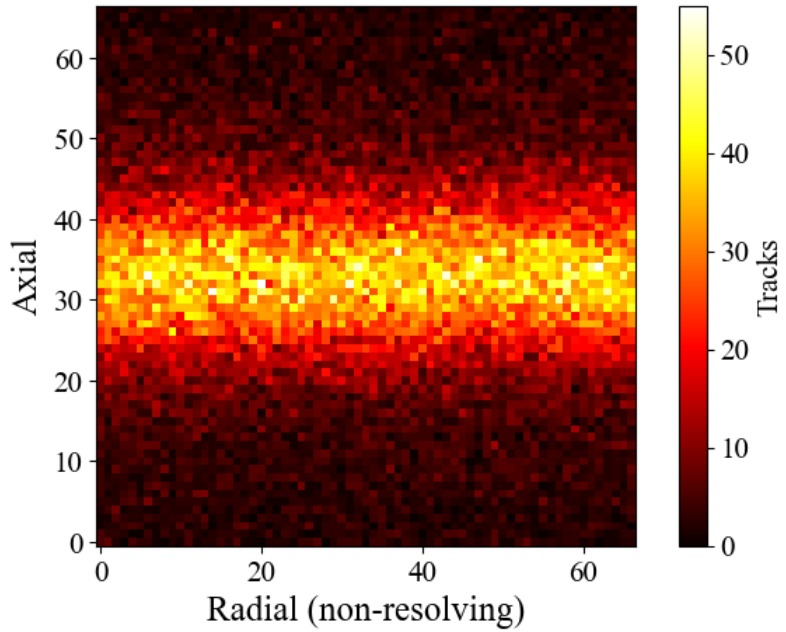

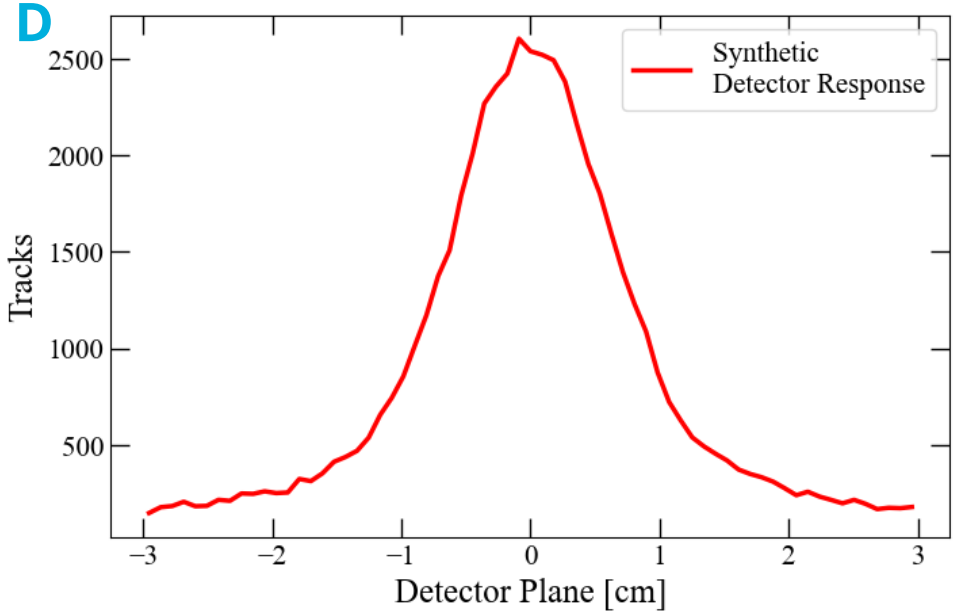

Image Reconstruction Methods

Fredholm Integral Equation of the First Kind

$$\int_a^b P(x,y)G_0(y)dy = N_0(x), c \leq x \leq d$$

Kernel/ Instrument Response Function

Neutron Source

Neutron Image Data

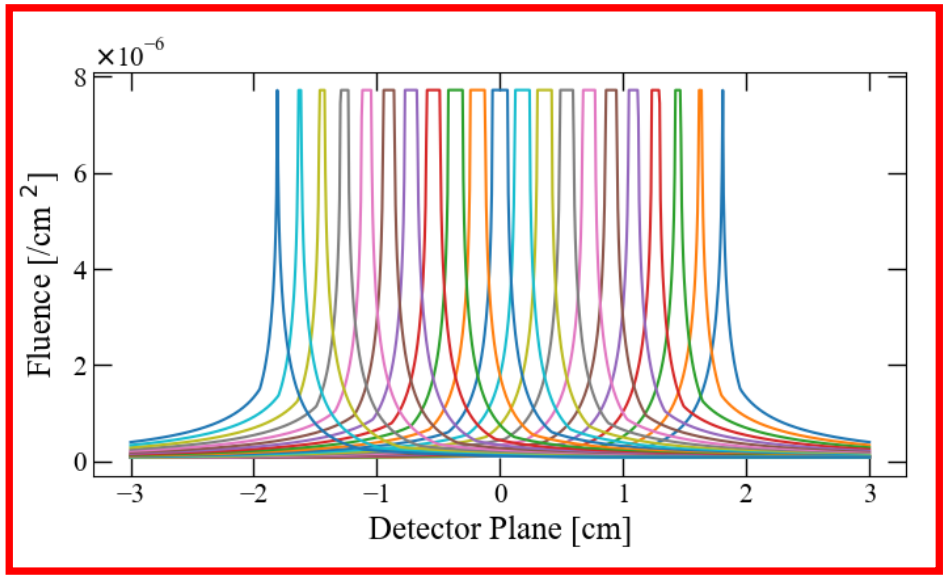

?

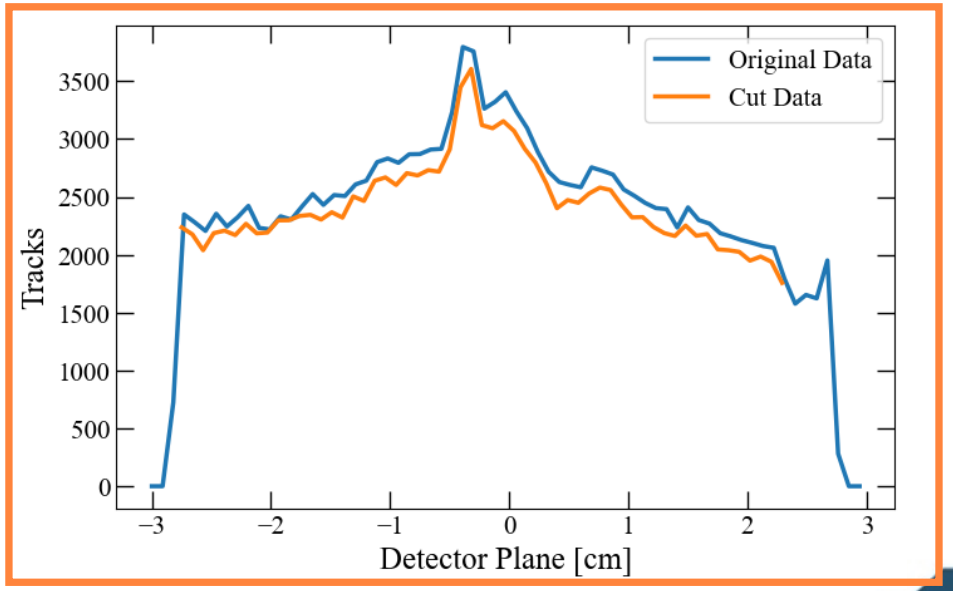

Image Reconstruction Methods

- Least Squares Fit
  - Selects a solution which minimizes the square of the residual

$$LSF : \min_G \sum_{i=1}^{n} R_i(G)^2 = \min_G \sum_{i=1}^{n} (Y_i - \sum_{j=1}^{m} P_{ij} G_j)^2$$

- Non-Negative Least Squares Fit
  - Implements non-negativity constraint for Least Squares Fit

$$NNLSF : \min_G \|Y - PG\|_2^2,$$

- Maximum Likelihood Estimation
  - Iterative algorithm which converges to a solution that maximizes a likelihood function
  - Can factor in the type of noise (Gaussian or Poissonian)
  - Poissonian has non-negativity constraint

$$g_{MLE} = arg \max_g \log L(g) = arg \max_g \log p(y|g),$$

- Generalized Expectation Maximization
  - Iterative algorithm with a regularization parameter 1/β which implements a smoothing to the solution
  - Low β smooths the solution
  - Large β has no smoothing and approaches Maximum Likelihood Poissonian

$$g_{GEM} = arg \max_g \log p(y|g) - \frac{1}{\beta} \sum_{c \in C} V_c(g),$$

Chosen Synthetic Sources

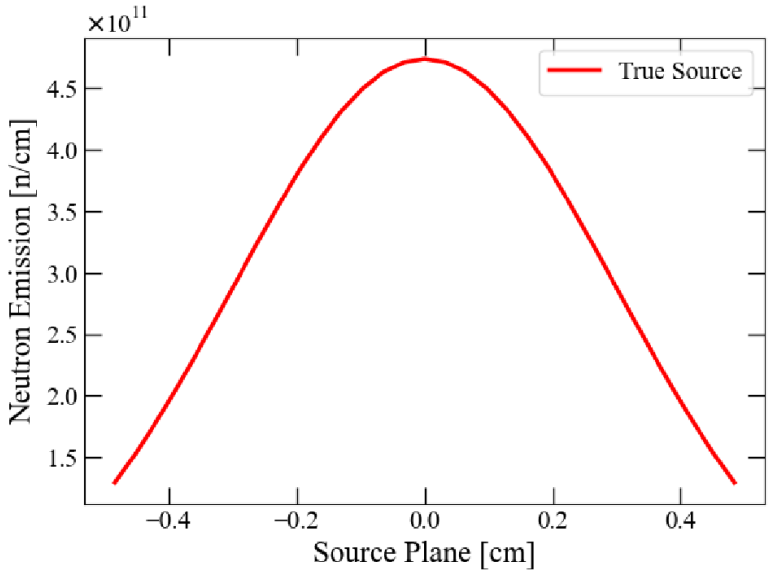

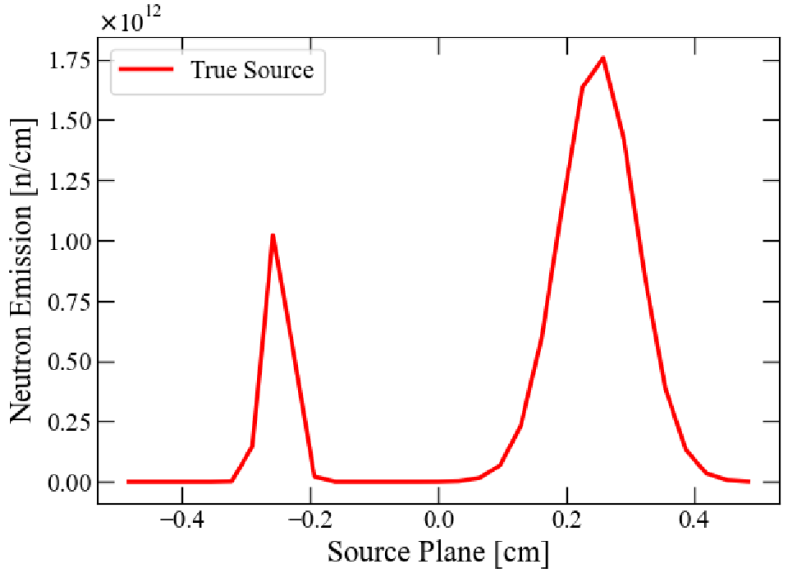

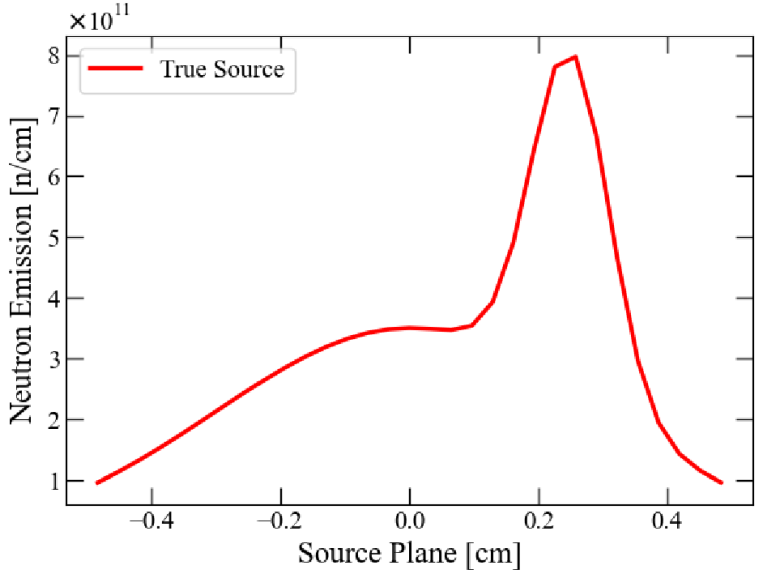

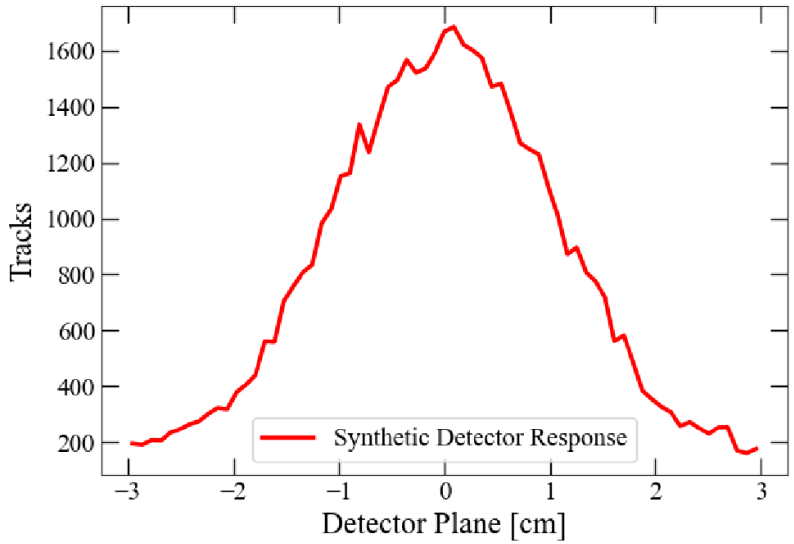

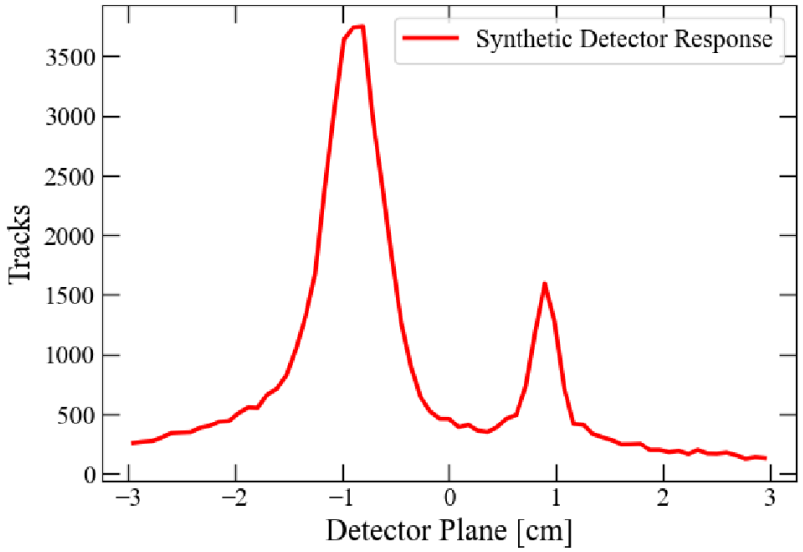

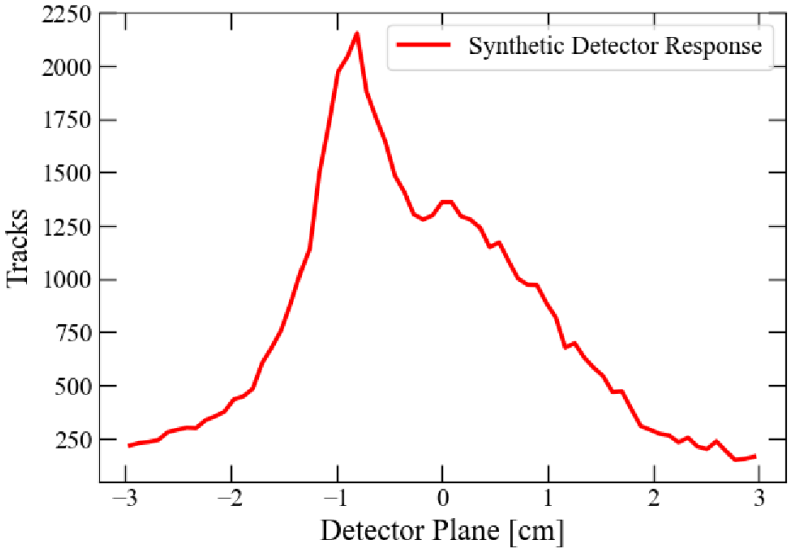

Low Frequency (LF) **High Frequency (HF)** **Mixed Frequency (MF)**

LSF and NNLSF Synthetic Source Reconstructions

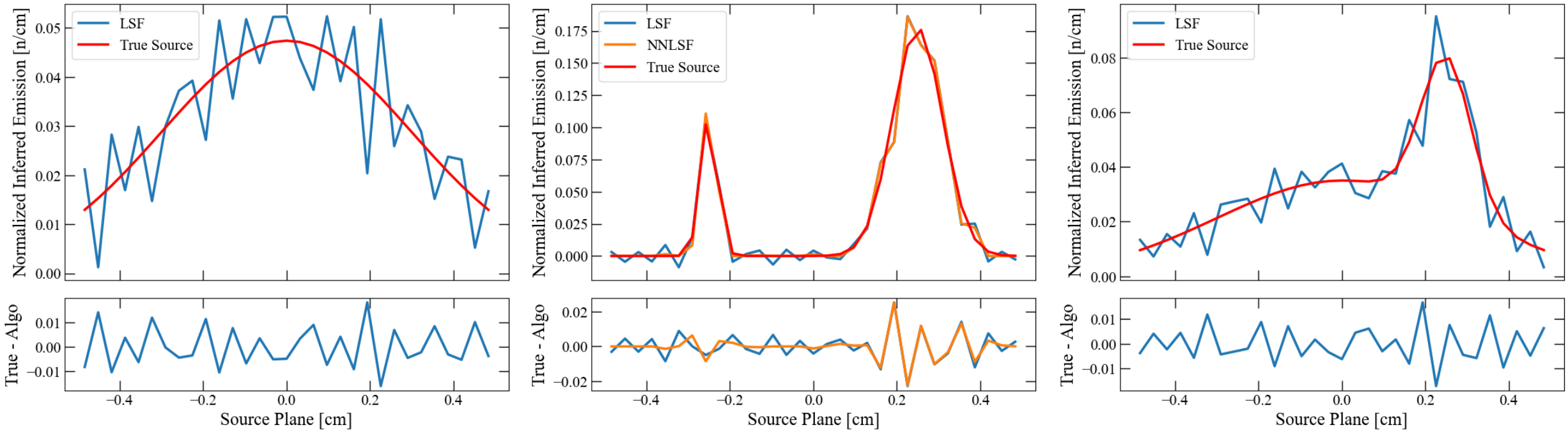

- LF and MF reconstructions have no difference in solutions
- HF reconstruction has negative source contributions in LSF
- Over-fitting smooth solutions due to noise

MLE_Gauss and MLE_Poiss Synthetic Source Reconstructions

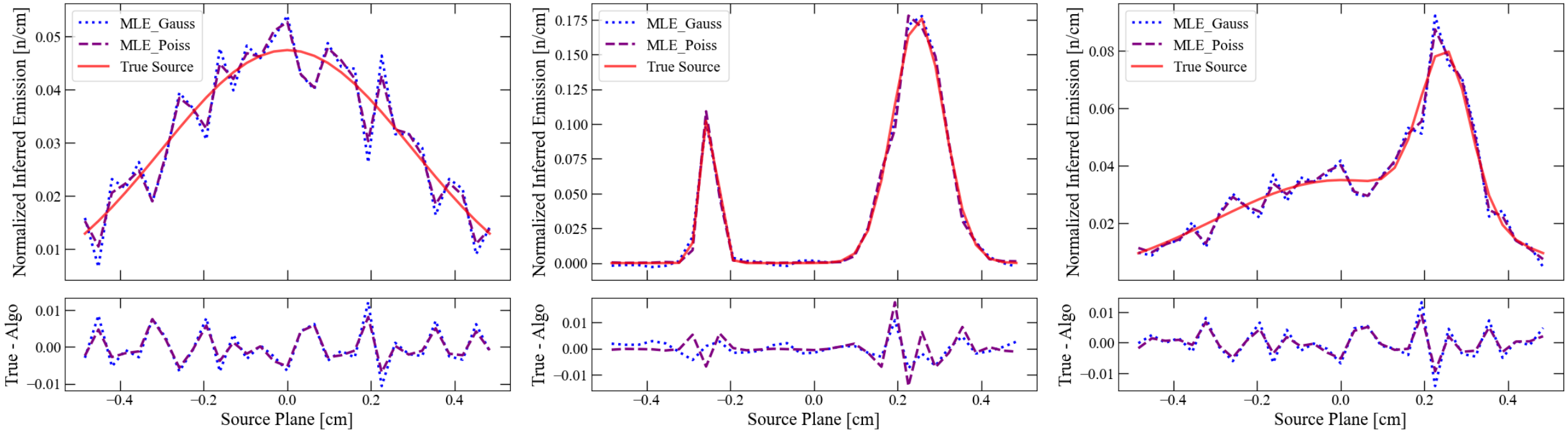

- HF reconstruction has negative source contributions in MLE_Gauss
- MLE_Poiss performs slightly better in smooth areas

GEM Regularization - Effect of β

$$g_{GEM} = arg\max_{g} \log p(y|g) - \frac{1}{\beta}\sum_{c\in C} V_c(g),$$

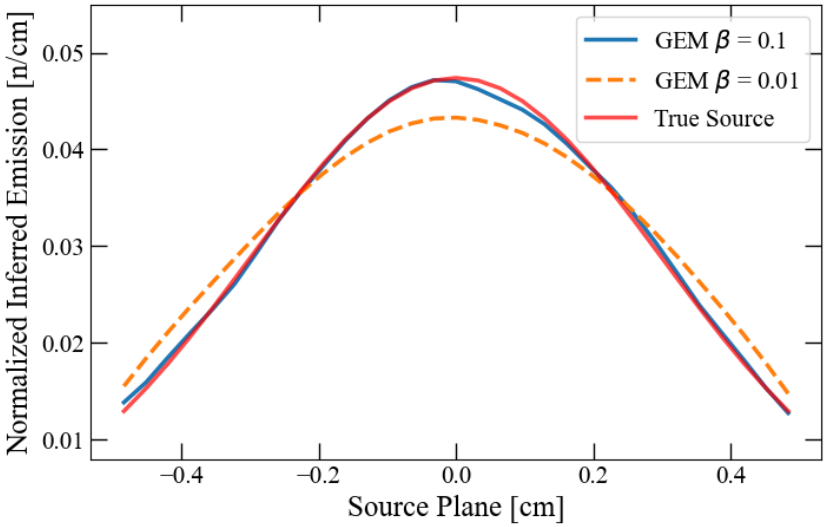

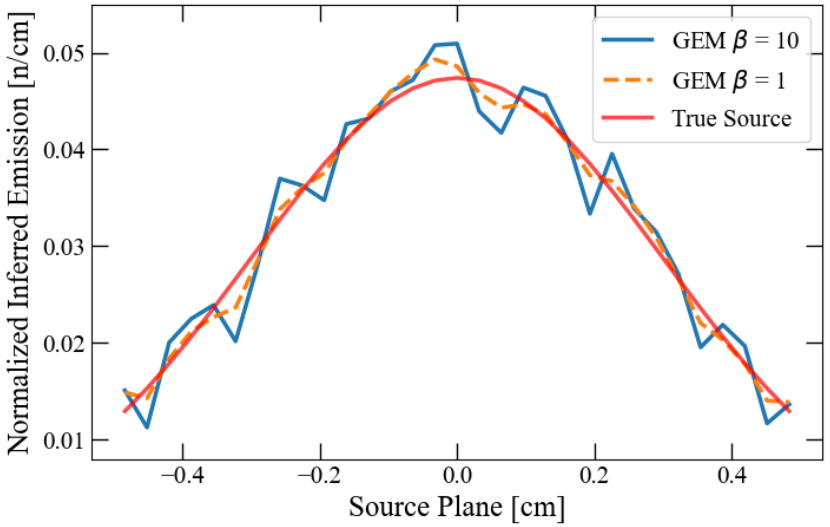

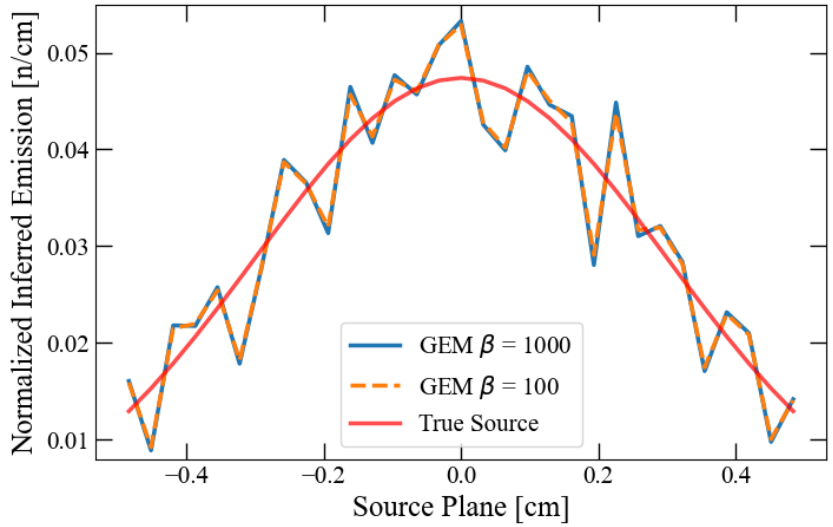

- As β increases, the influence of the Gibbs prior is reduced
- As B approaches + ∞, solution approaches MLE_Poiss

β Selection Method: k-Fold Cross Validation

1. Randomize order of 1D data points
2. Split data into k sections
3. First section becomes validation data, remaining sections are used as training data to generate a solution with a given β
4. Solution is forward propagated and compared to validation data
5. Iterate through each k section
   - Allows each data point to be part of training and testing
6. Repeat steps 3 - 5 over a range of β values

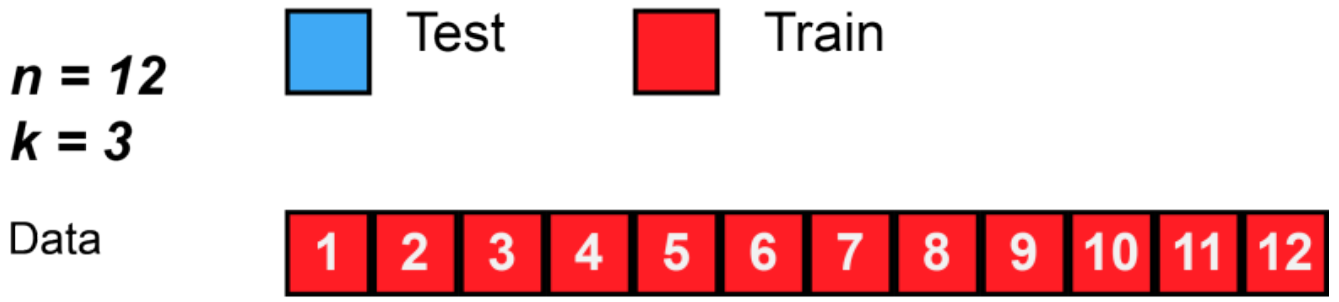

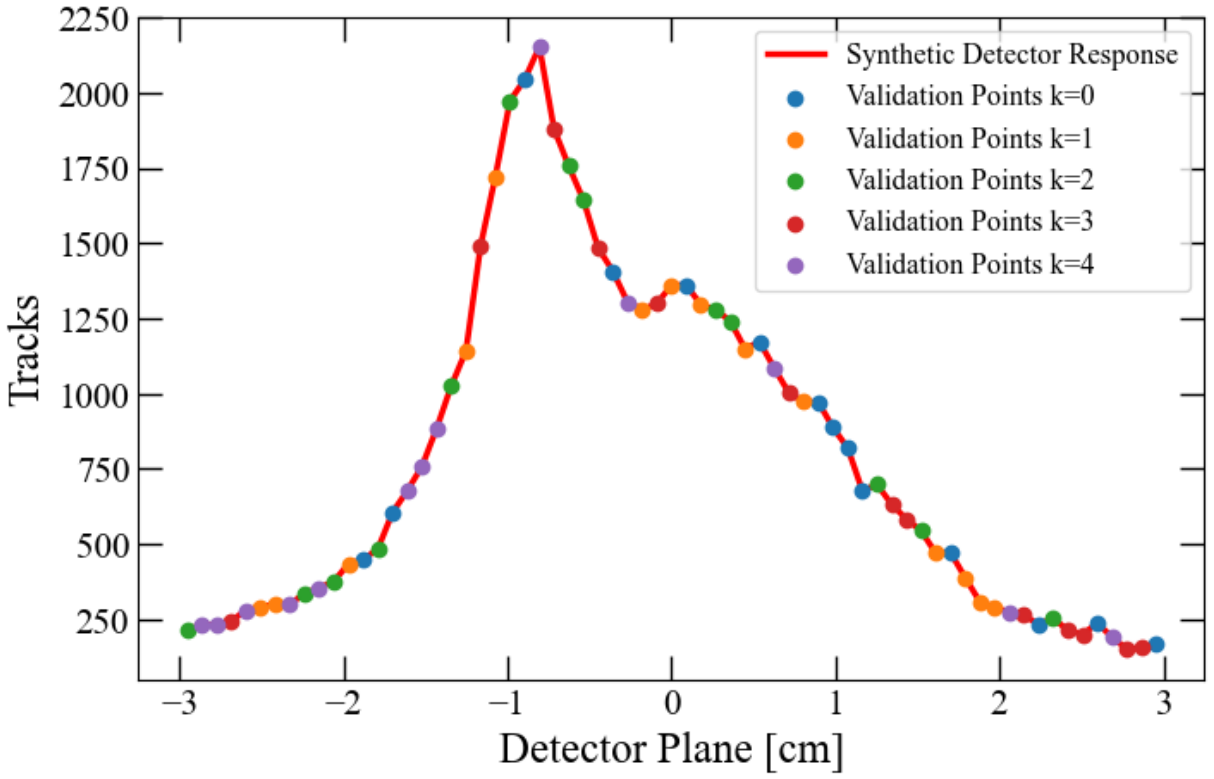

GEM Synthetic Source Reconstructions

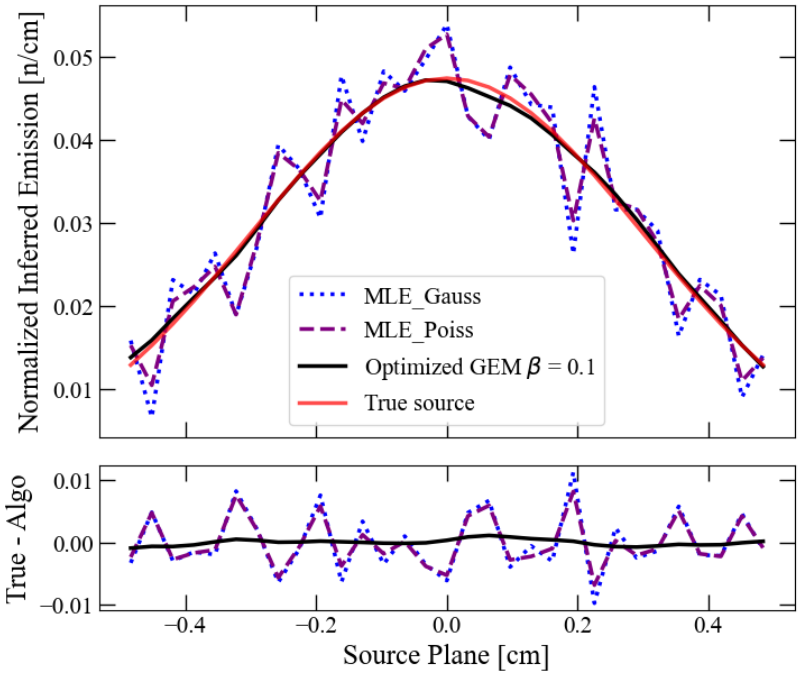

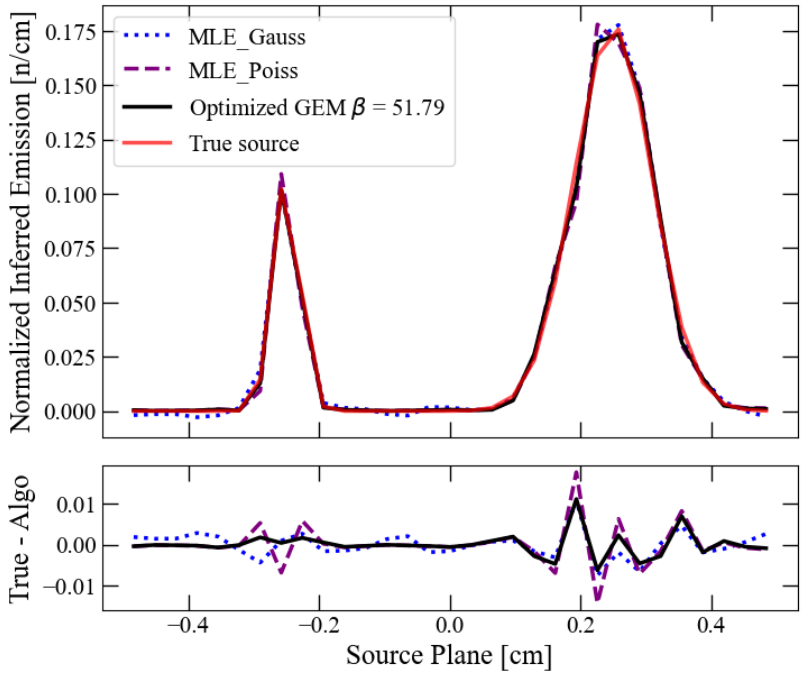

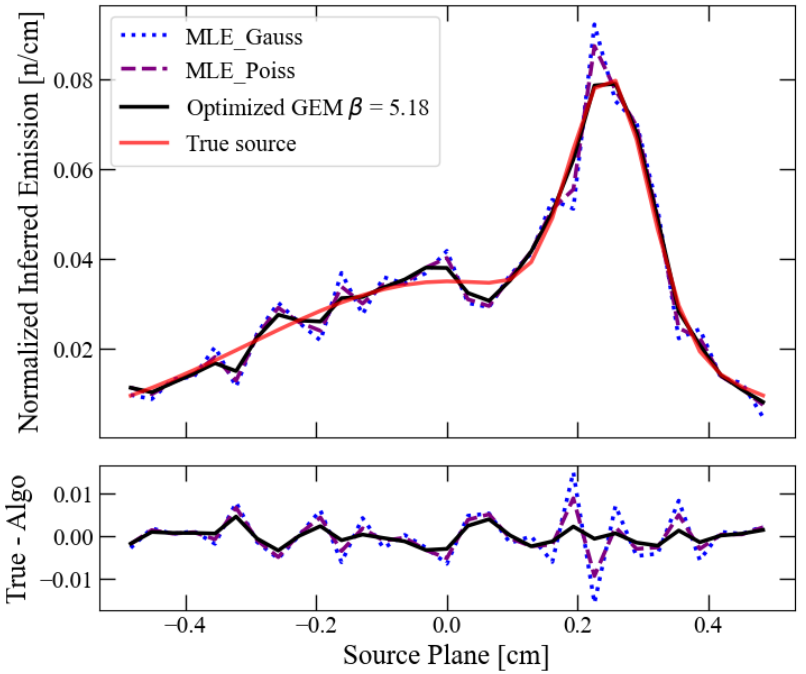

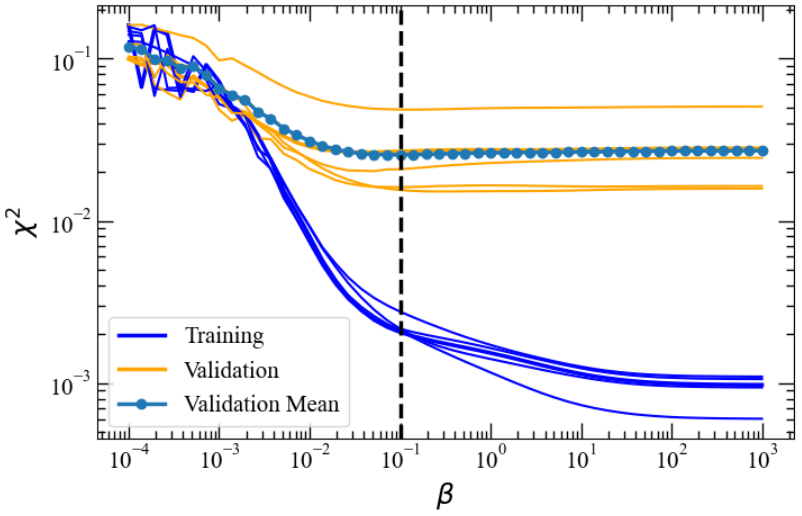

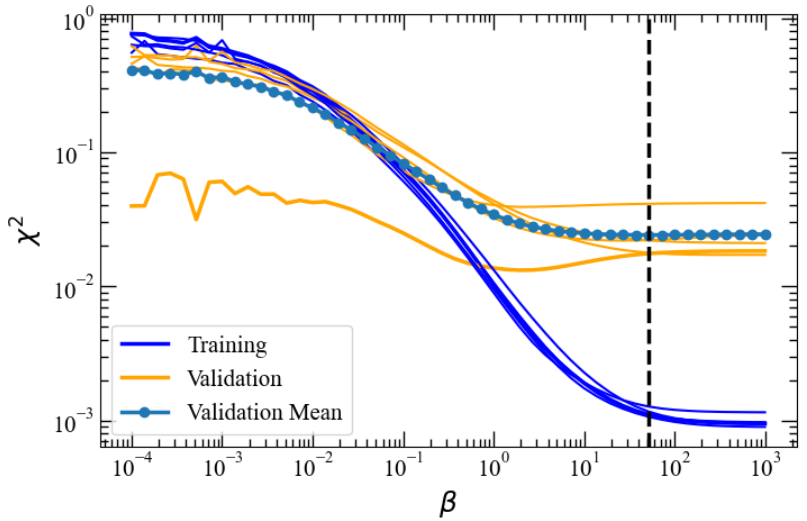

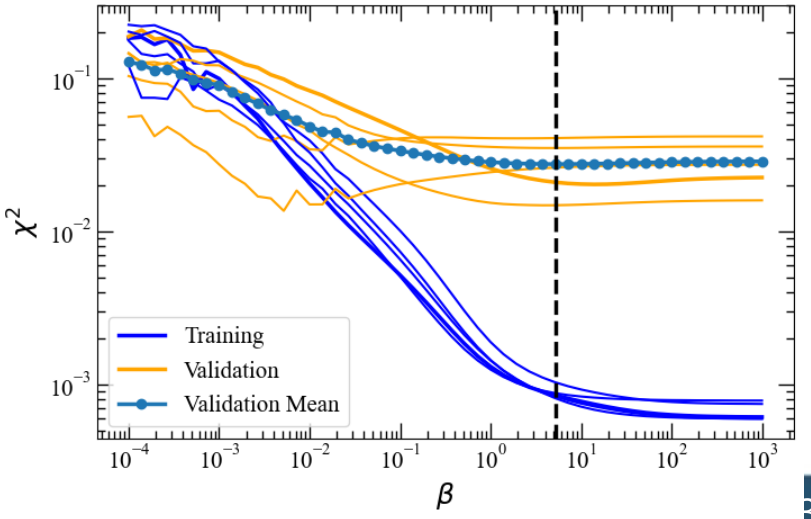

ODIN Forward Model Sensitivity Analysis

ODIN Model Parameters

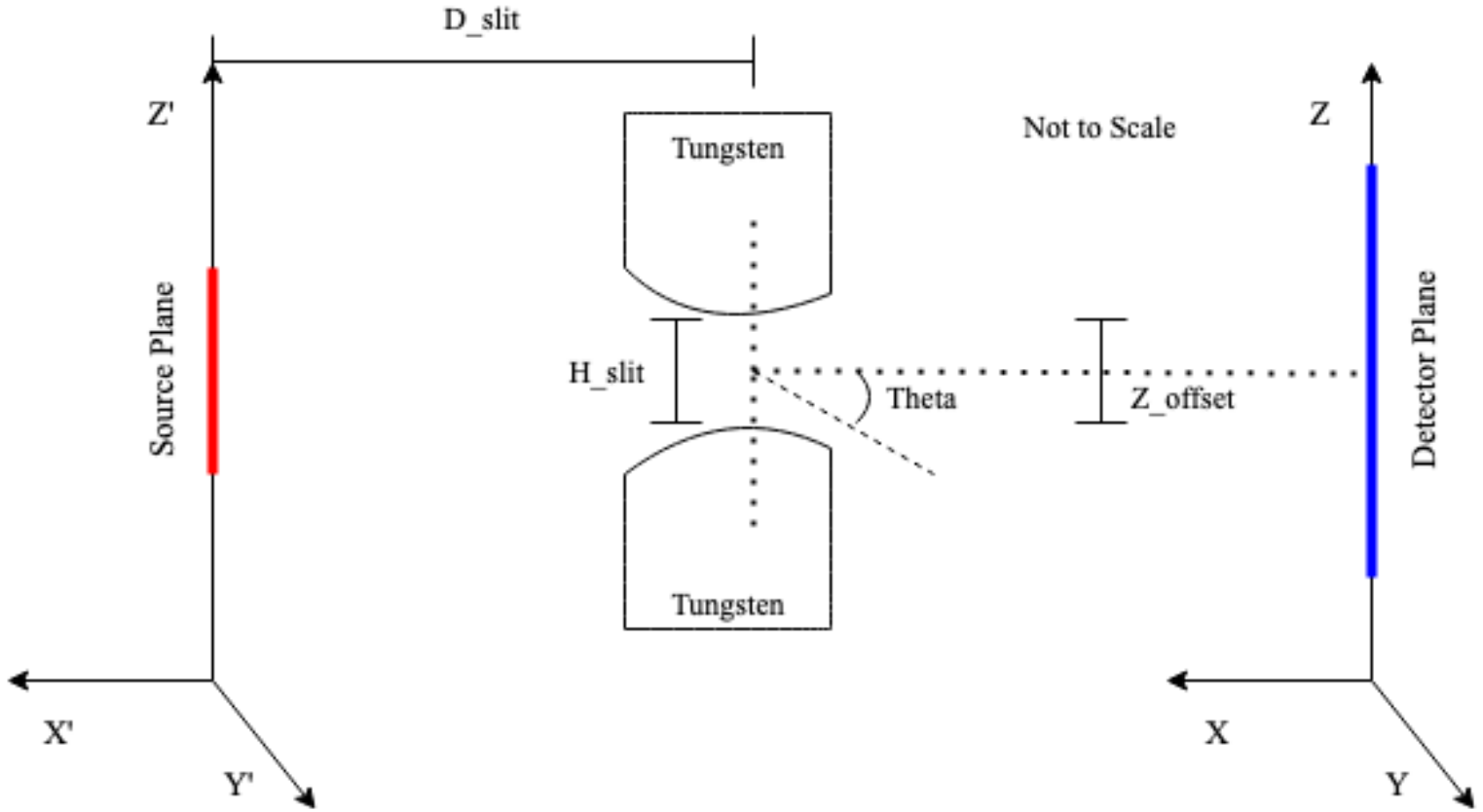

- Each parameter has some variability when fielding ODIN
- Reconstructions with synthetic data can determine the sensitivity of each parameter

Sensitivity Study Methodology

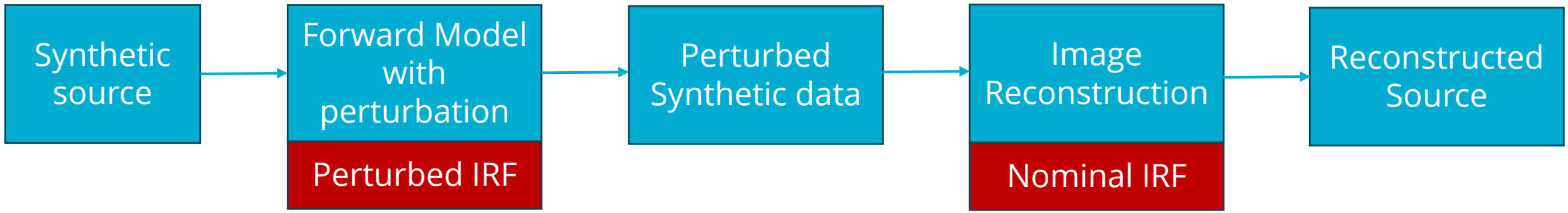

Varying source profiles representing experimental possibilities

Perturbed IRF represents some type of error in experimental setup, changes in model parameter space

Synthetic experimental data from perturbed model

Image reconstruction with nominal IRF using various methods

Reconstructed source variation will quantify how sensitive perturbed parameter is

- In addition, the sensitivity to noise variations will be tested by generating multiple synthetic detector responses from the nominal IRF matrix

Noise Variation

- 10 synthetic detector responses were generated for each source type (1E13)
- Increased deviations in reconstructions when sources contain lower frequencies
- GEM solutions under predict peaks, have low variation (this is a common issue with regularization)

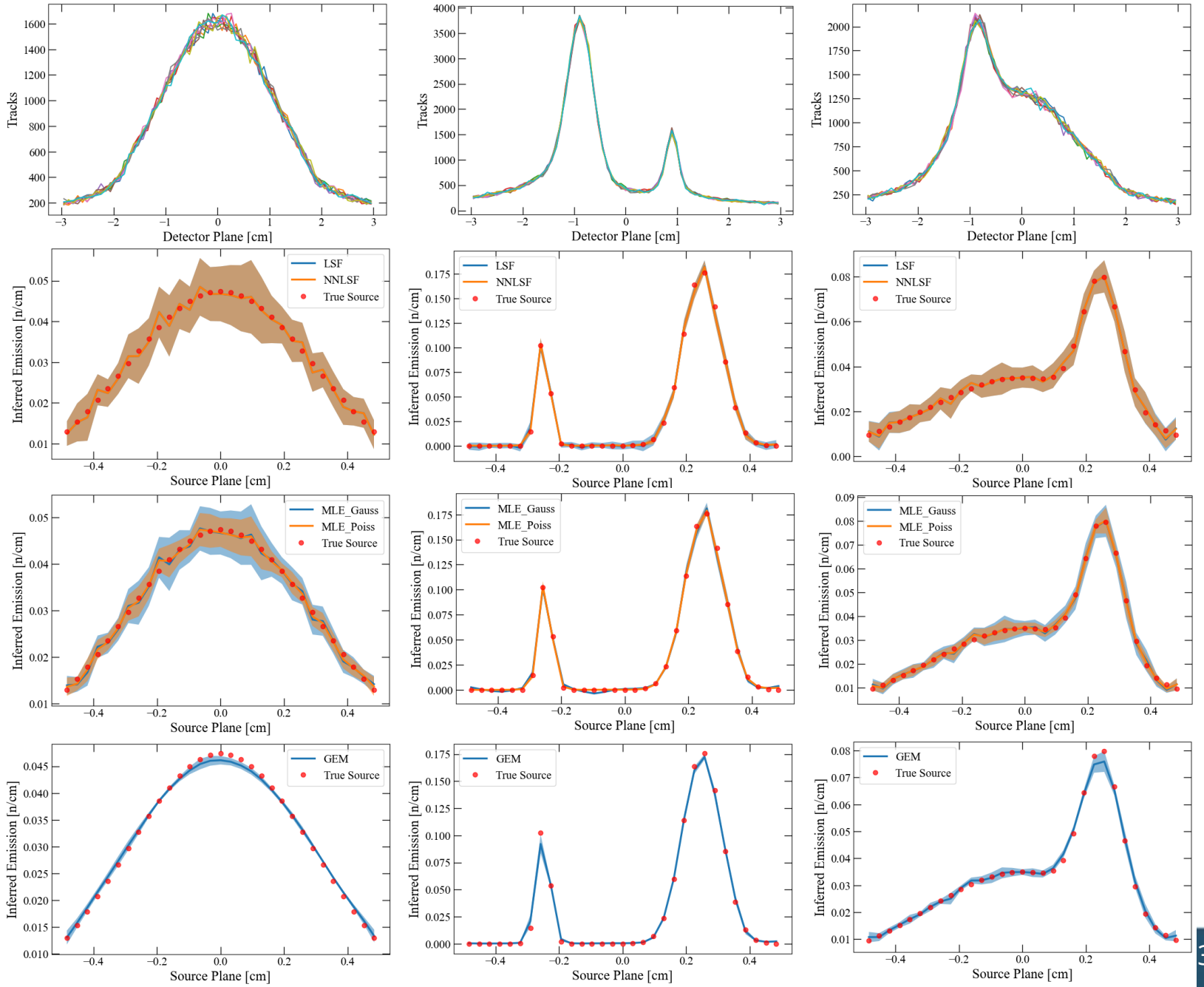

D_slit Variation

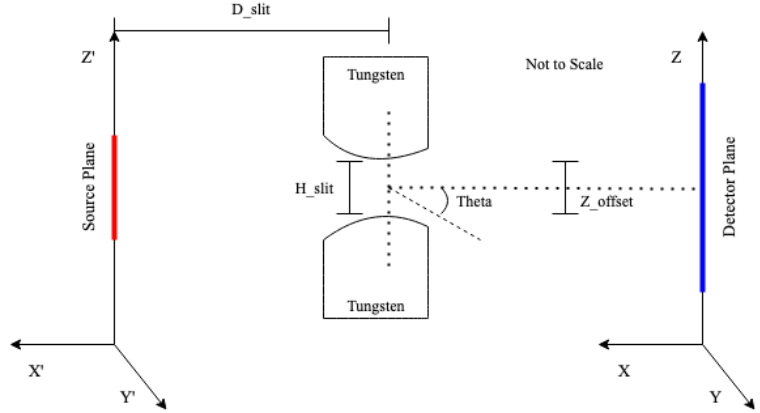

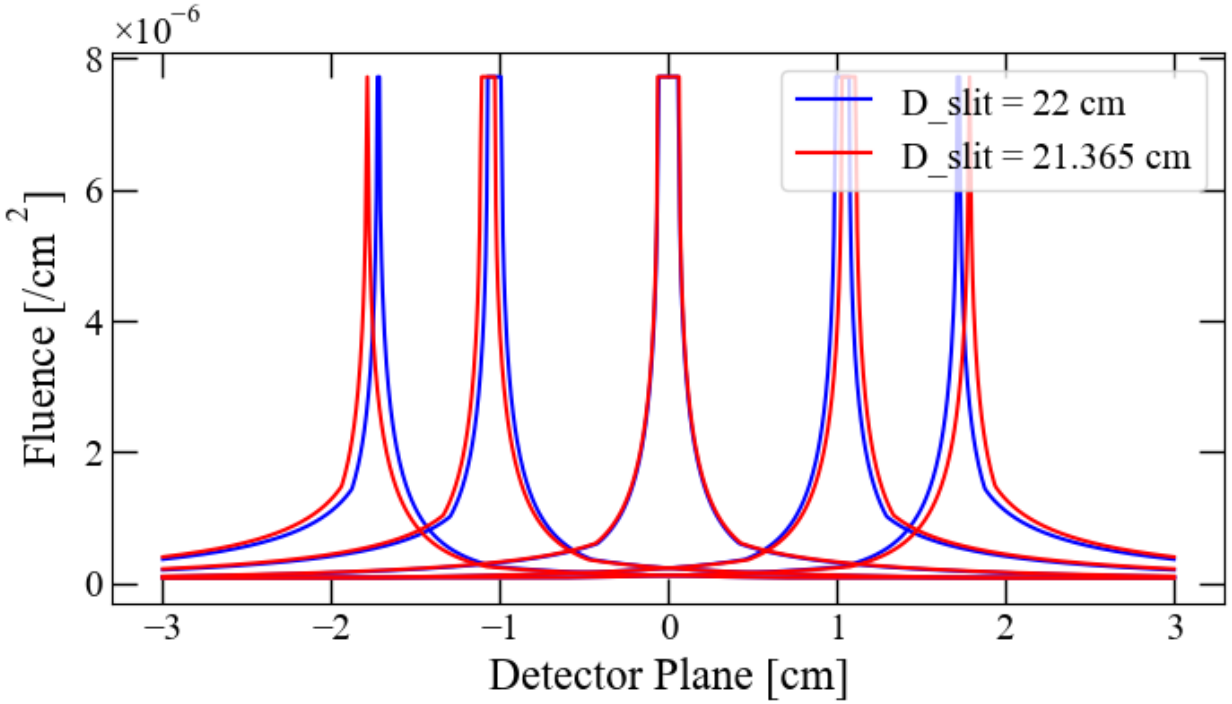

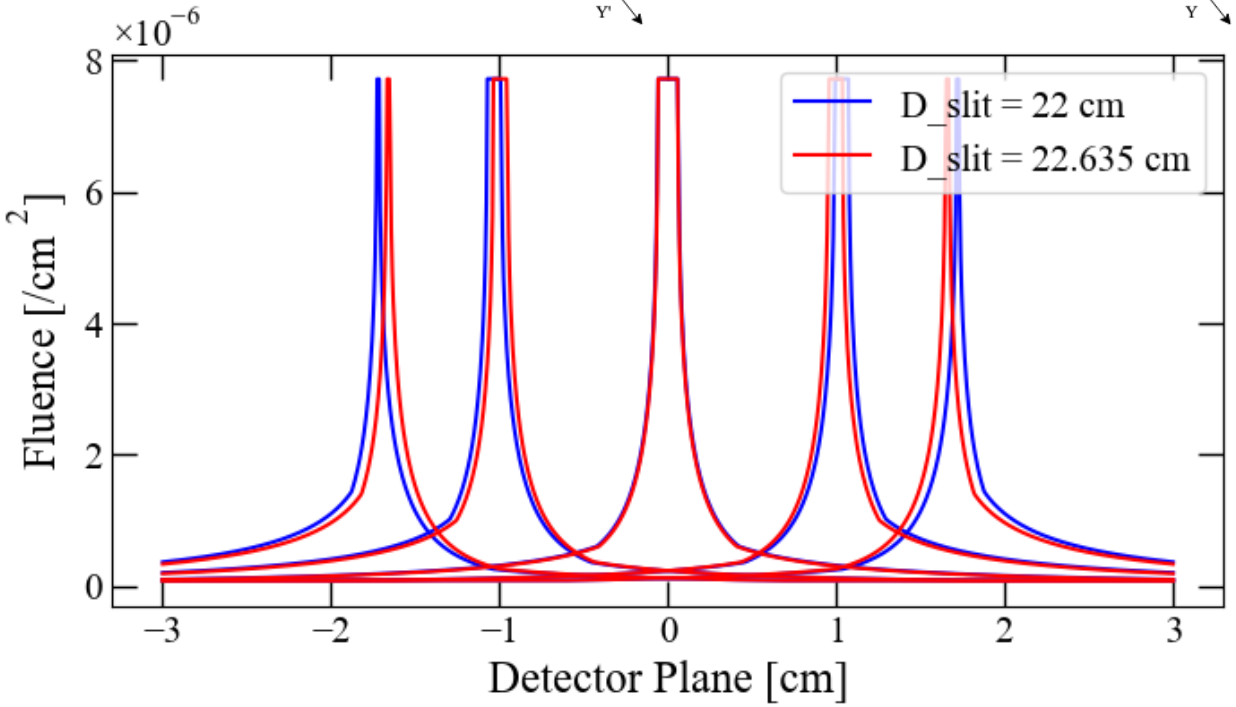

- D_slit alters the magnification of the image onto the detector plane
- Moving the aperture closer to the source increases the magnification
- The edge nominal IRFs can no longer account for increases in signal toward the edges

D_slit Variation Reconstruction Effects

- Increases in magnification cause the outermost source points to try and compensate for signal near the edge of the detector
- This is a mathematical property of searching for the best forward fit, edges must compensate
- This effect is not seen in HF synthetic source reconstructions due to having less tracks near the edge of the detector

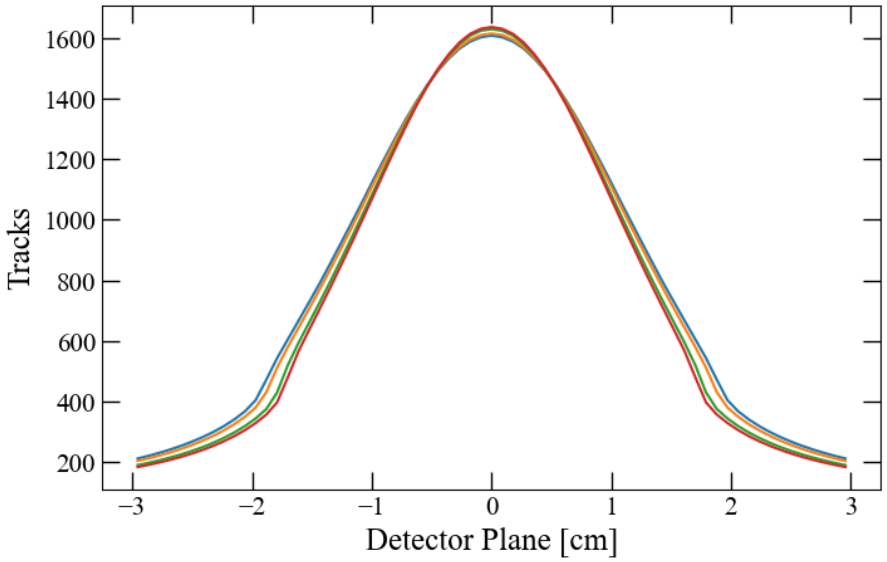

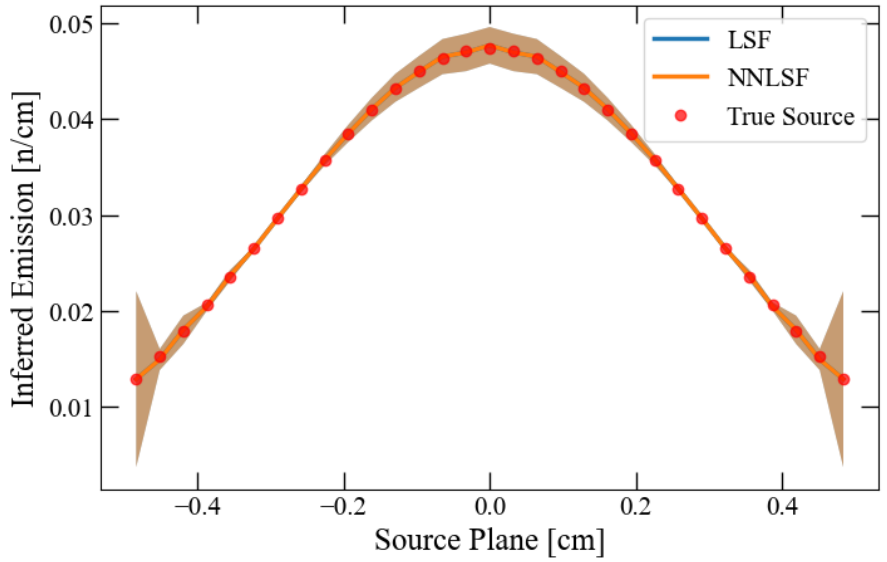

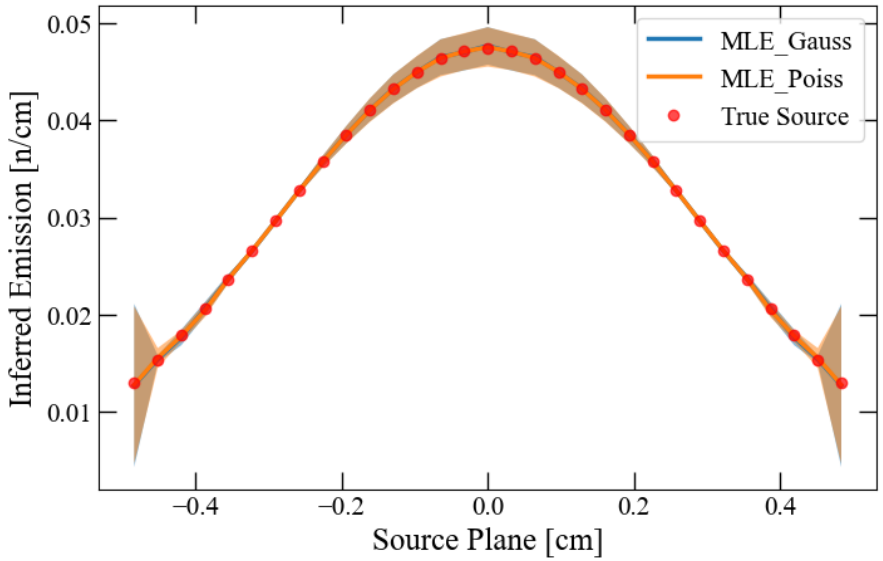

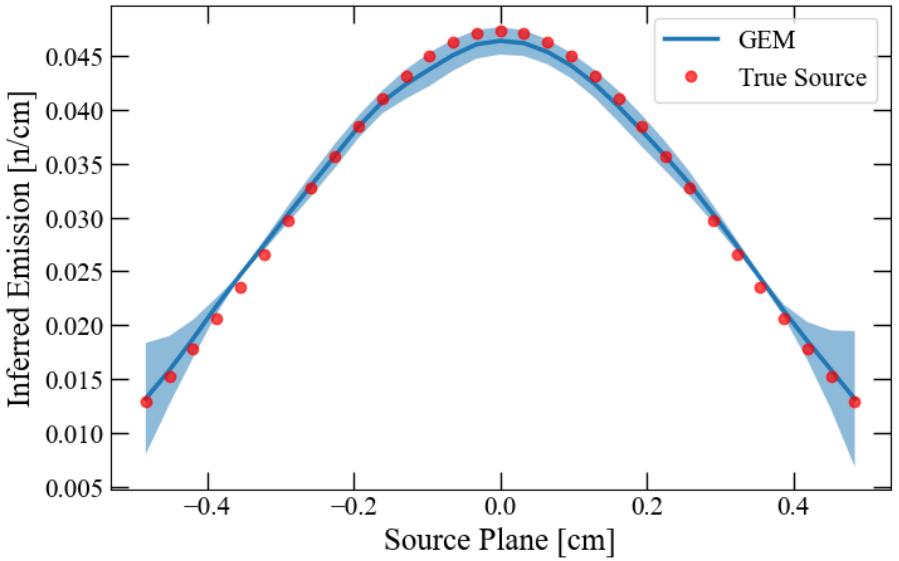

h_slit Variations

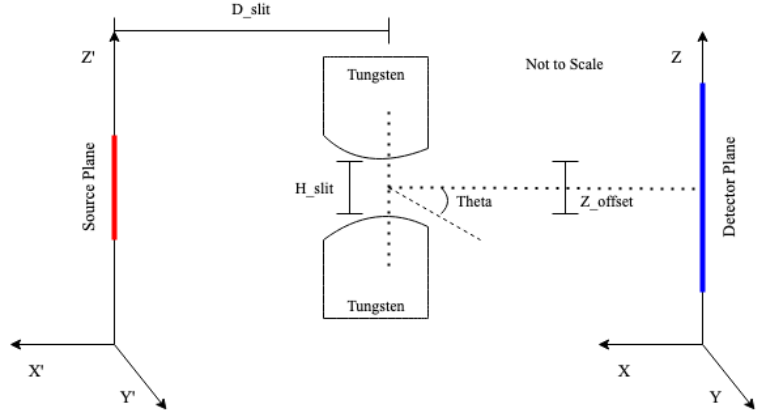

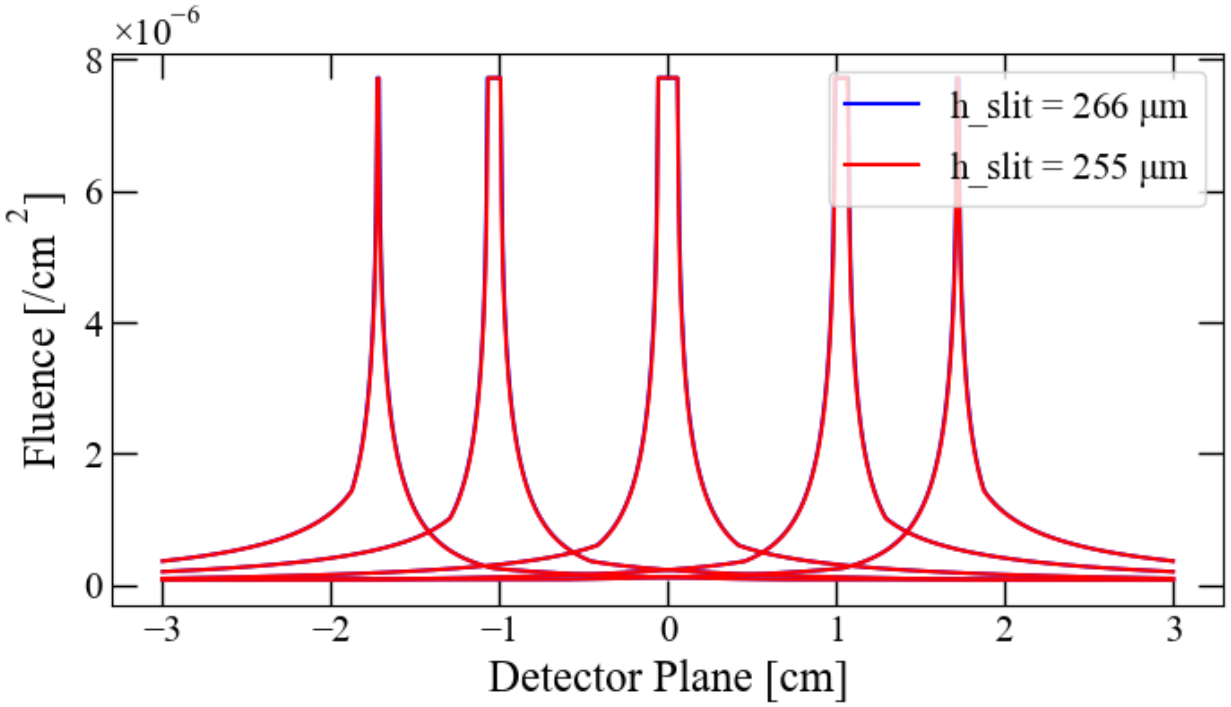

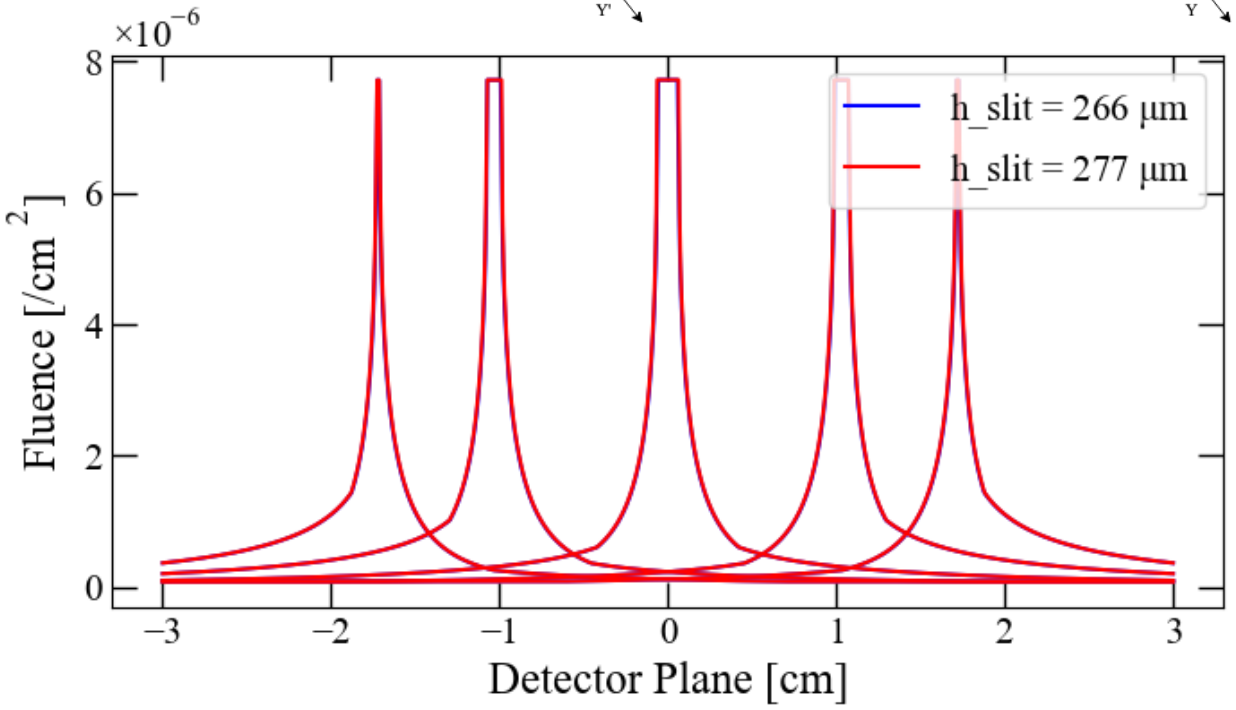

- Increasing or decreasing the aperture size has little effect on the IRFs
- Alters the flat top widths by an insignificant amount
- No variations in reconstructions (GEM still underpredicts peaks)

Z_offset Variations

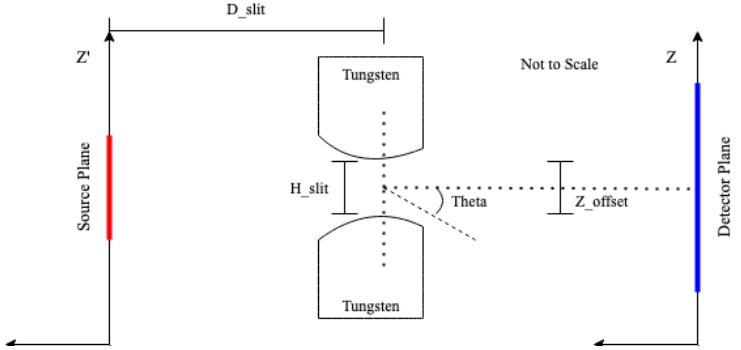

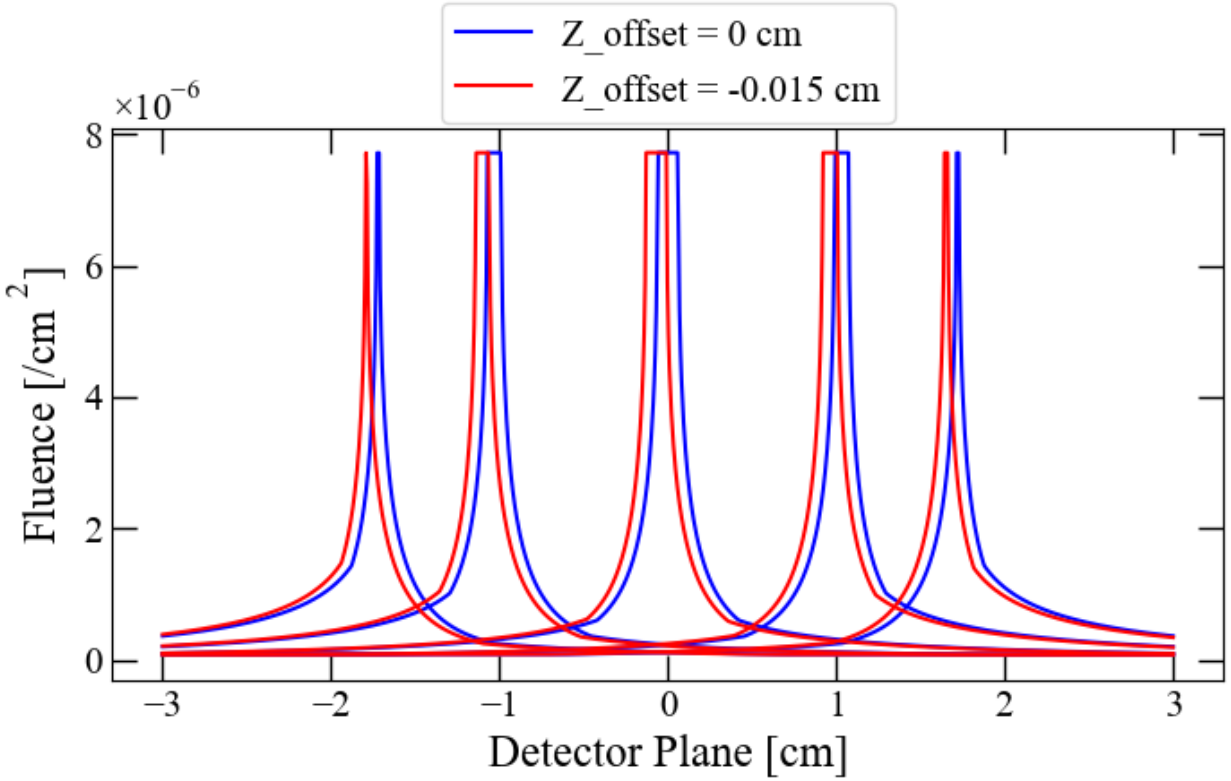

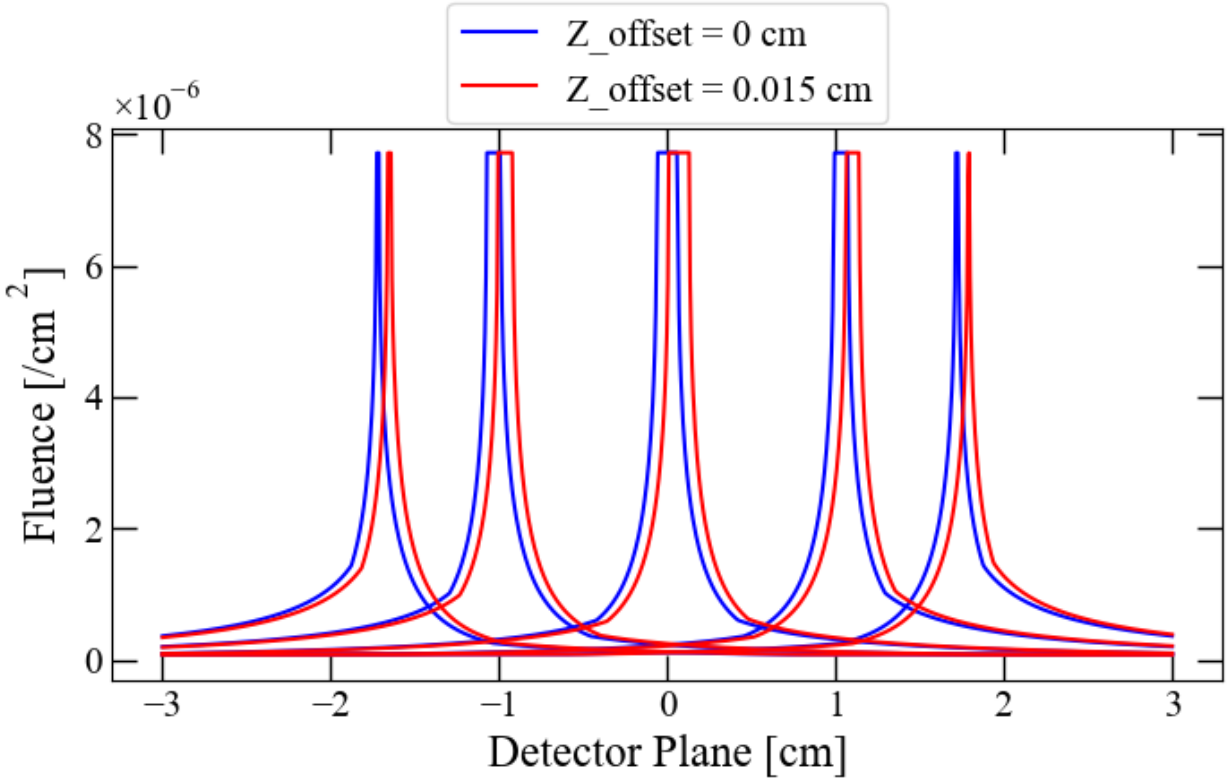

- Shifts the location of each IRF
- Flat tops get wider or smaller as the direct line of sight changes
- Variation is symmetric in +/- direction

Z_offset Variation Reconstruction Effects

- Detector response peaks shift in location due to all IRFs being altered
- Edge effects appear due to outermost IRF shifts
- Has larger standard deviation in HF features (peak areas) compared to D_slit

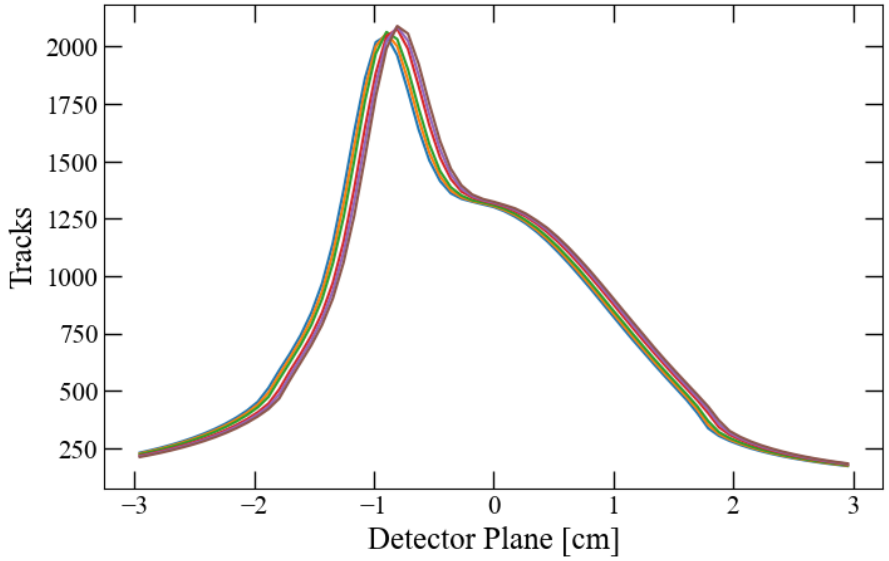

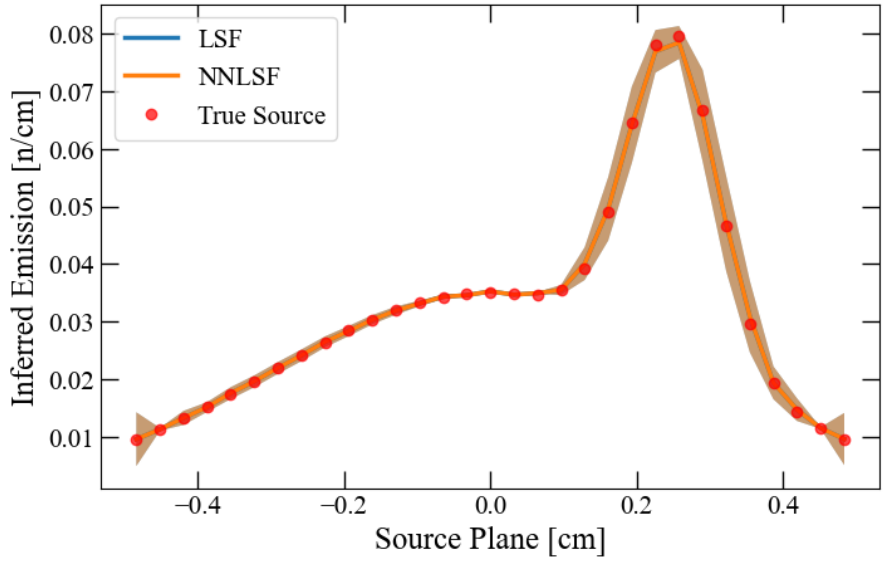

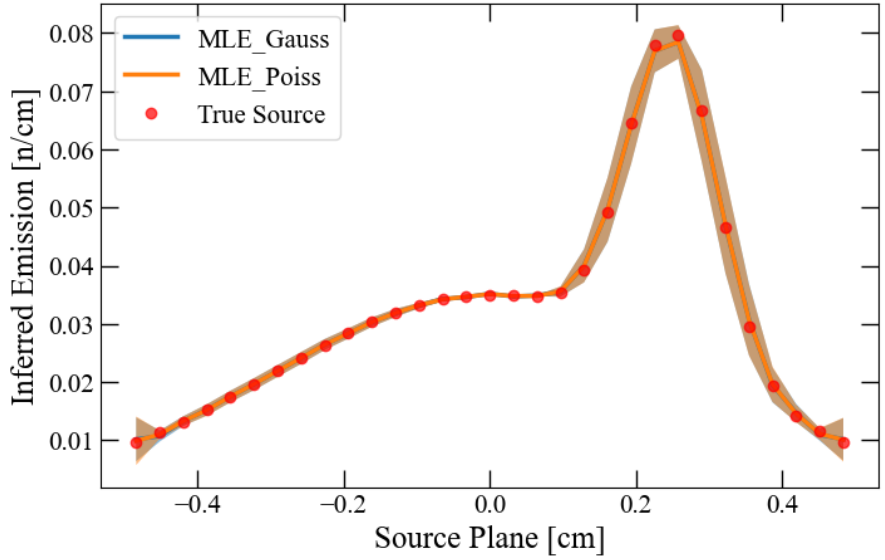

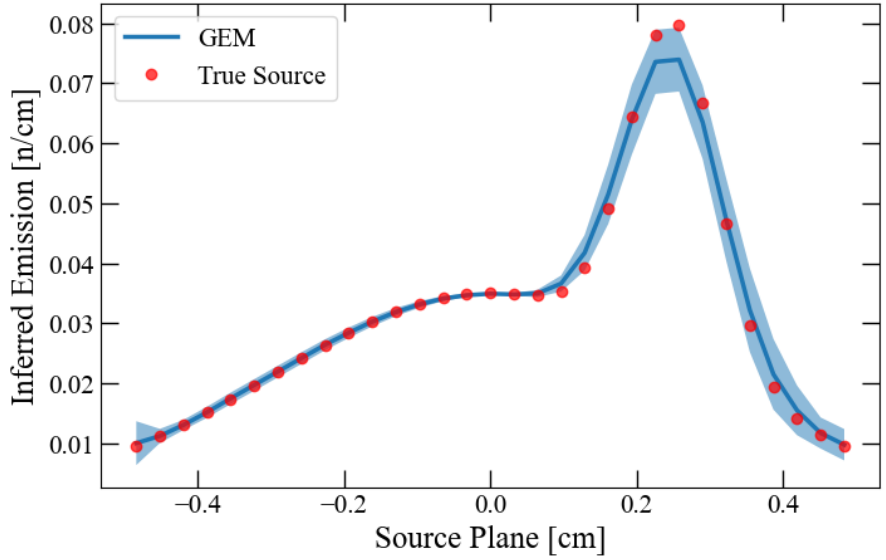

Theta

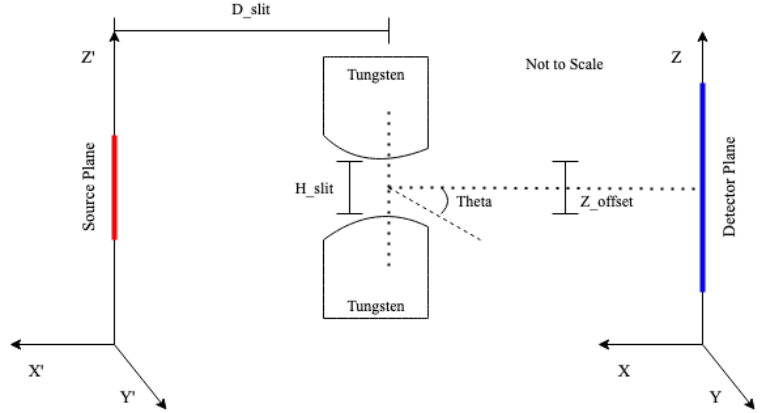

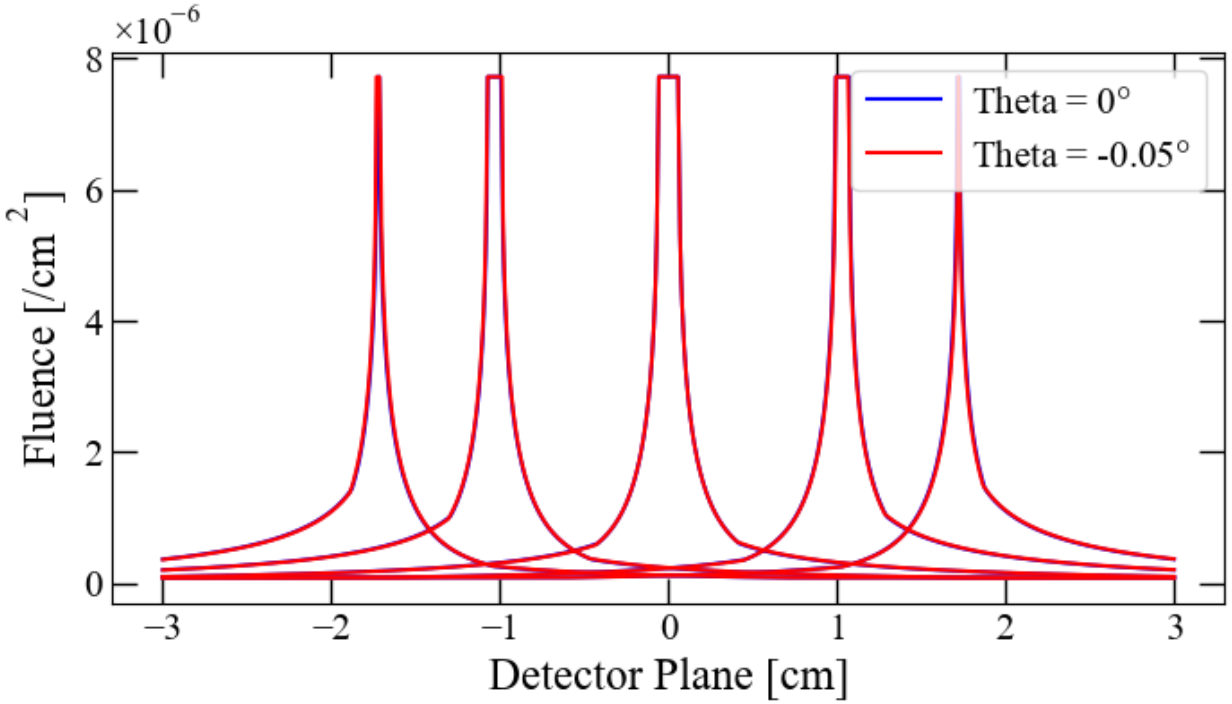

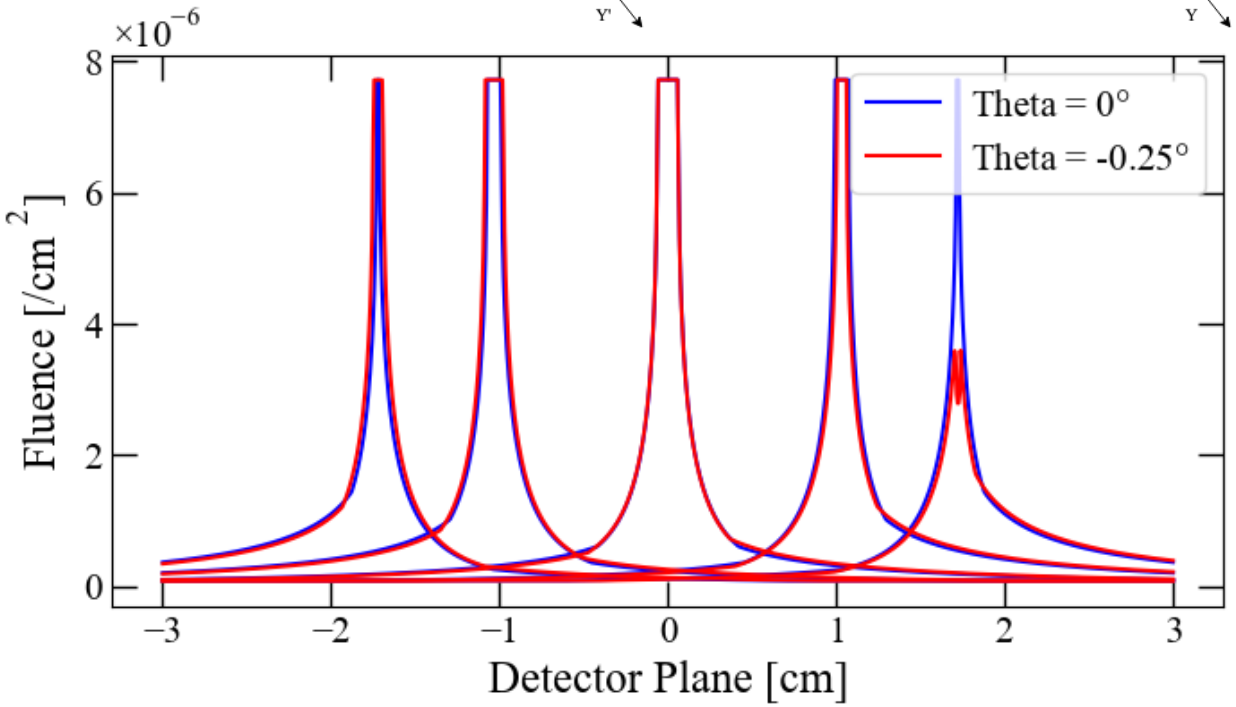

- Changes the shape of each IRF
- Source points near the top of the stagnation column see a larger aperture opening
- Source points near the bottom eventually have no direct line of sight through the aperture

Theta Variation Reconstruction Effects

- Increases the contribution from positive source points
- Edge effects appear once again due to outermost IRF compensation, but appear asymmetrically

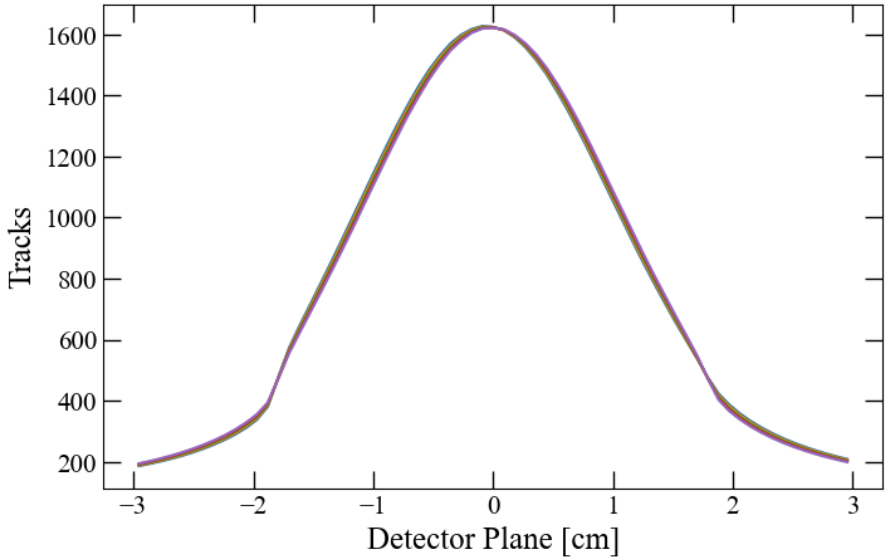

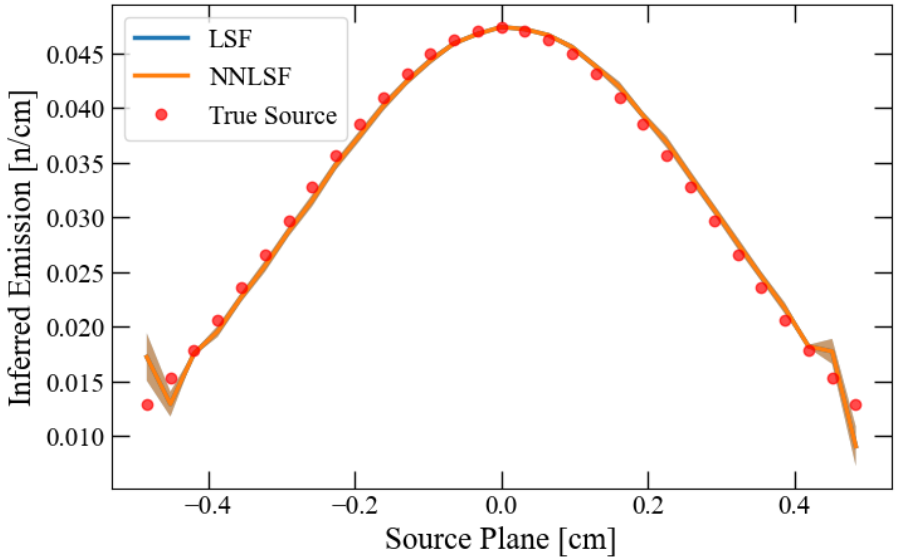

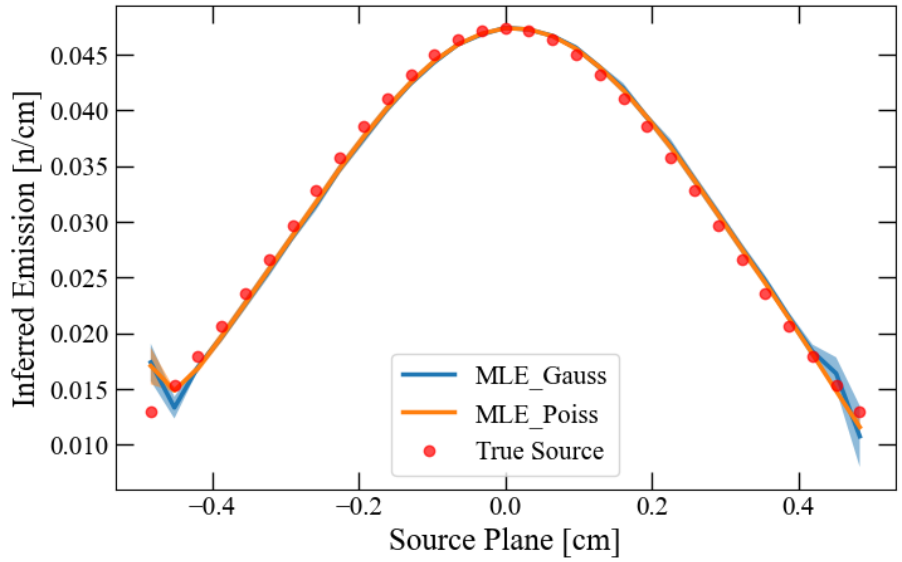

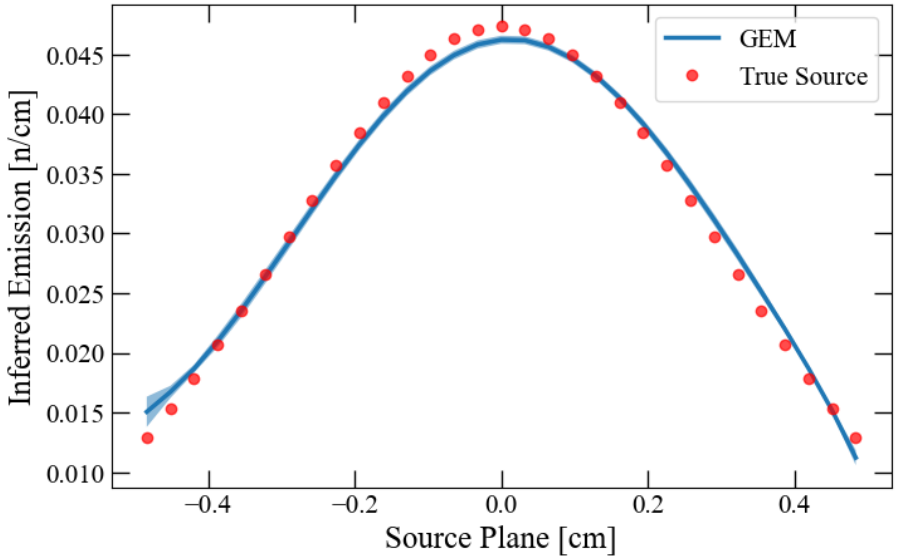

Error Estimation - Latin Hypercube Sampling (LHS)

- LHC is a sampling is used to avoid biasing in parameter selection, to create more uniform sampling in the parameter space

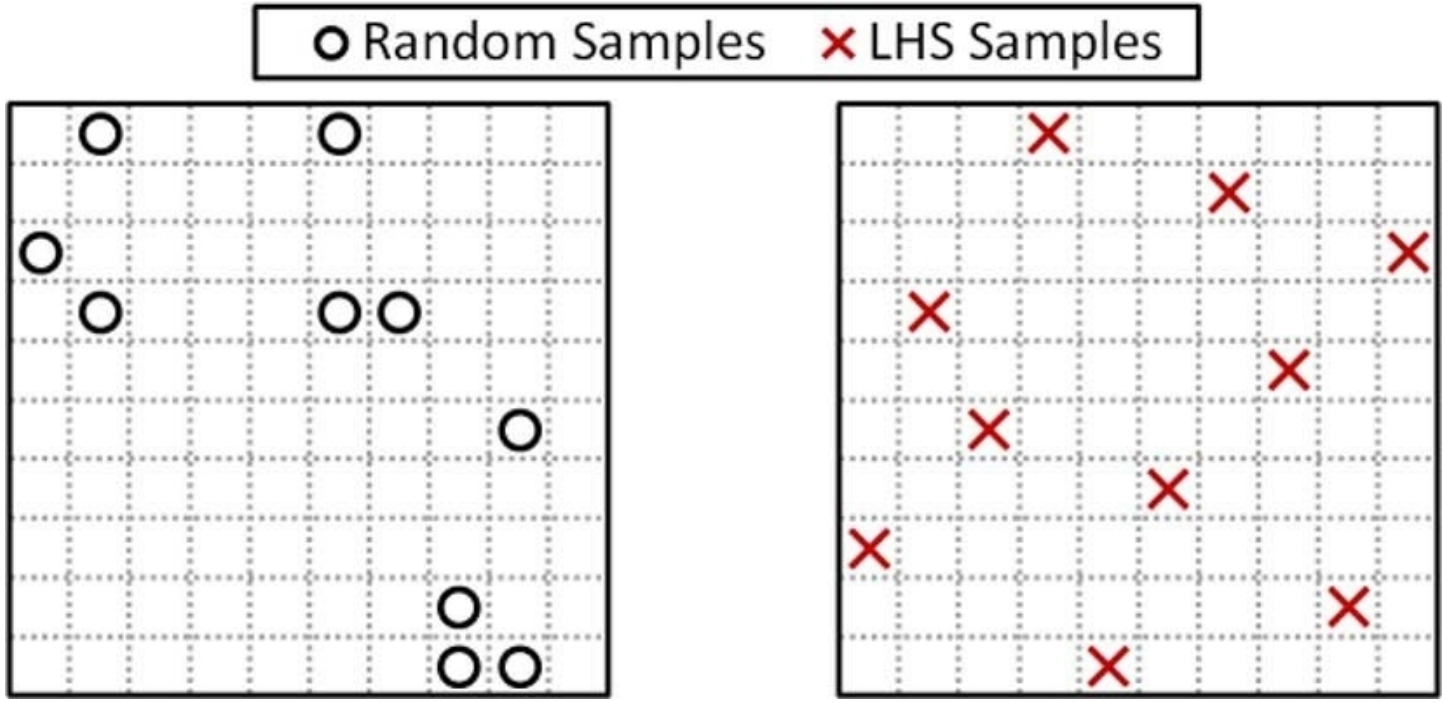

Preece, Robin & Milanović, Jovica. (2015). Efficient Estimation of the Probability of Small-Disturbance Instability of Large Uncertain Power Systems. IEEE Transactions on Power Systems. 31. 1-10. 10.1109/TPWRS.2015.2417204.

Low Frequency LHS Reconstructions

- Provides a range of possible detector responses from our parameter uncertainties
- Reconstructions represent an estimated error propagation from the accumulation of parameters

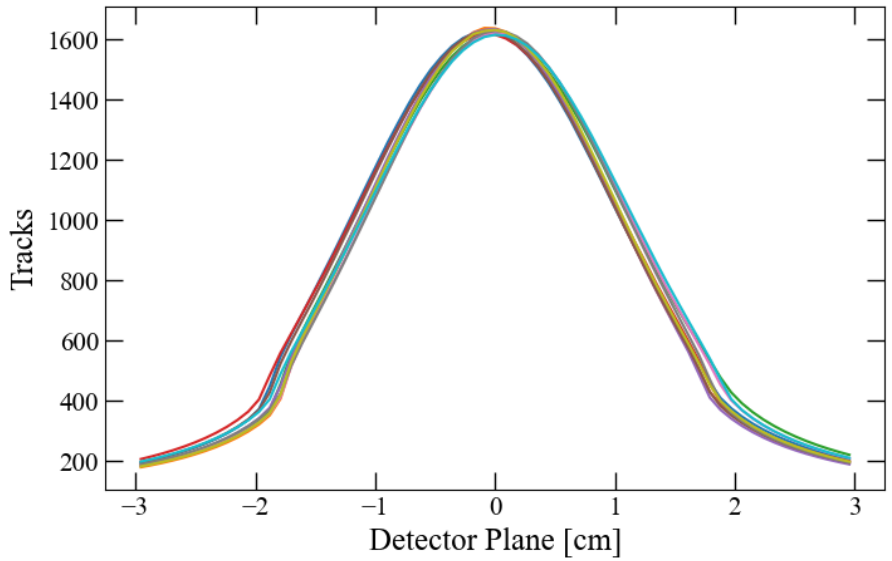

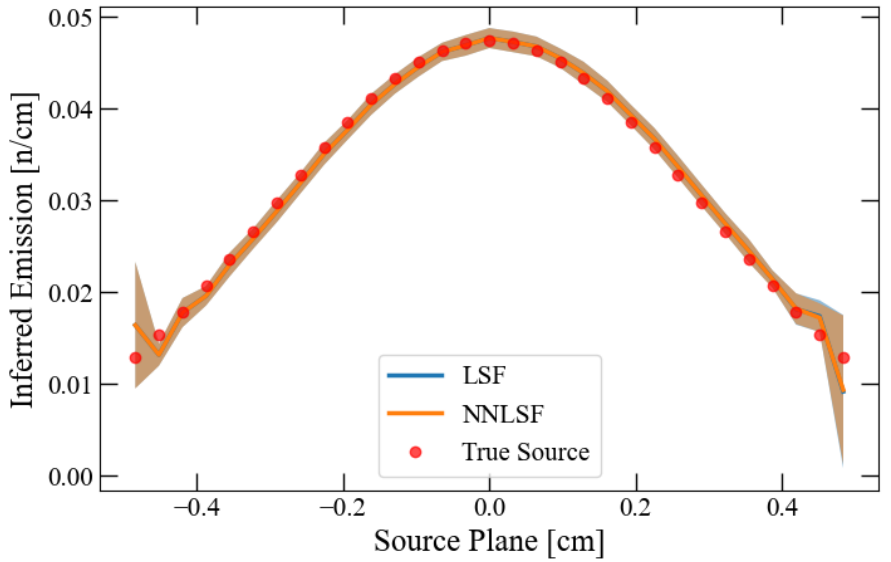

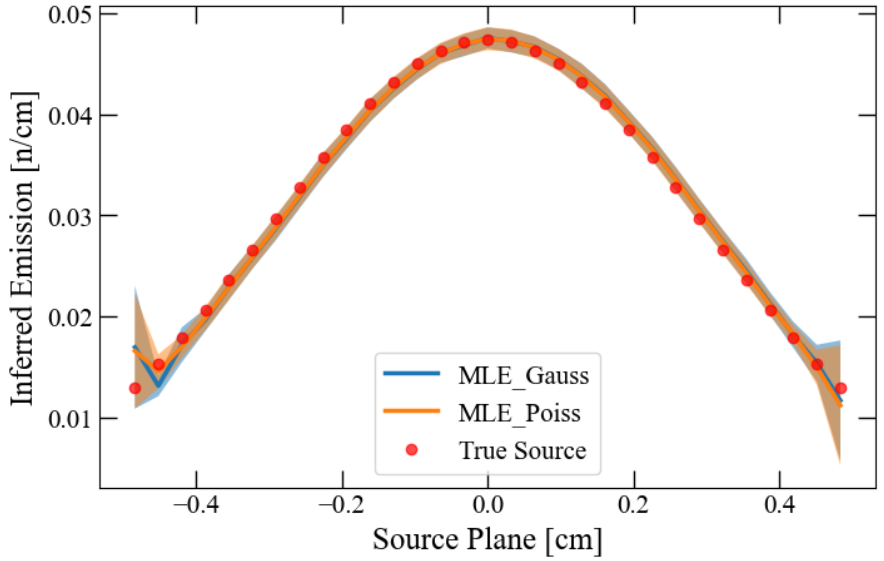

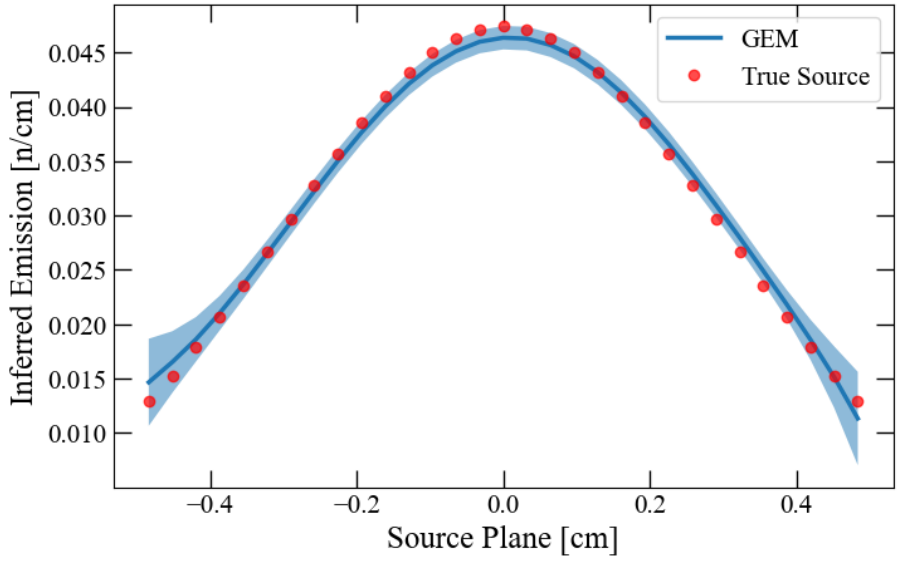

LHS + Yield Noise

- Synthetic yields of 2E12, 1E13, and 5E13 (5X multiples)
- Increasing yields increases the signal to noise (SNR)
- It is clear the standard deviation is reduced with increased yield, approaching only the parameter error propagation
- GEM appears to be the best performing algorithm

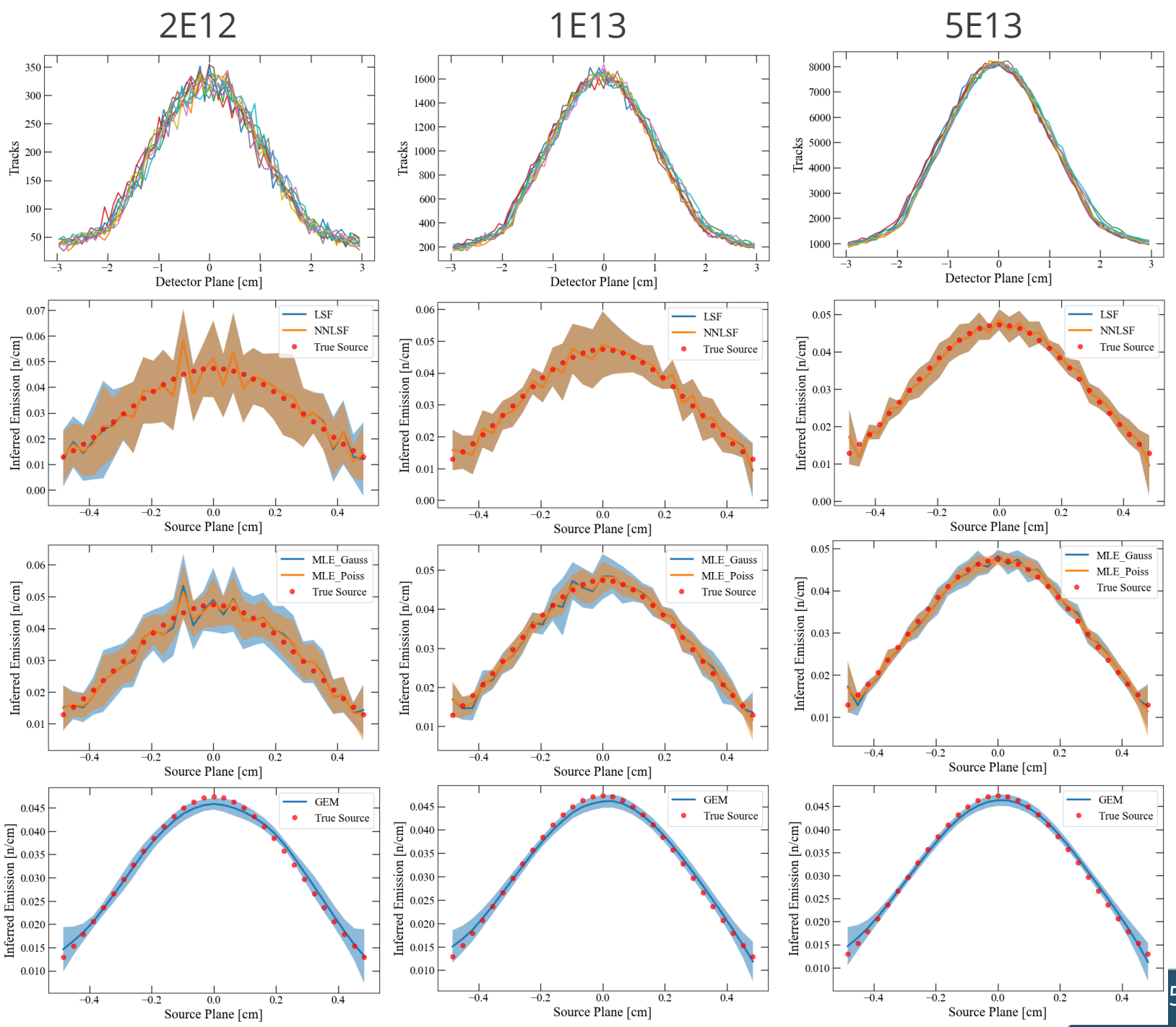

Error Estimation - Bootstrapping

- LHS error propagation is difficult to implement into real data, as well as computationally expensive
- An quick alternative approach to estimate error, is by bootstrapping the data
- This method resamples the original data based on the central limit theorem, and generates multiple data sets

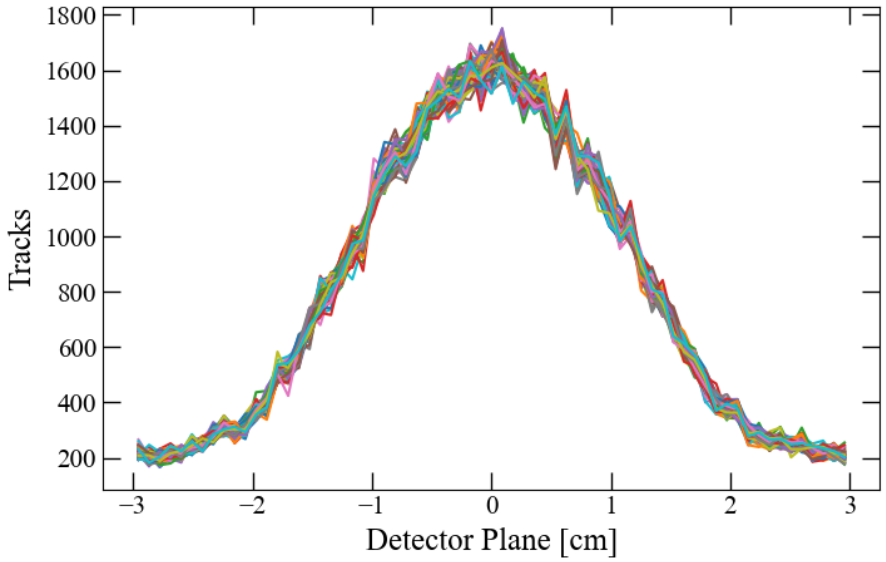

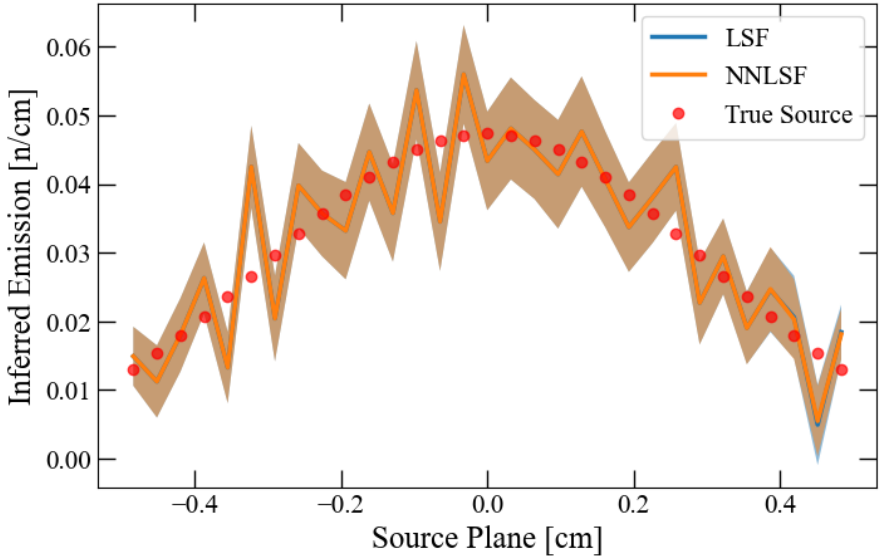

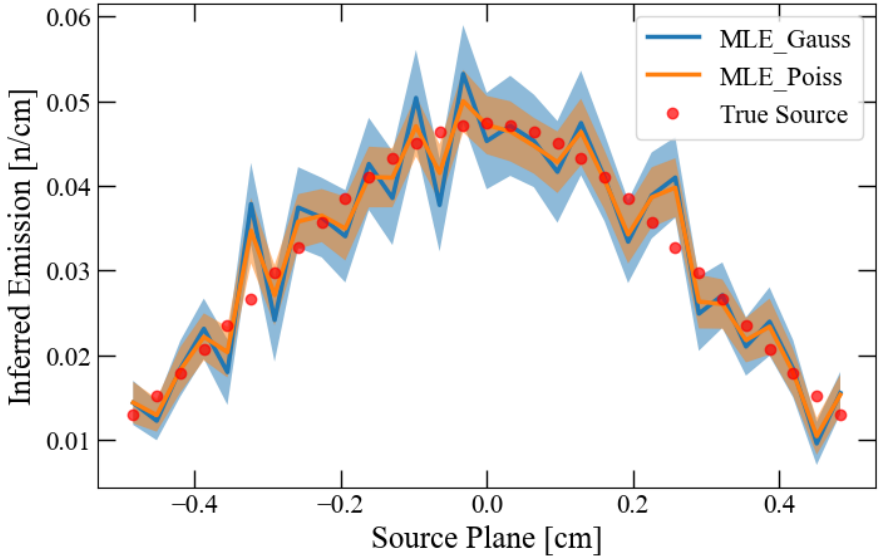

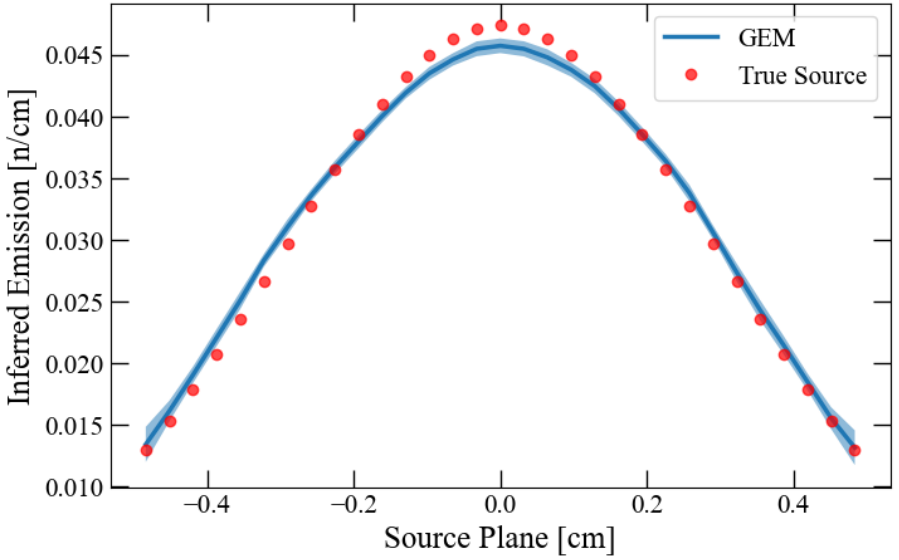

Source Reconstruction from ODIN Data

z3289 and z3926 CR-39 Data

z3289

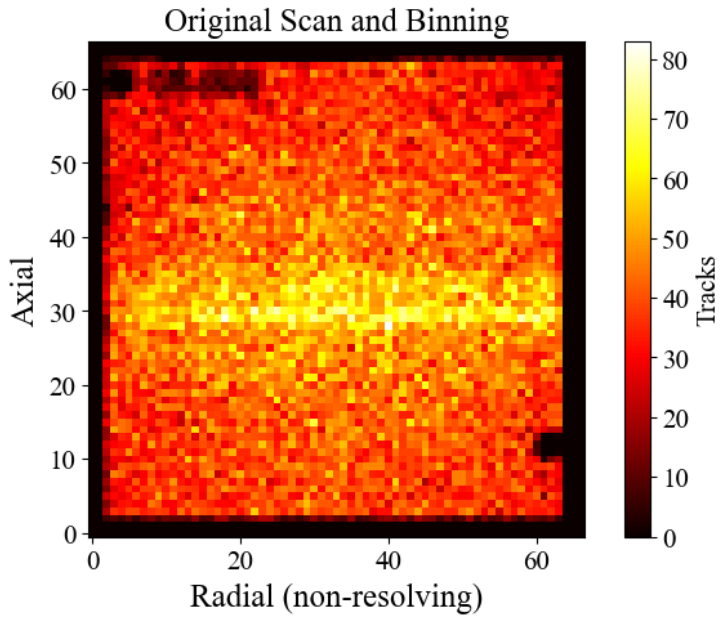

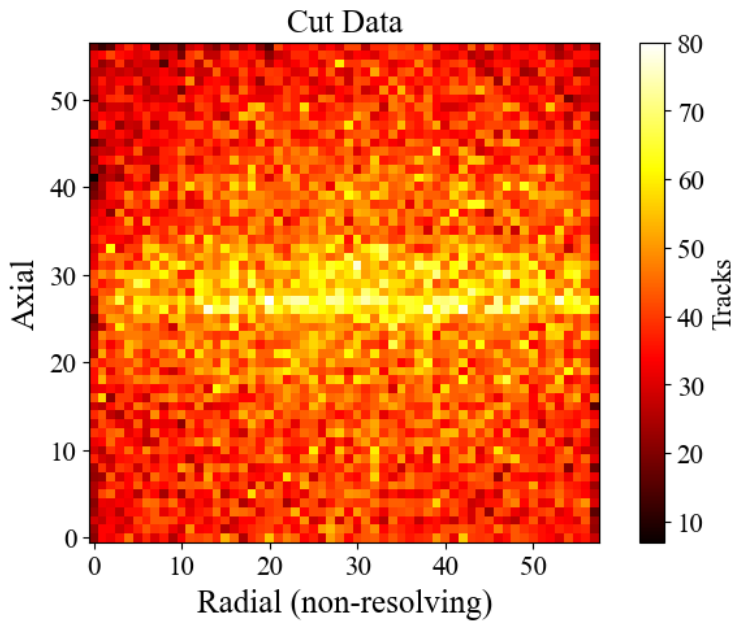

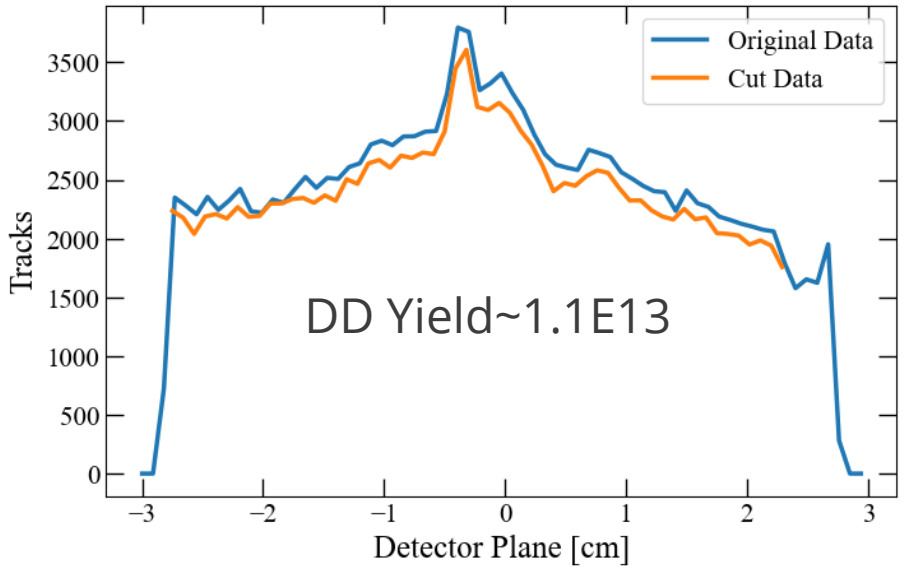

z3926

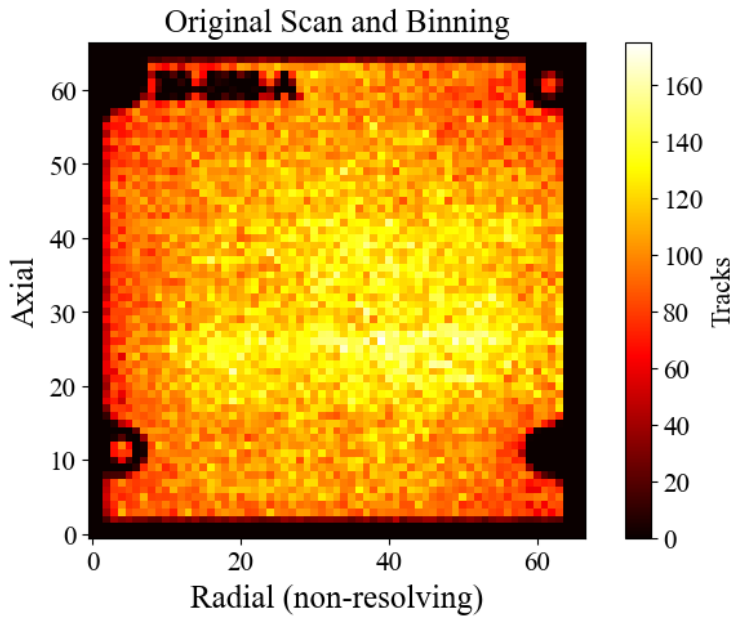

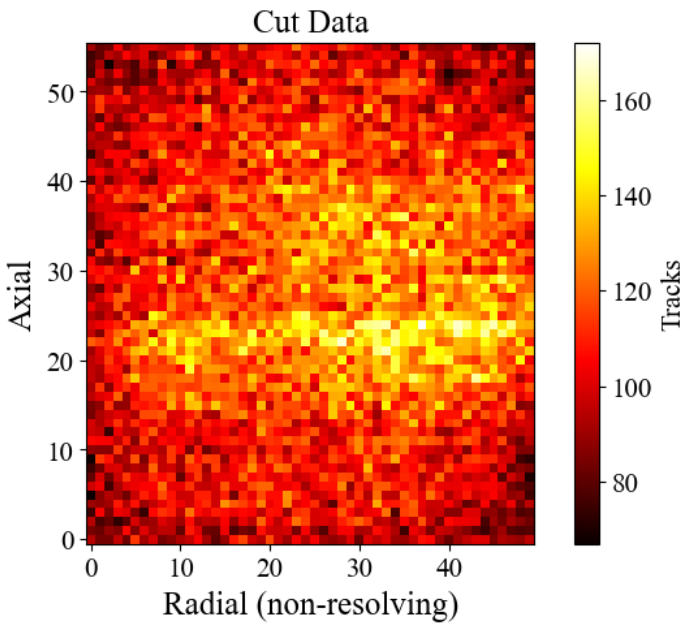

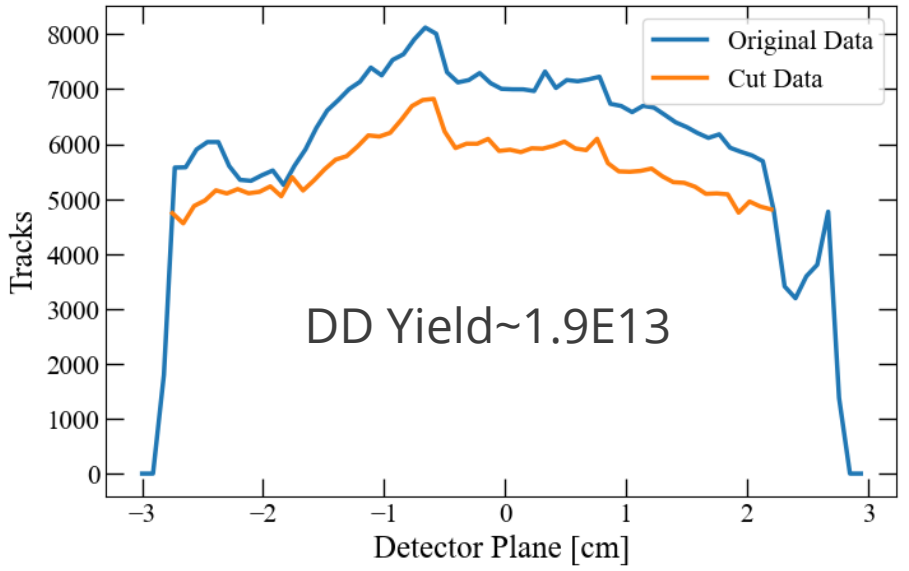

z3289 Reconstruction

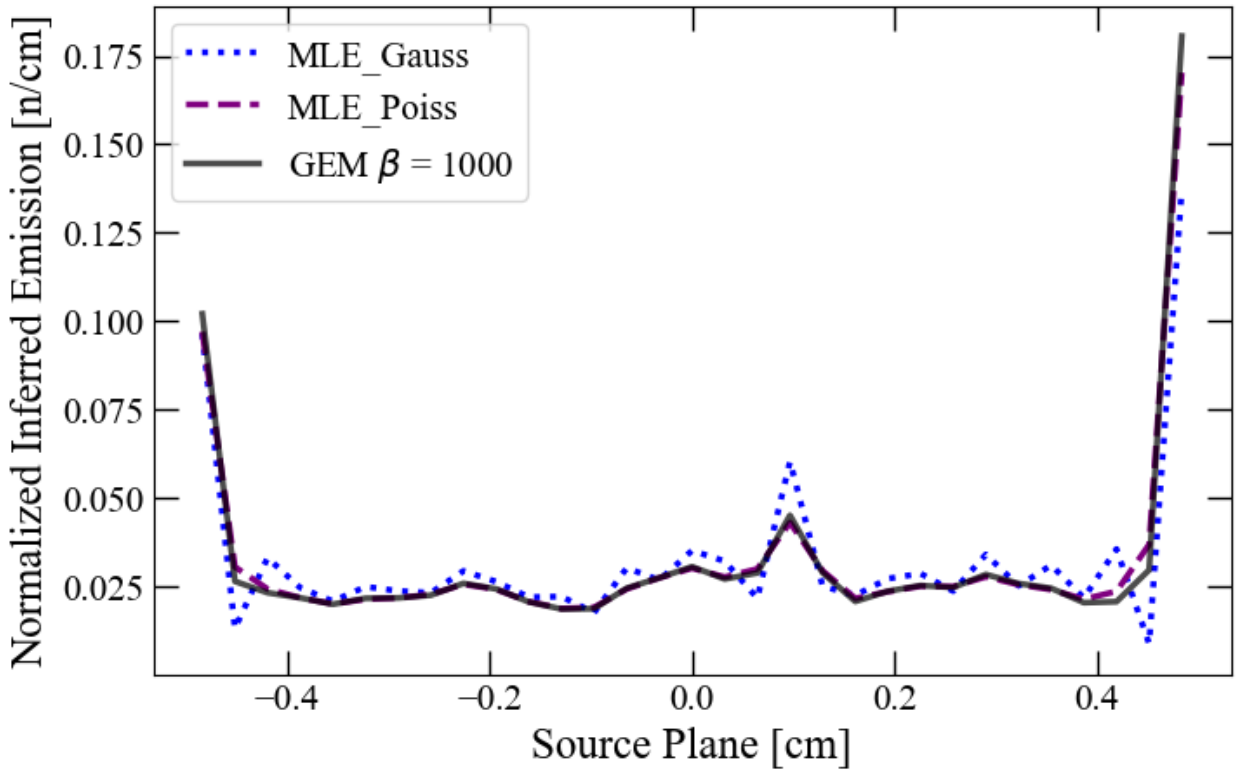

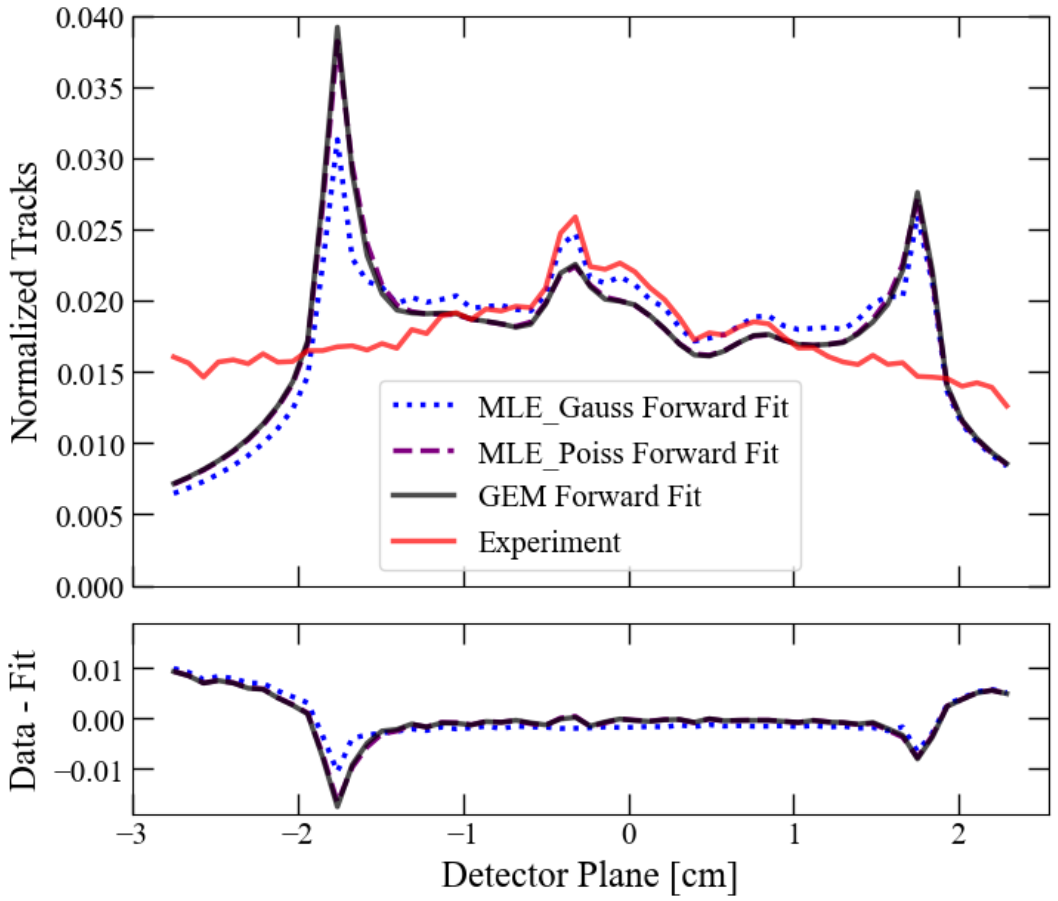

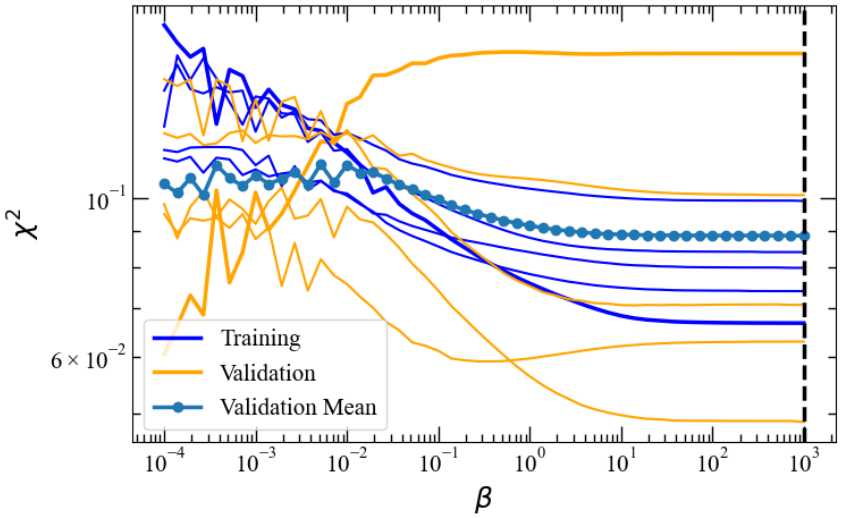

- Edge effects appear in all methods
- There is clear compensation in the forward fit

Issues of Background

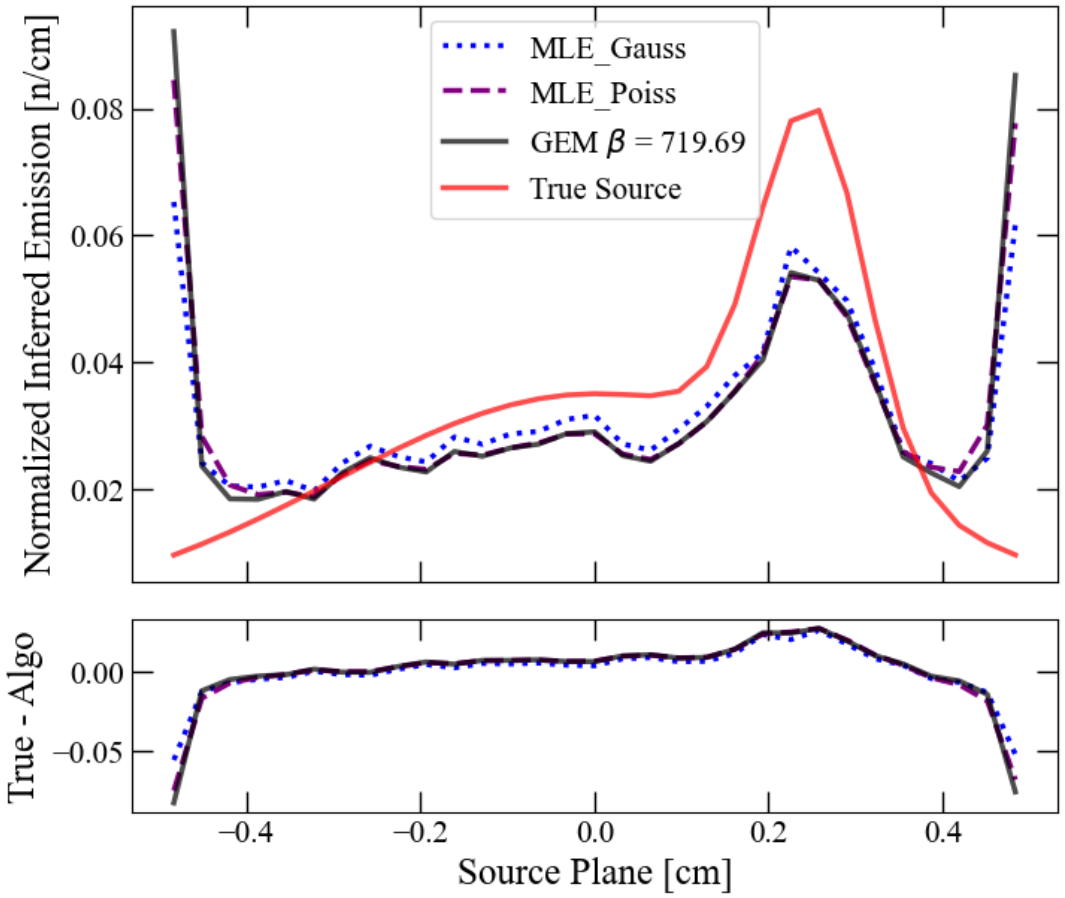

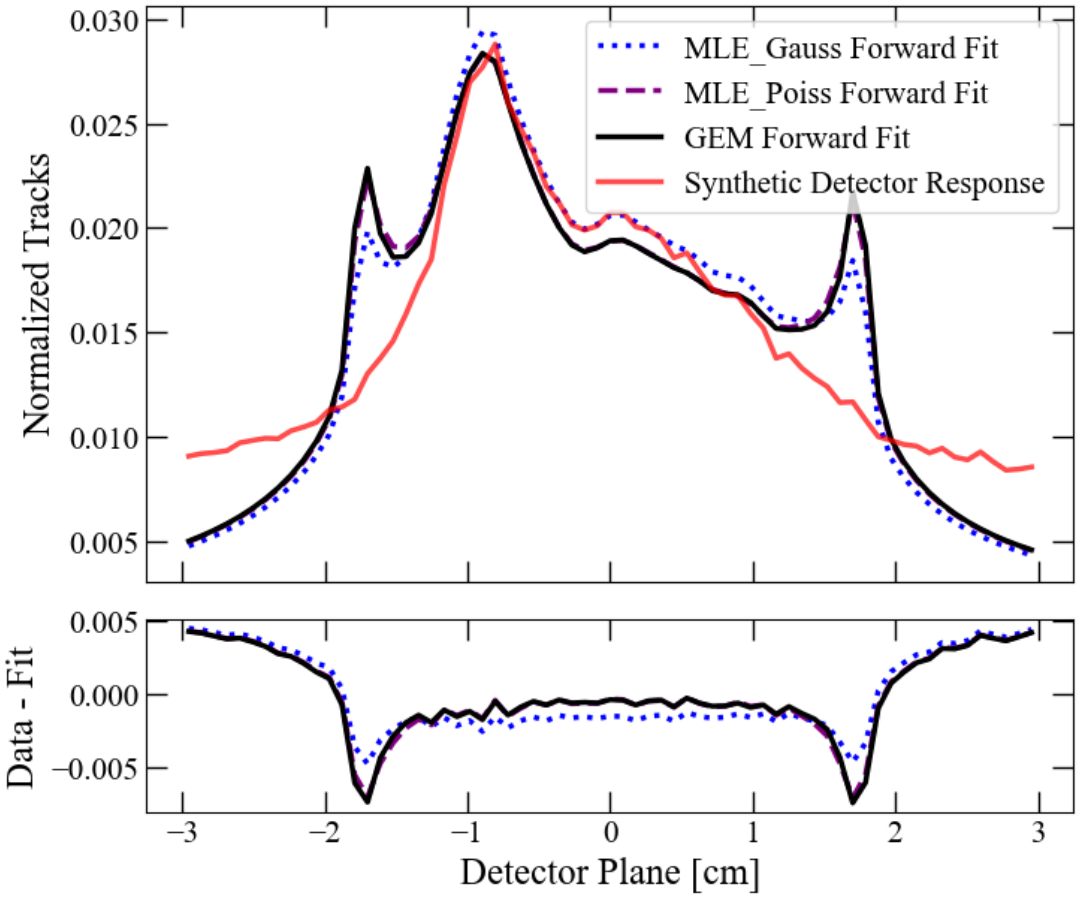

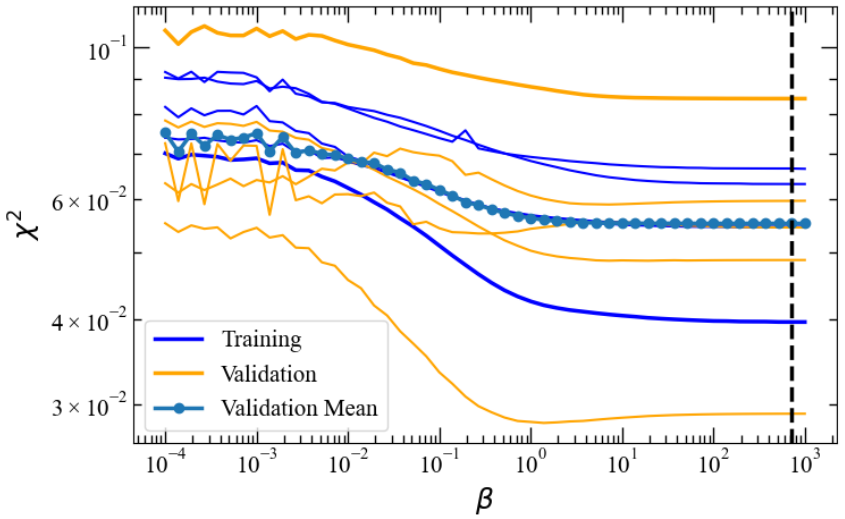

- Addition of a uniform background to MF synthetic response recreates the edge effects seen in z3289
- There is an unknown background in the CR-39 data not being accounted for in the reconstructions

Modified GEM Method (GEM_BG)

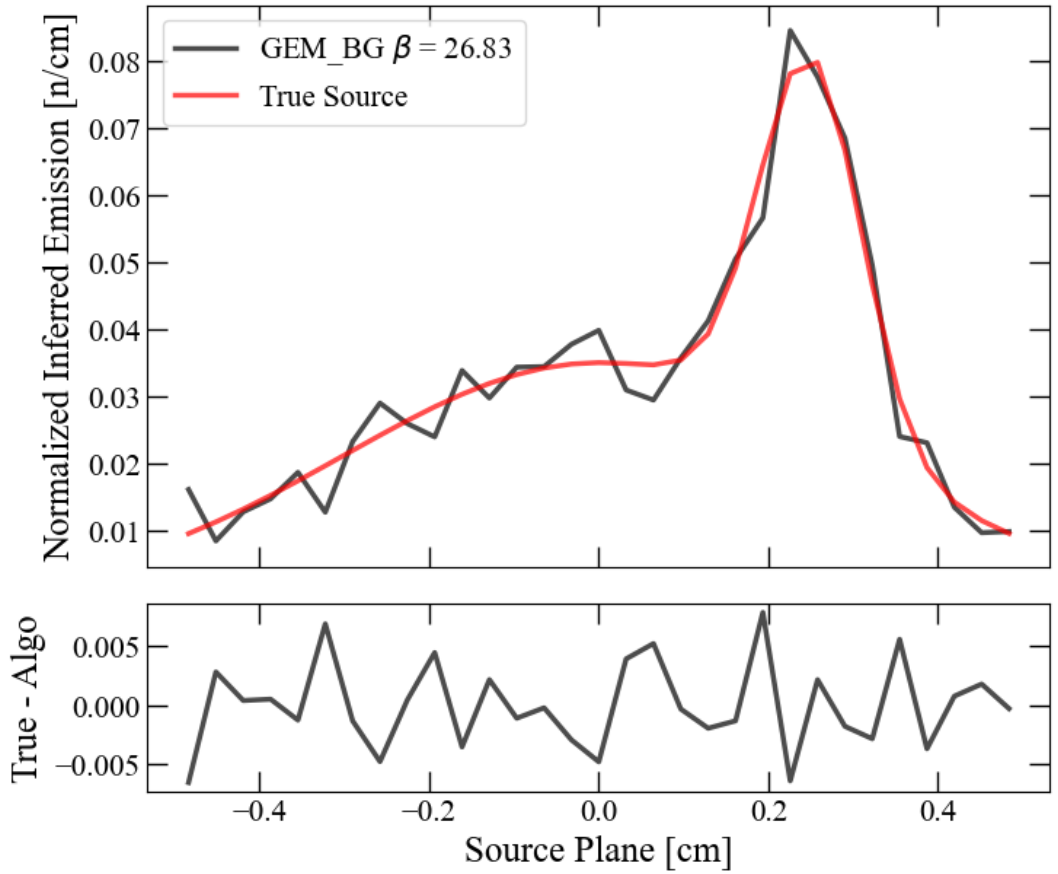

$$[P, B] = \begin{bmatrix} G \\ \mu \end{bmatrix} = Y$$

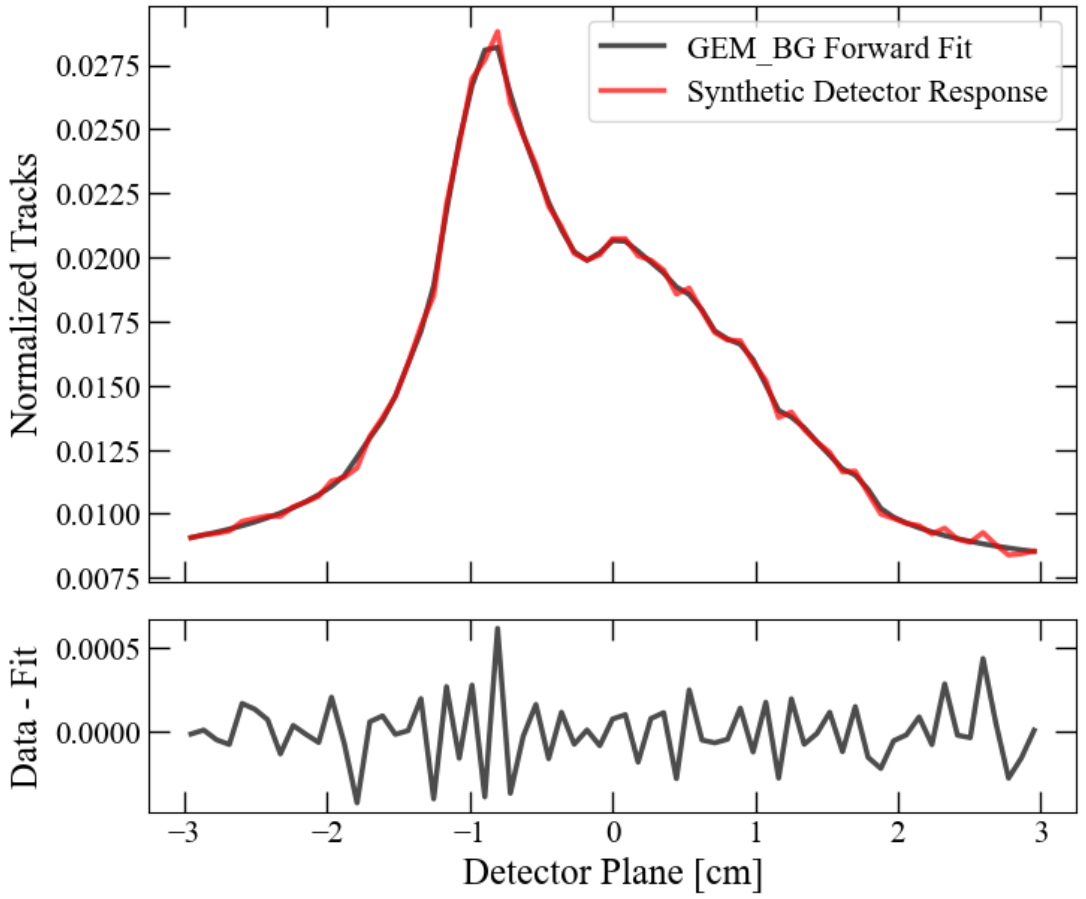

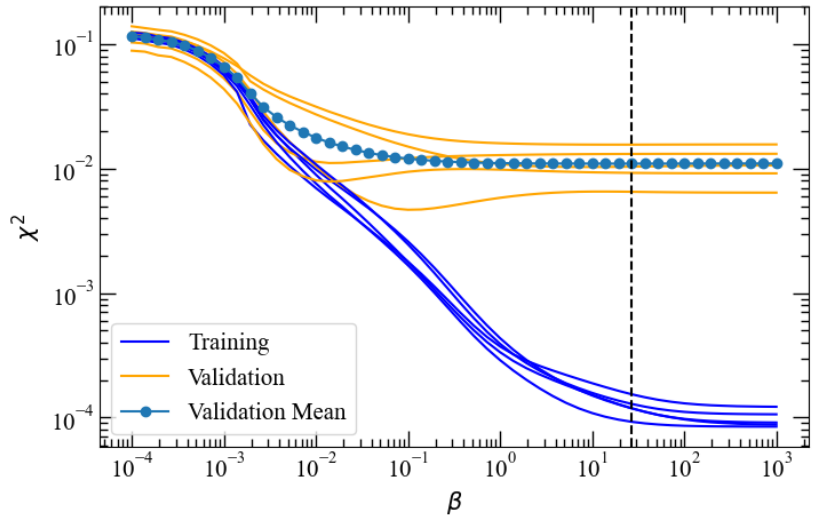

- Modified method computes an unknown background using three basis functions *B* (constant, ascending, descending), and corresponding coefficients, μ

Modified GEM z3289 Results

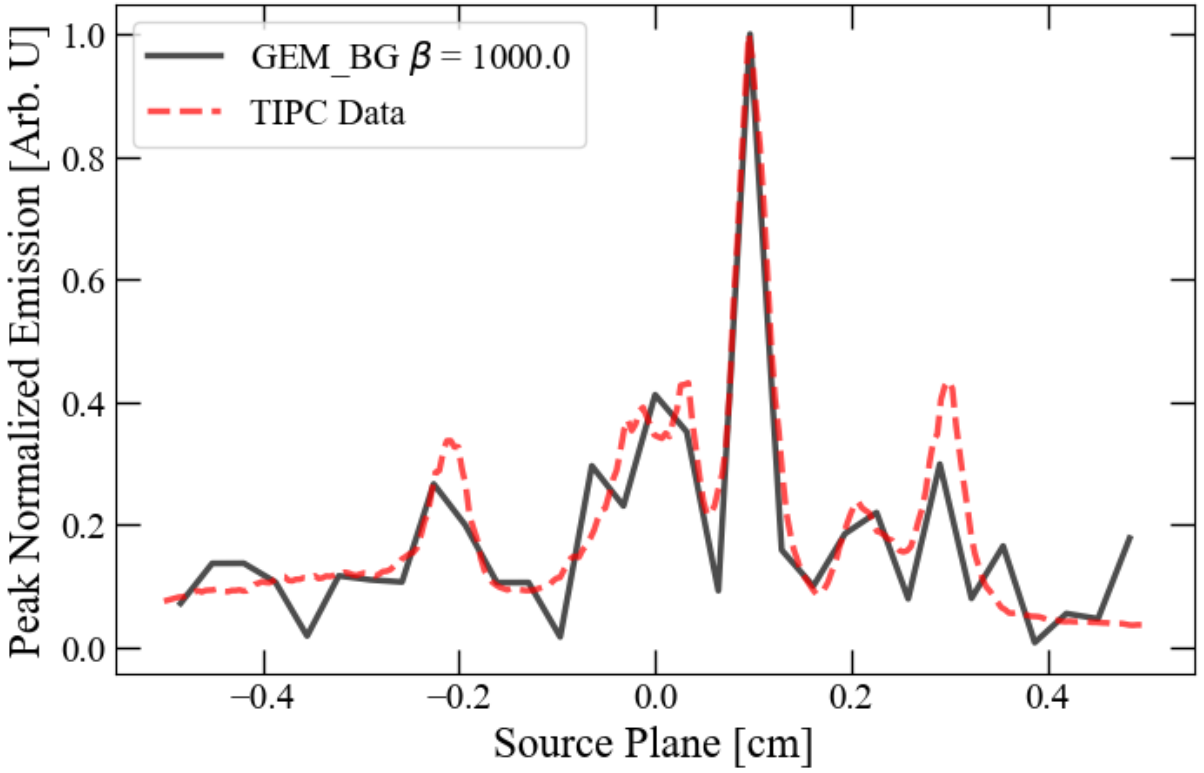

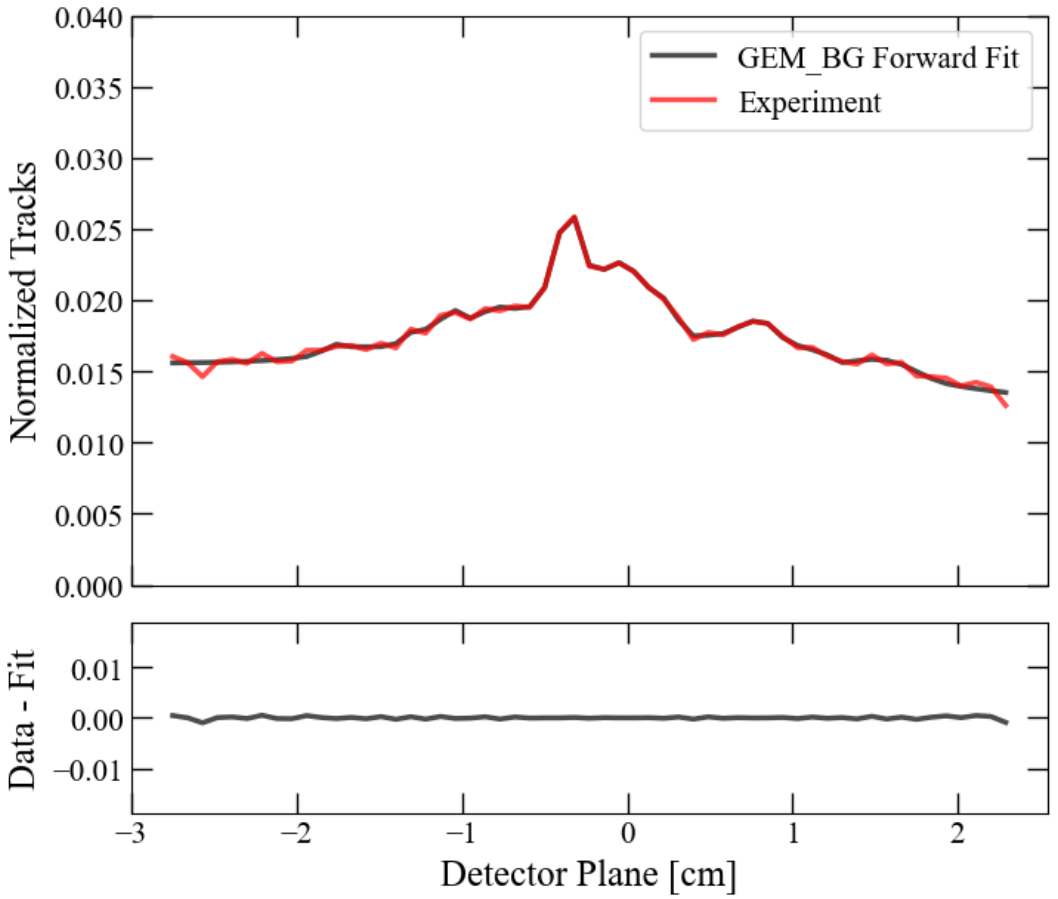

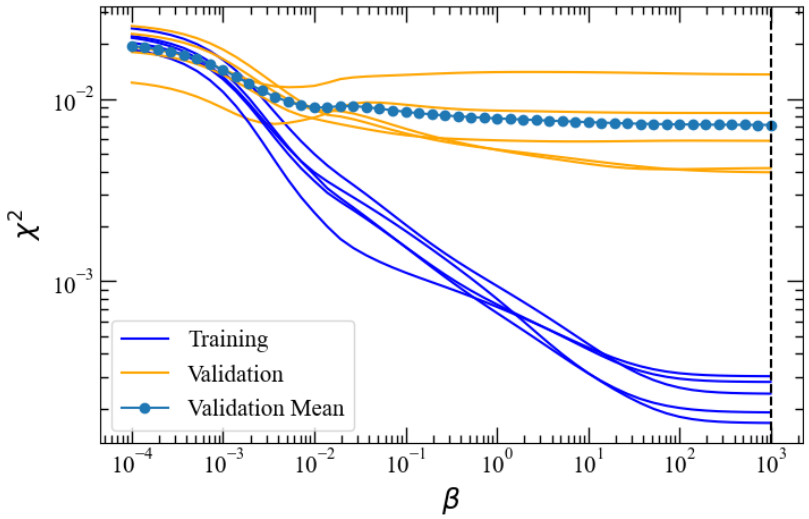

- GEM_BG successfully removes edge effects
- Verified by co-registering peak-normalized time-integrated pinhole camera (TIPC) x-ray data

S. A. Ricketts, M. A. Mangan, P. Volegov, D. N. Fittinghoff, W. E. Lewis, O. M. Mannion, J. E. Morel, M. L. Adams, D. J. Ampleford; Neutron source reconstruction using a generalized-expectation algorithm on one-dimensional neutron images from the Z Facility, American Institute of Physics - Review of Scientific Instruments, March 2024

Modified GEM z3926 Results

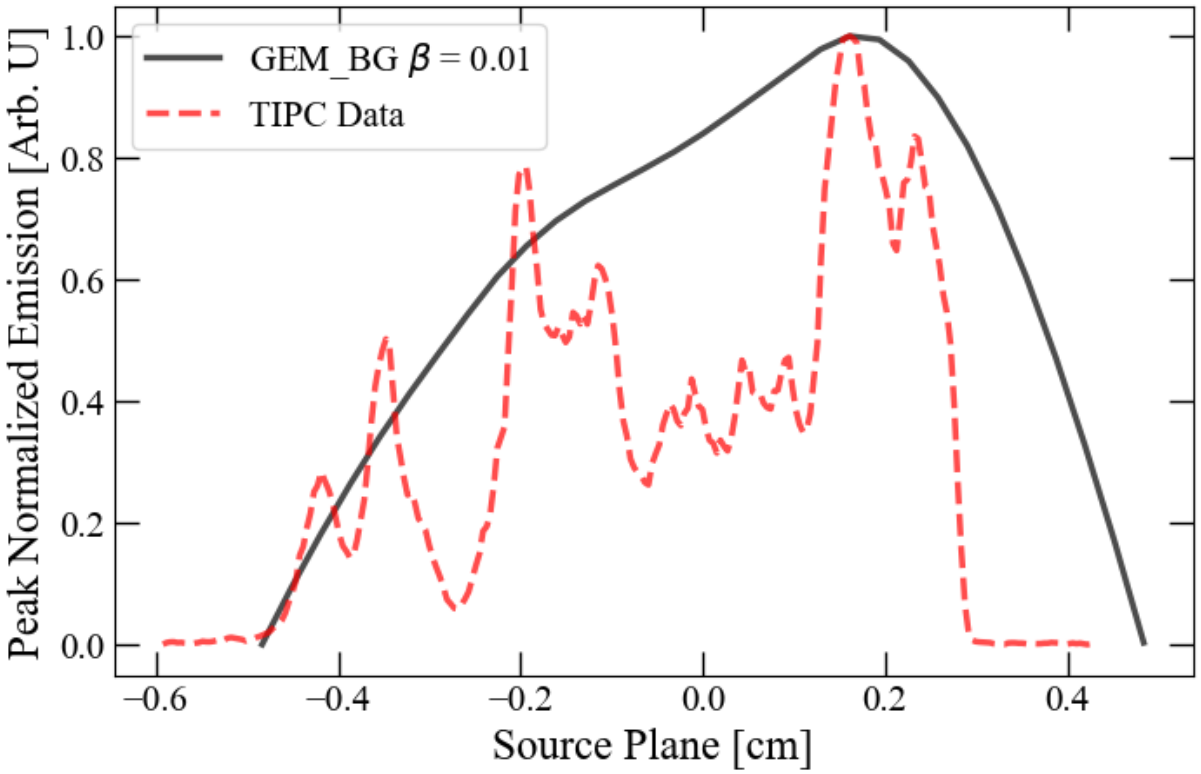

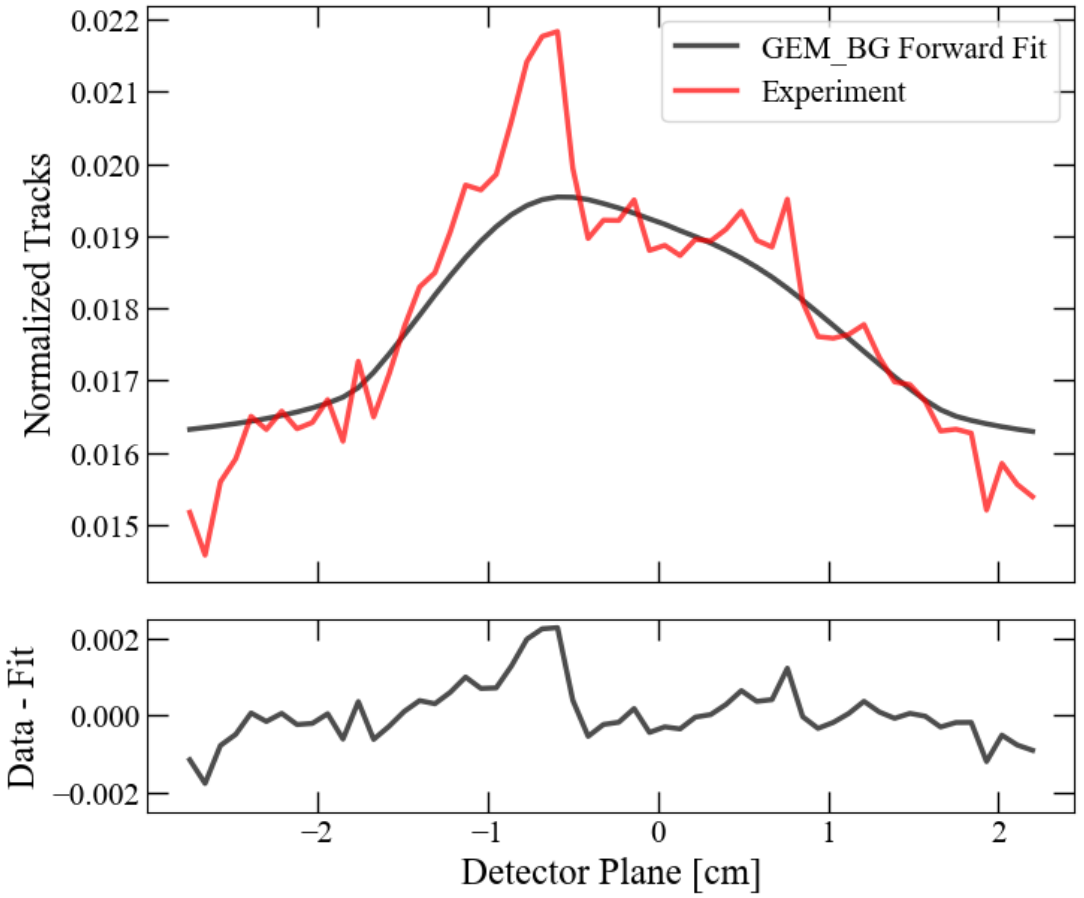

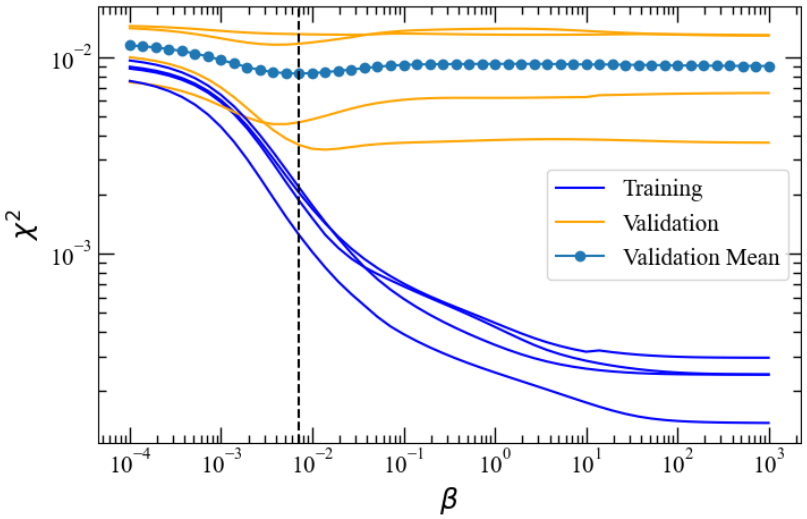

- GEM_BG consistently selected low β values
- Solution and forward fit show significant oversmoothing

K-fold Cross Validation Flaw on Synthetic Data

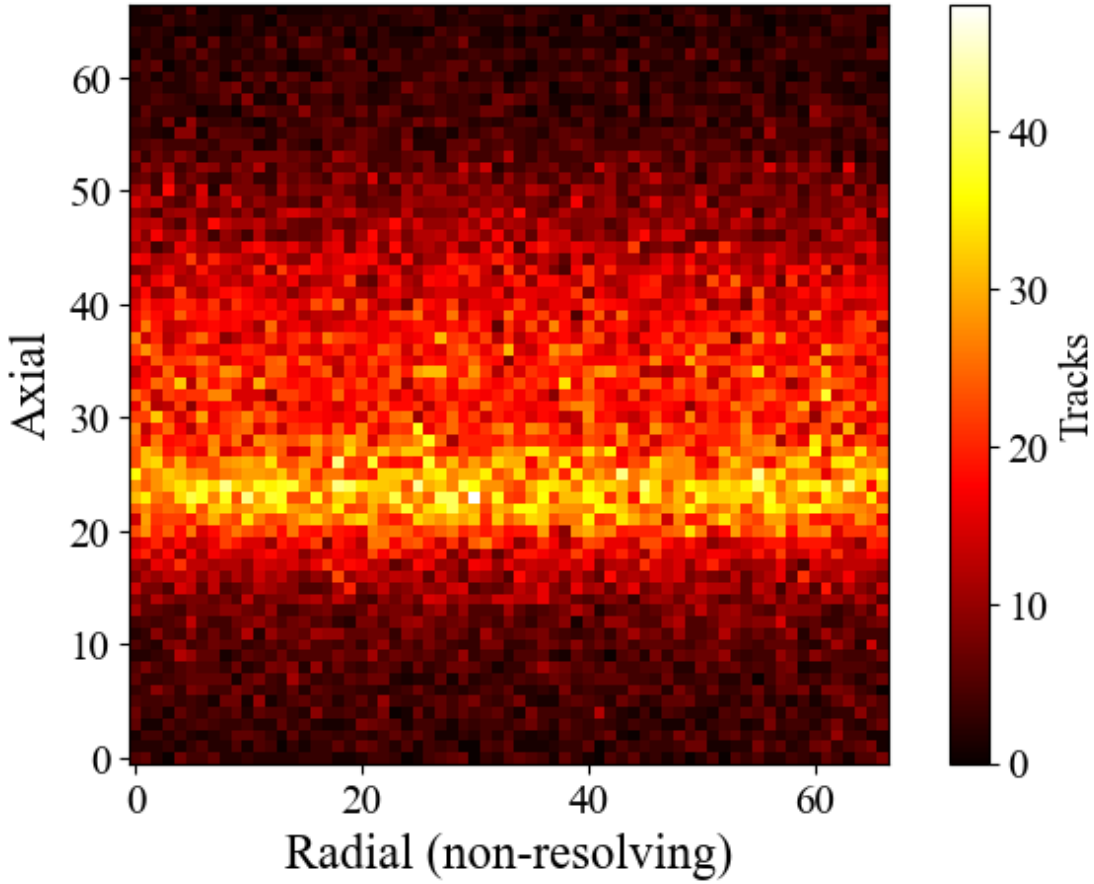

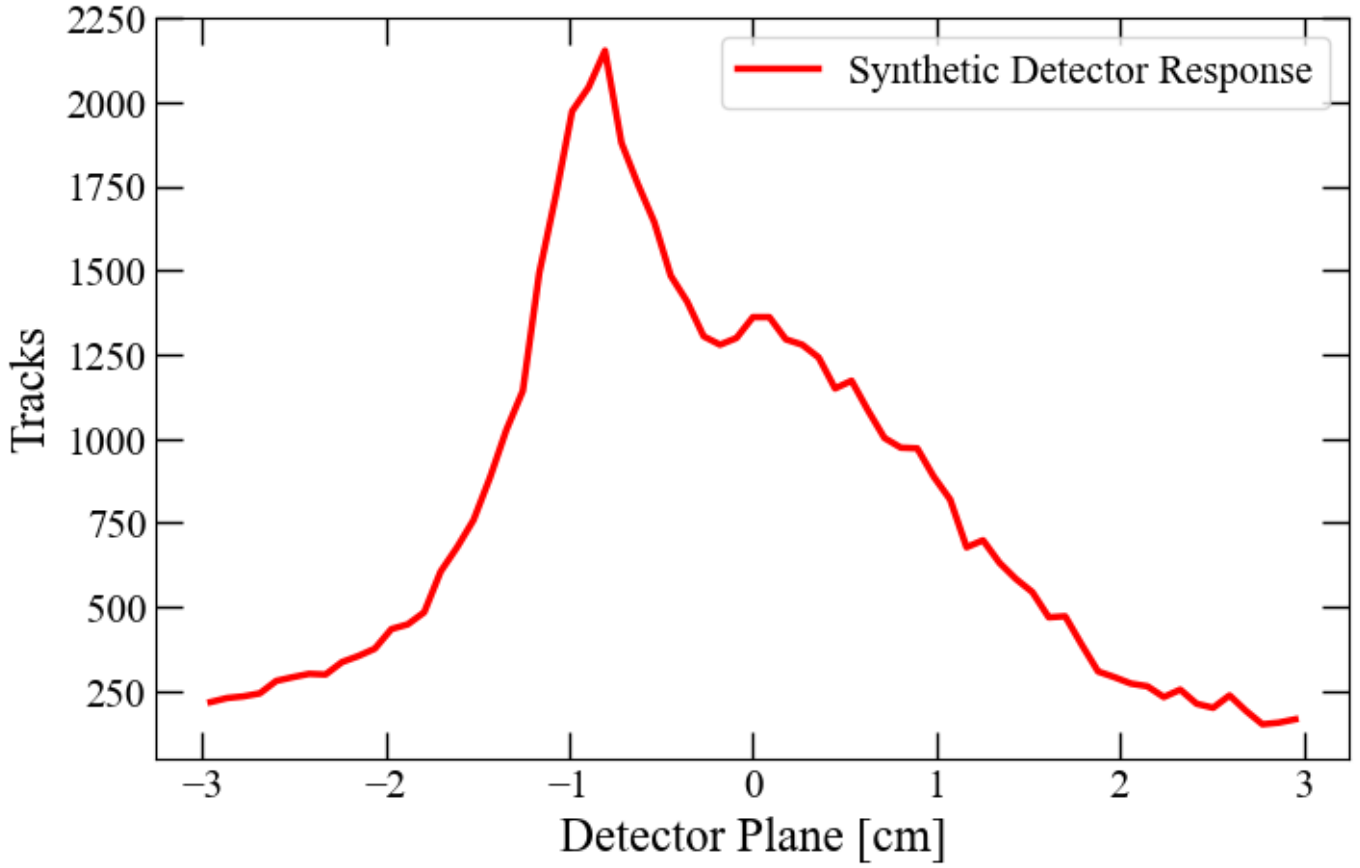

Randomization of Indices Problem

- ODIN's low resolution does not leave many data points to be split into k sections
- Different random seeds produce different points in each section k
- Here, sections k=1 and k=2 have no data points in the high frequency peak

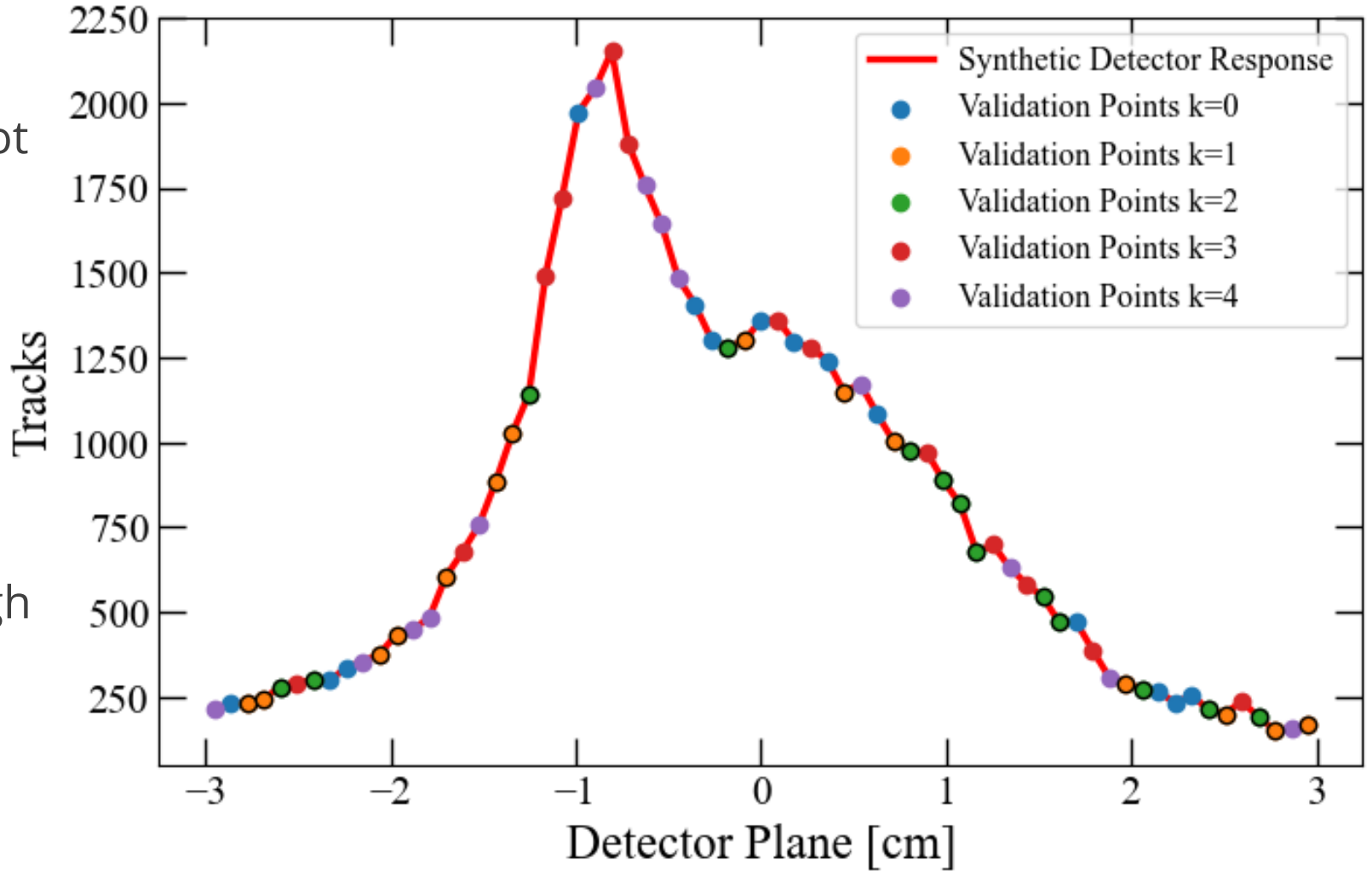

Validation Curve Effects

- Validation curves vary without inclusion of peaks, leading to oversmoothing

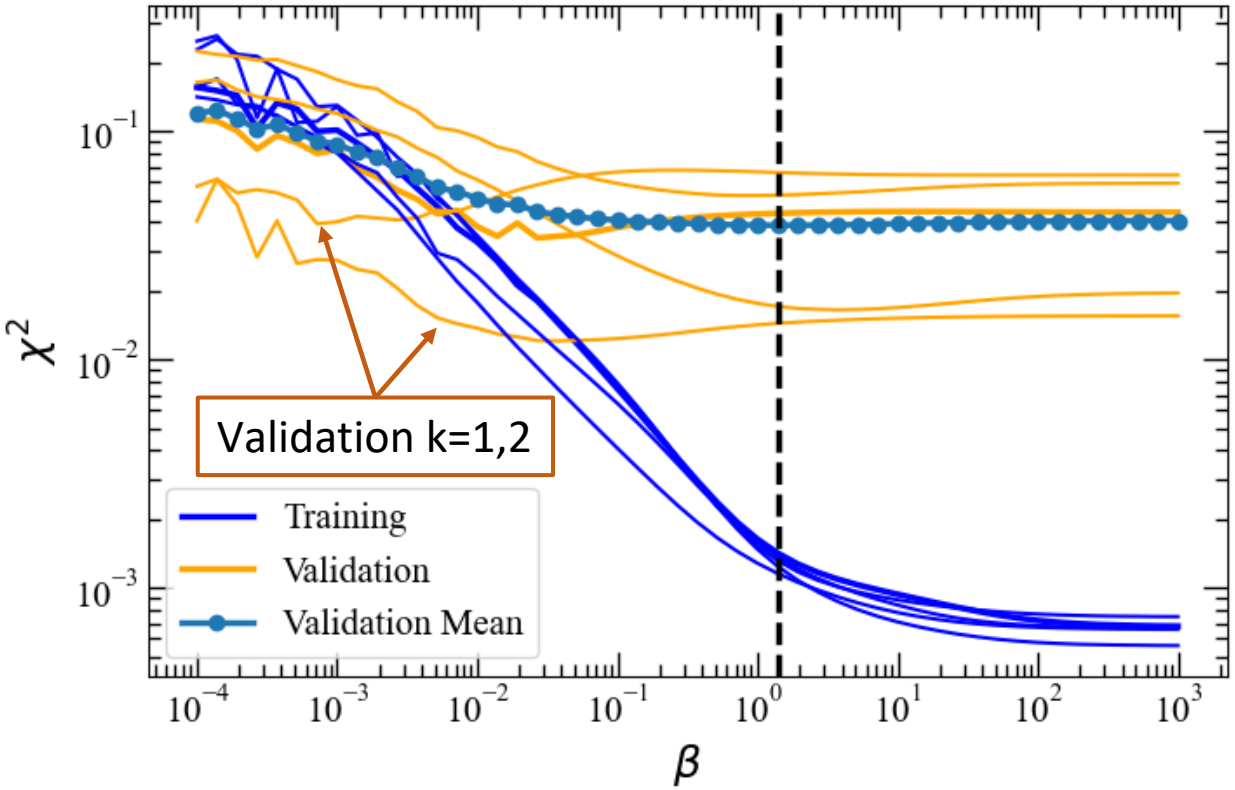

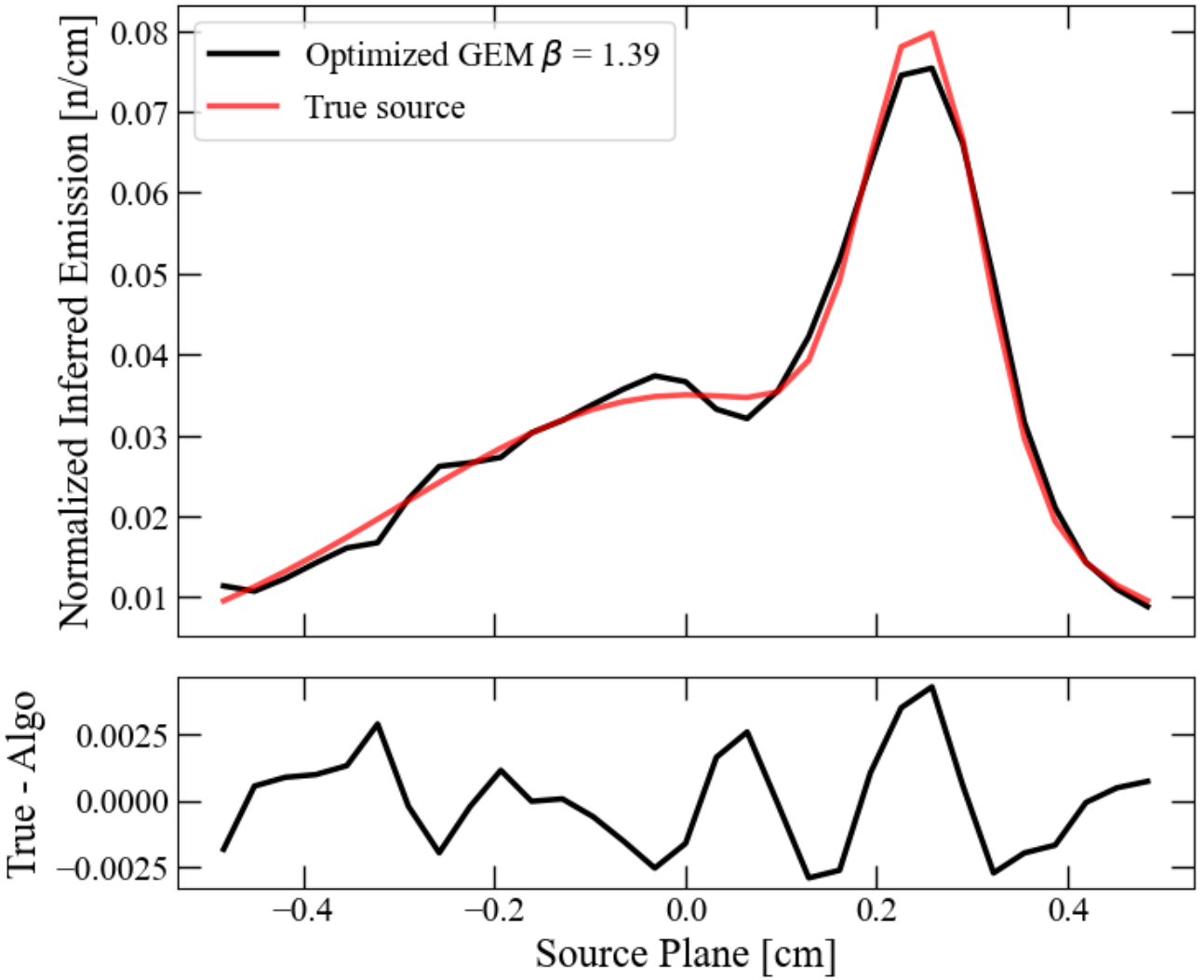

K-fold Cross Validation with 2-D Data

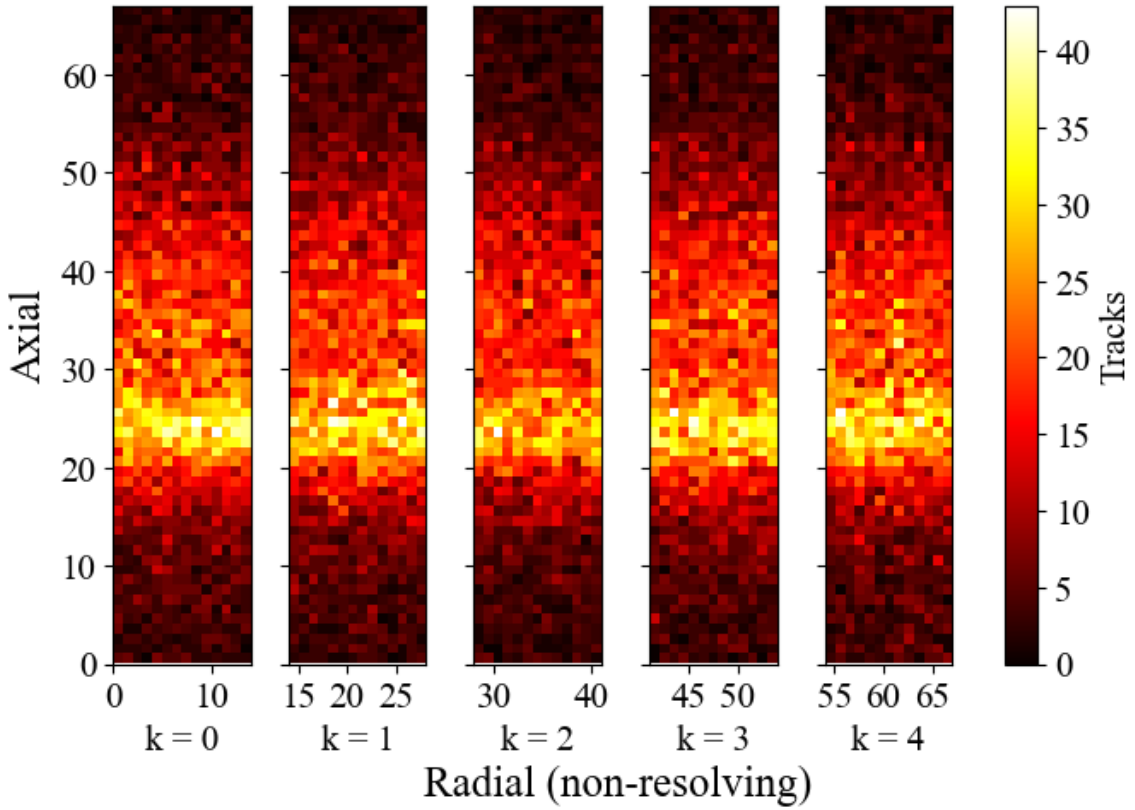

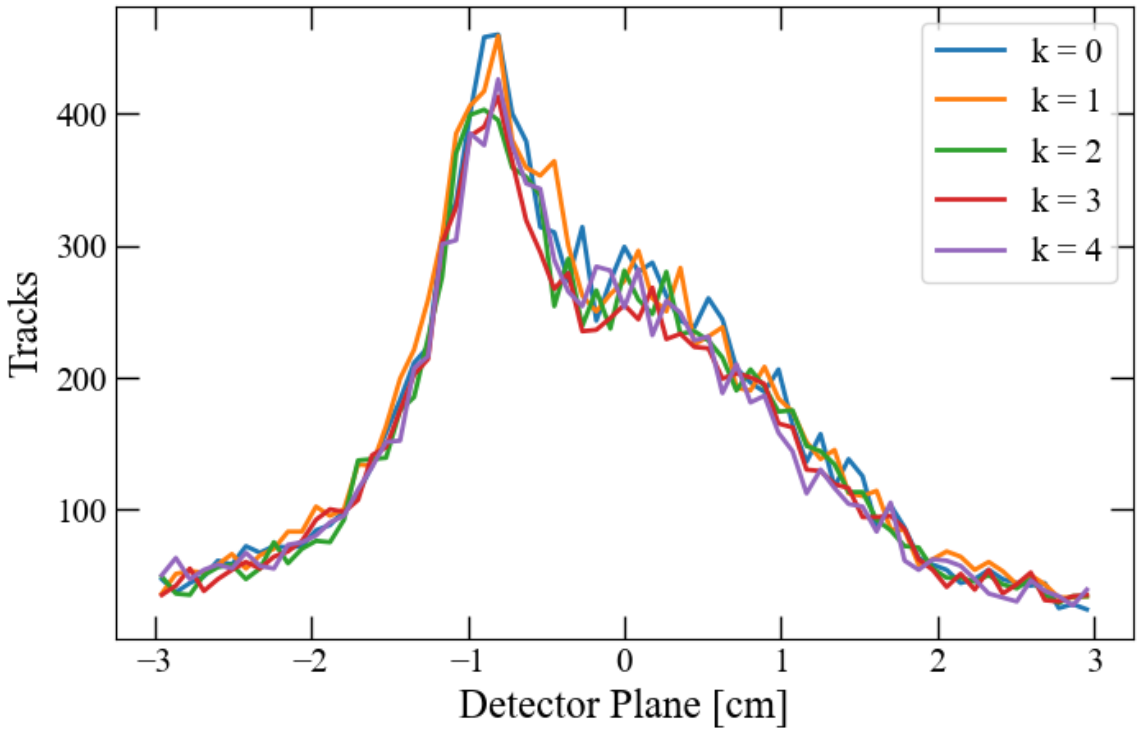

- By splitting the 2-D data into k sections, we can integrate each section along the non resolving axis
- This generates k 1-D profiles, but increases noise

Validation Curves Improve with 2-D K-fold

- No longer has an issue of randomness
- These training and validation curves will be the same when repeating the process

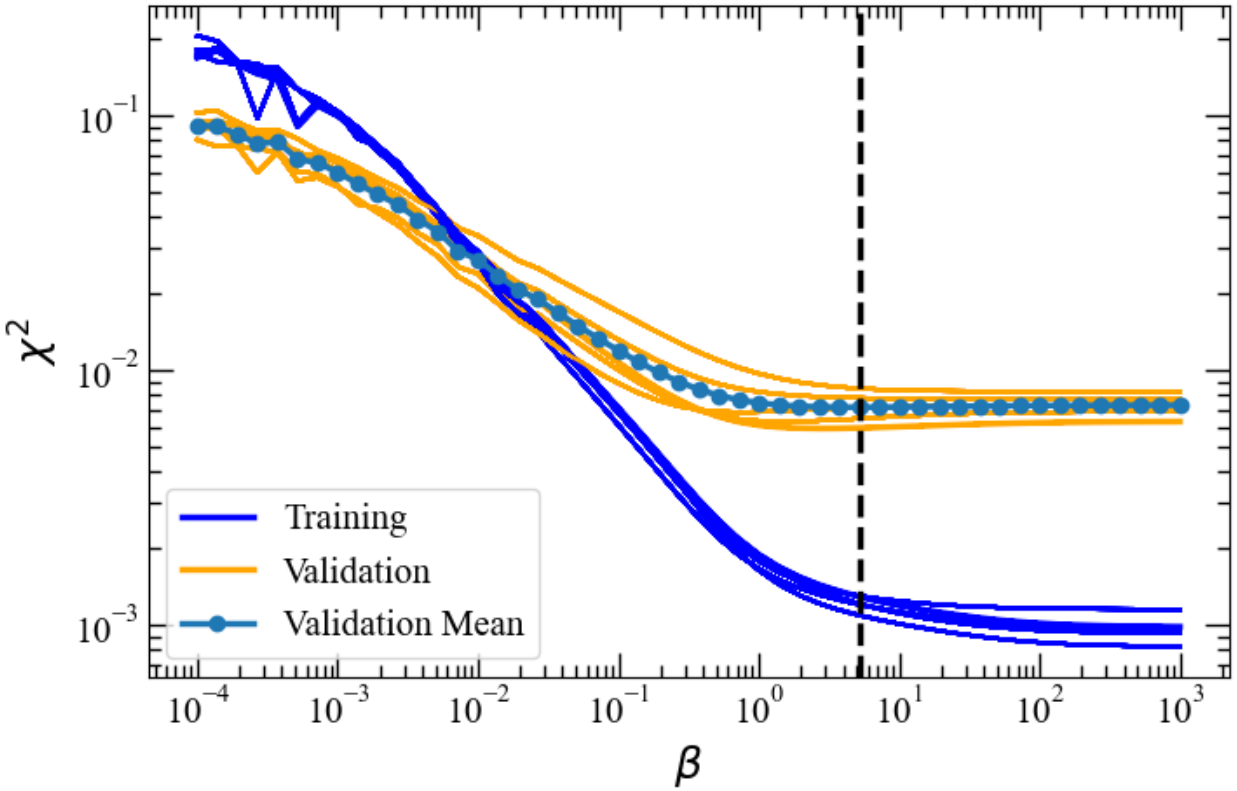

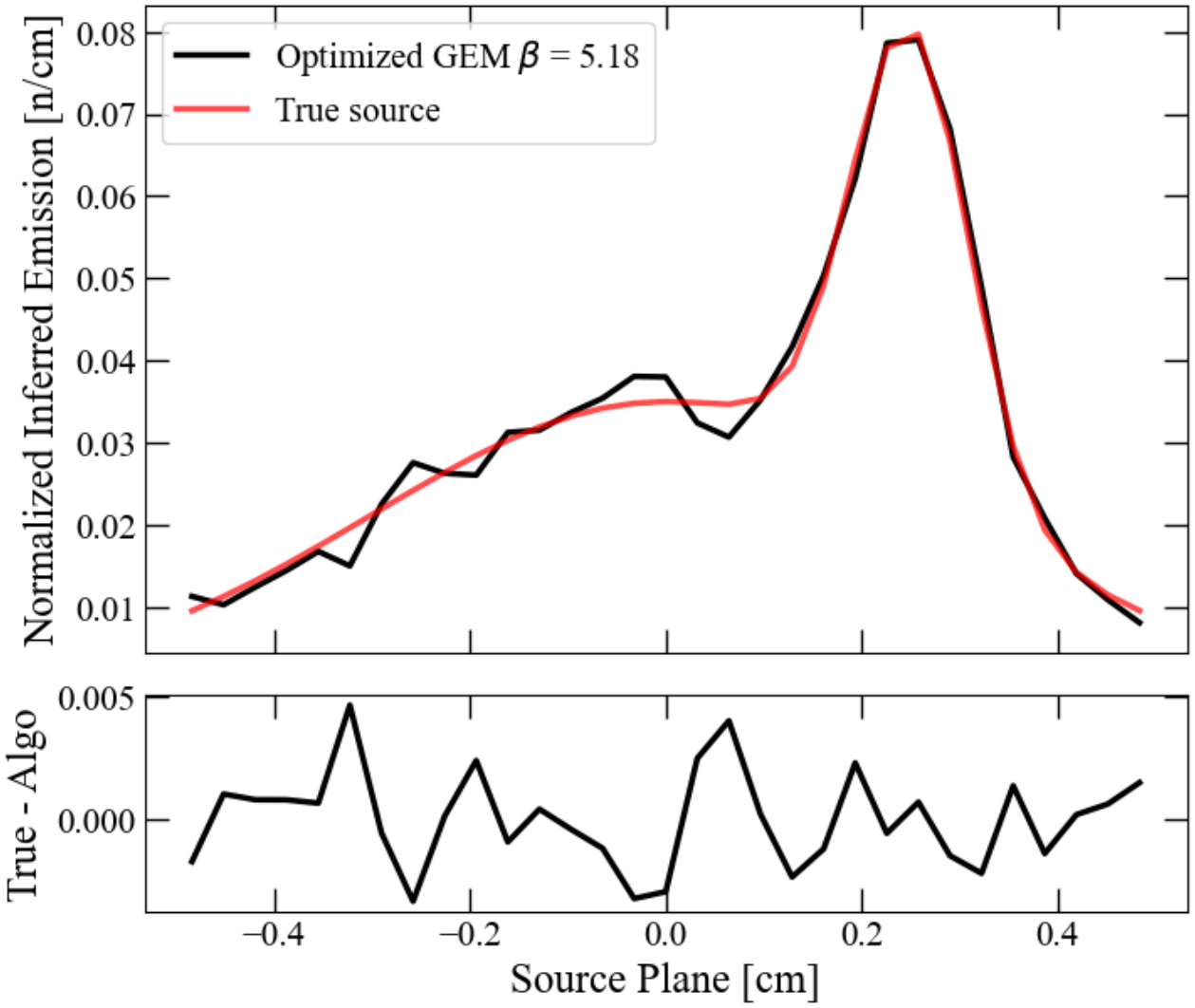

2-D K-Fold Selects β More Consistently

- MF synthetic source was reconstructed using the 1-D and 2-D methods
- 1-D k-fold was repeated (each having random indices)
- 2-D k-fold had column order randomized
- β selection is more consistent with the 2-D k-fold cross validation

MF Synthetic

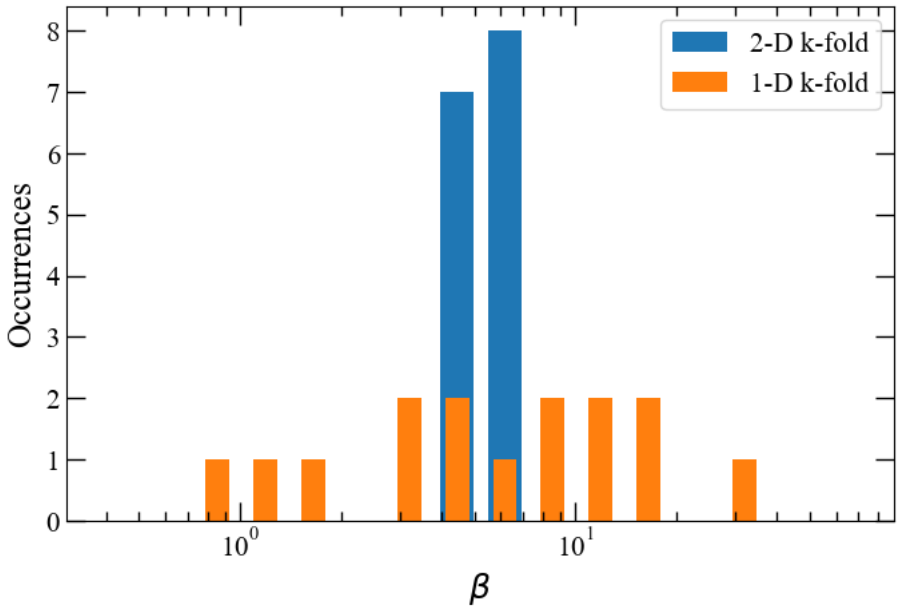

MF Synthetic + BG

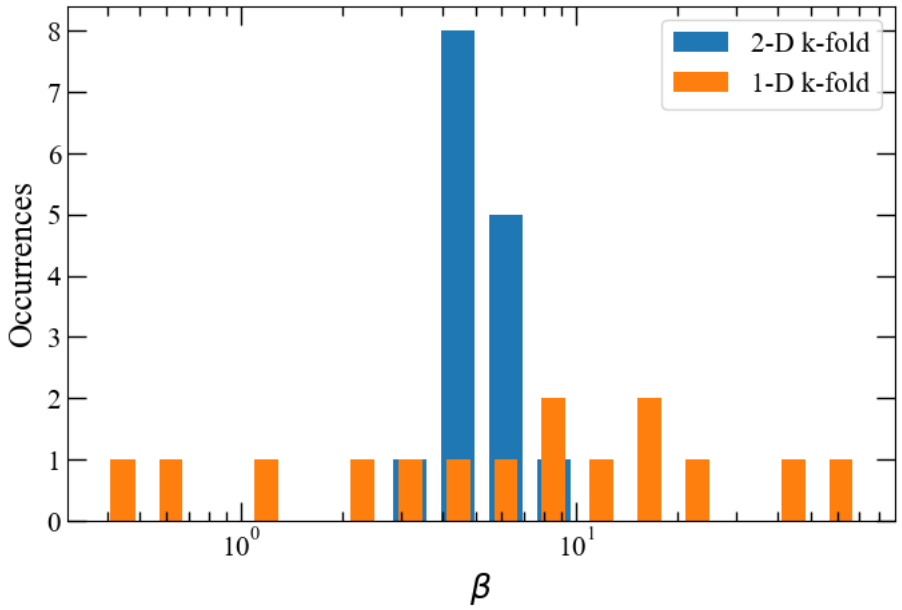

z3289 2-D K-fold Results

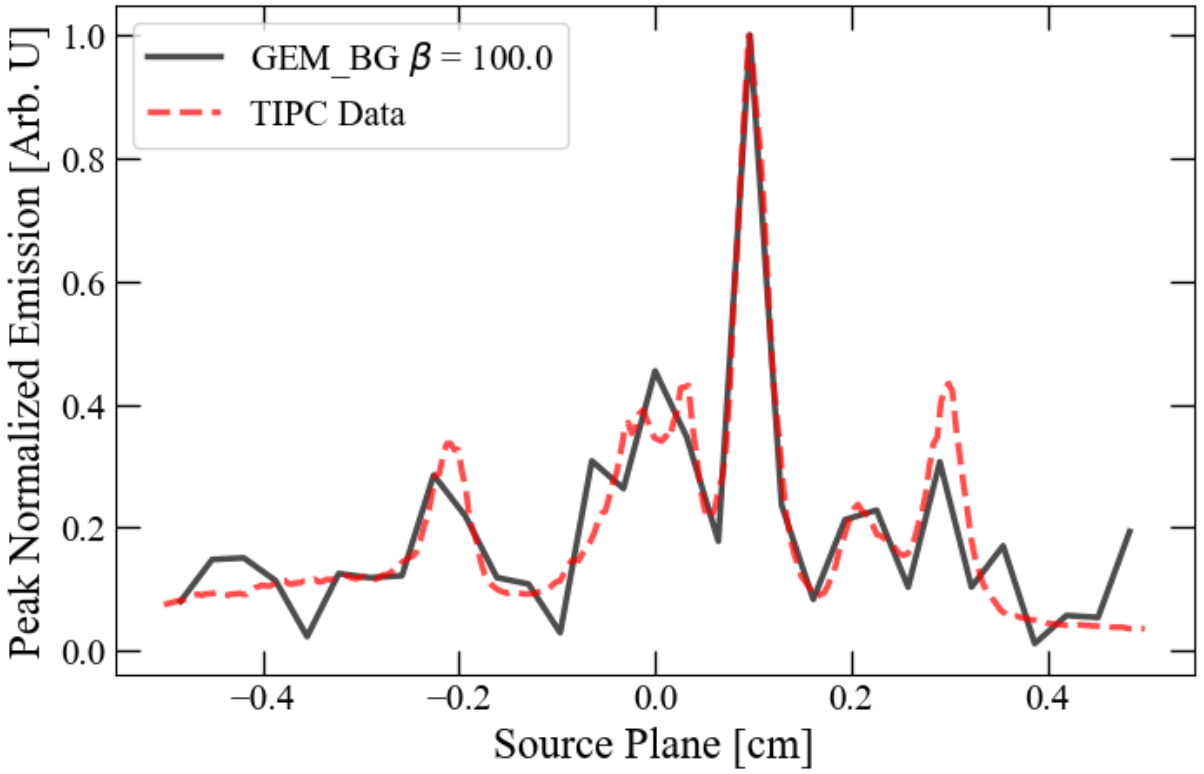

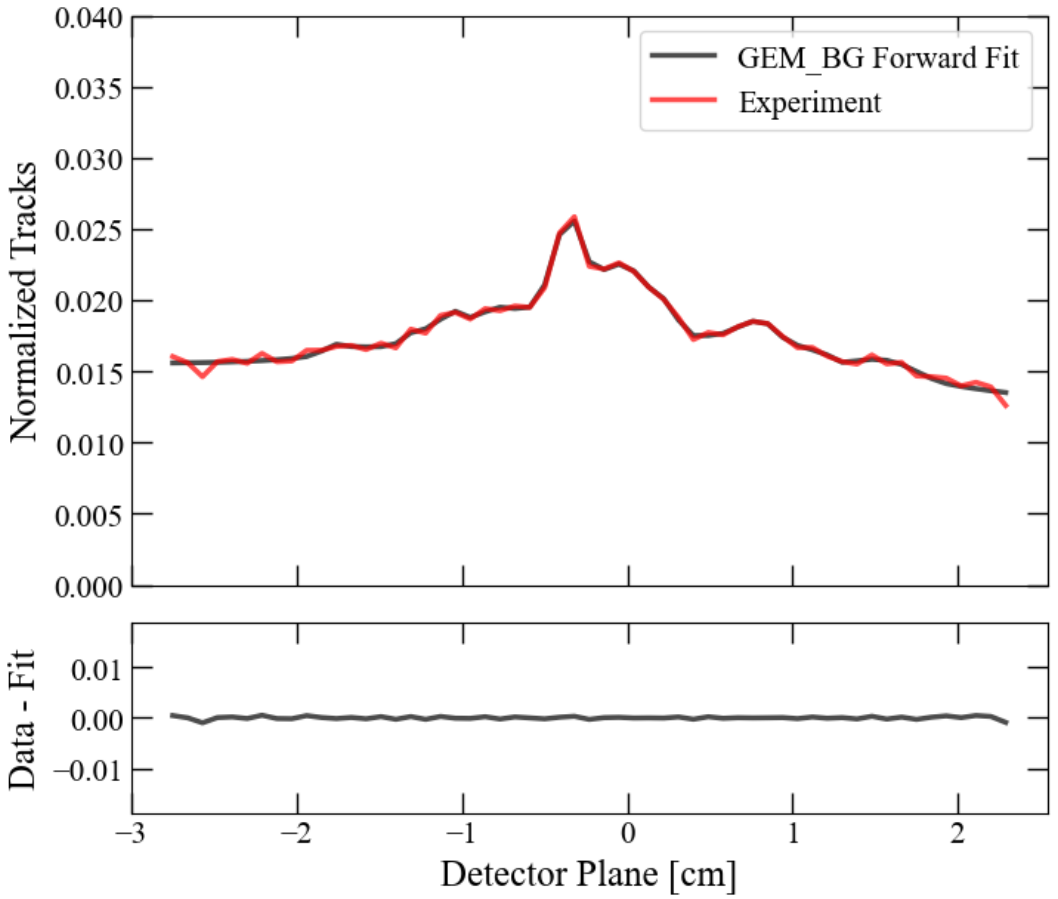

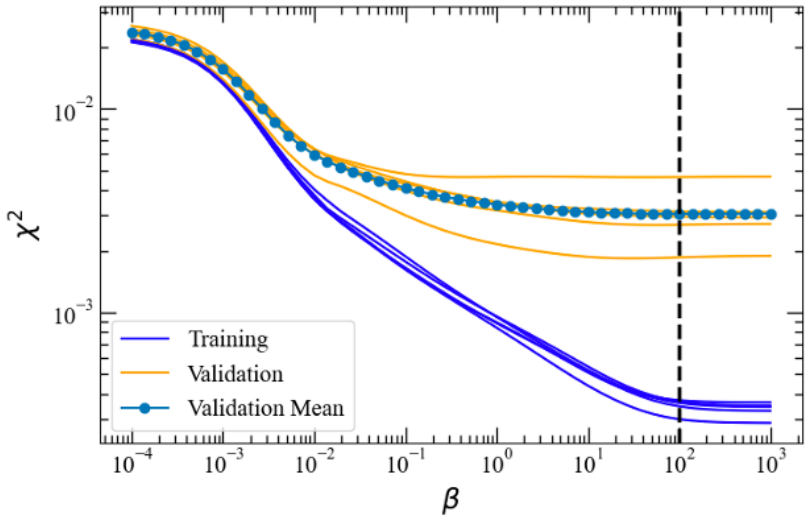

- GEM_BG 2-D k-fold results in β=100
- Minimal change to previous of β=1000

z3926 2-D K-fold Results

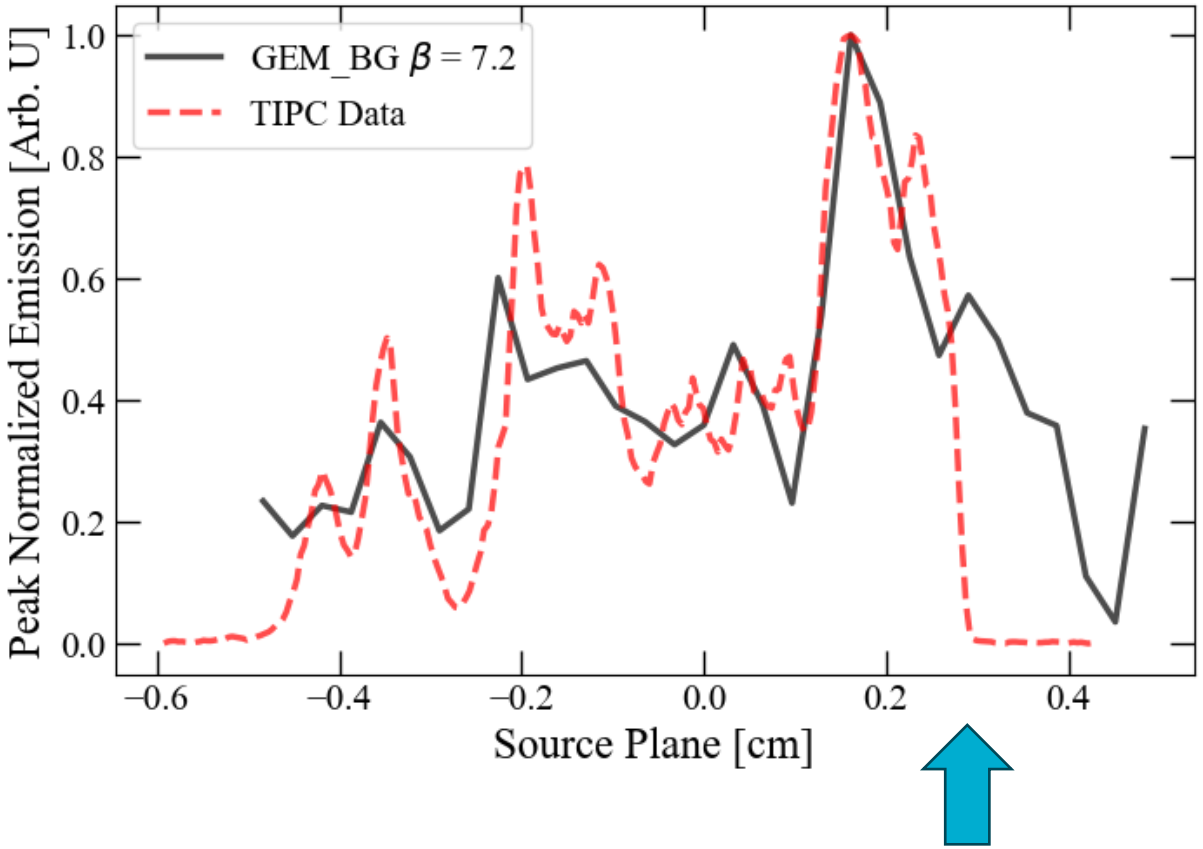

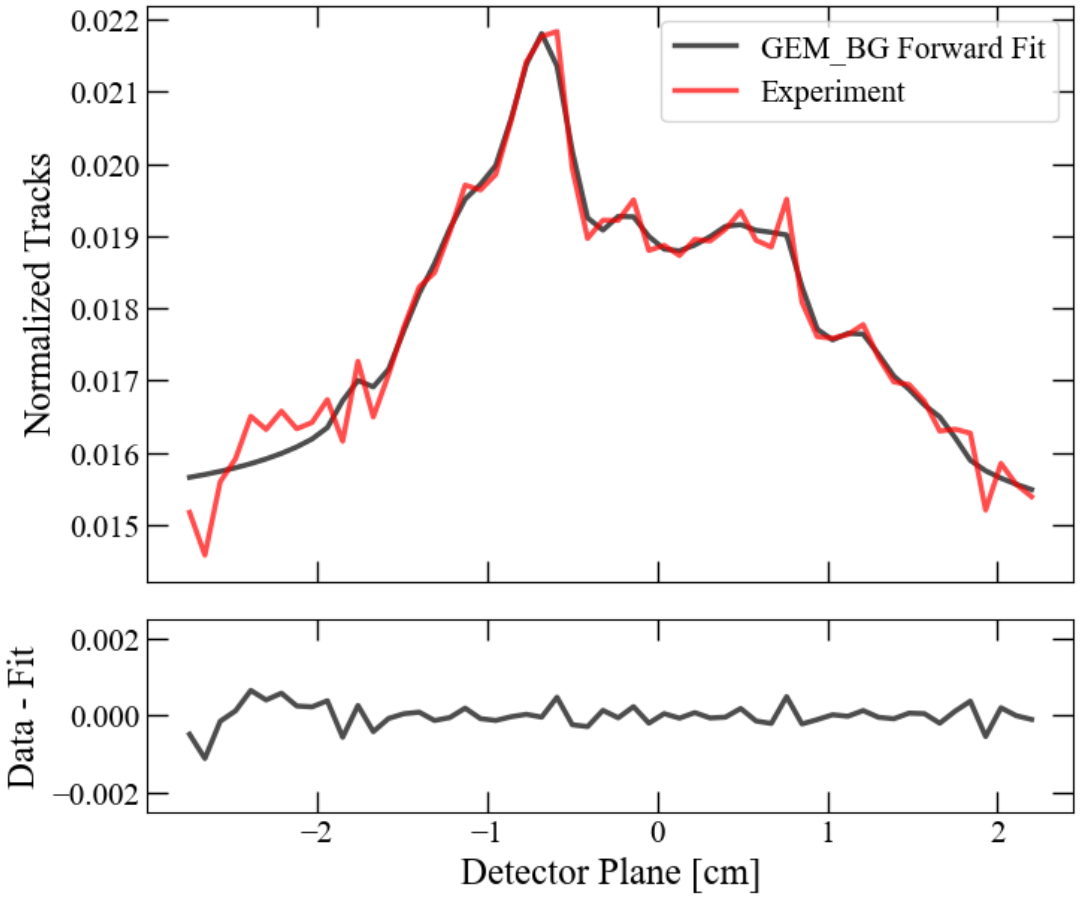

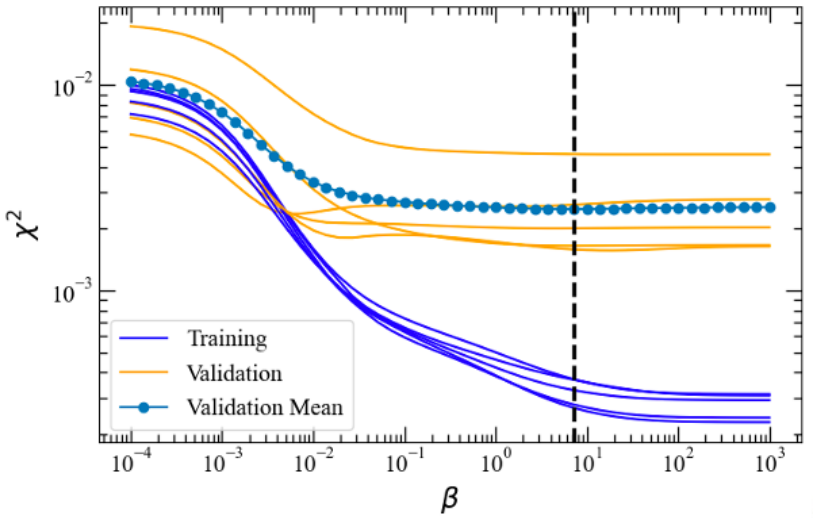

- GEM_BG 2-D k-fold results in β=7.2 and shows increased agreement between neutron and x-ray data
- Drop off near 0.3 in x-ray data believed to be artifact caused by object blocking x-rays

Experimental Results Error Estimation

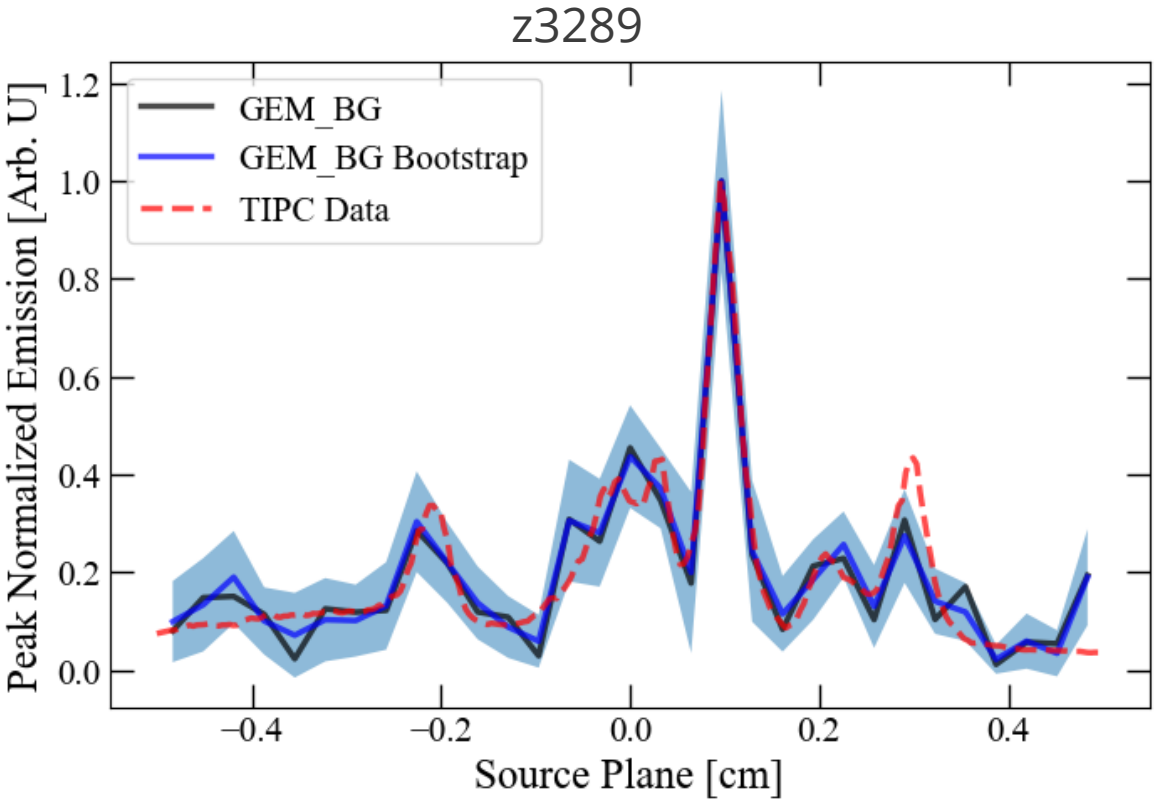

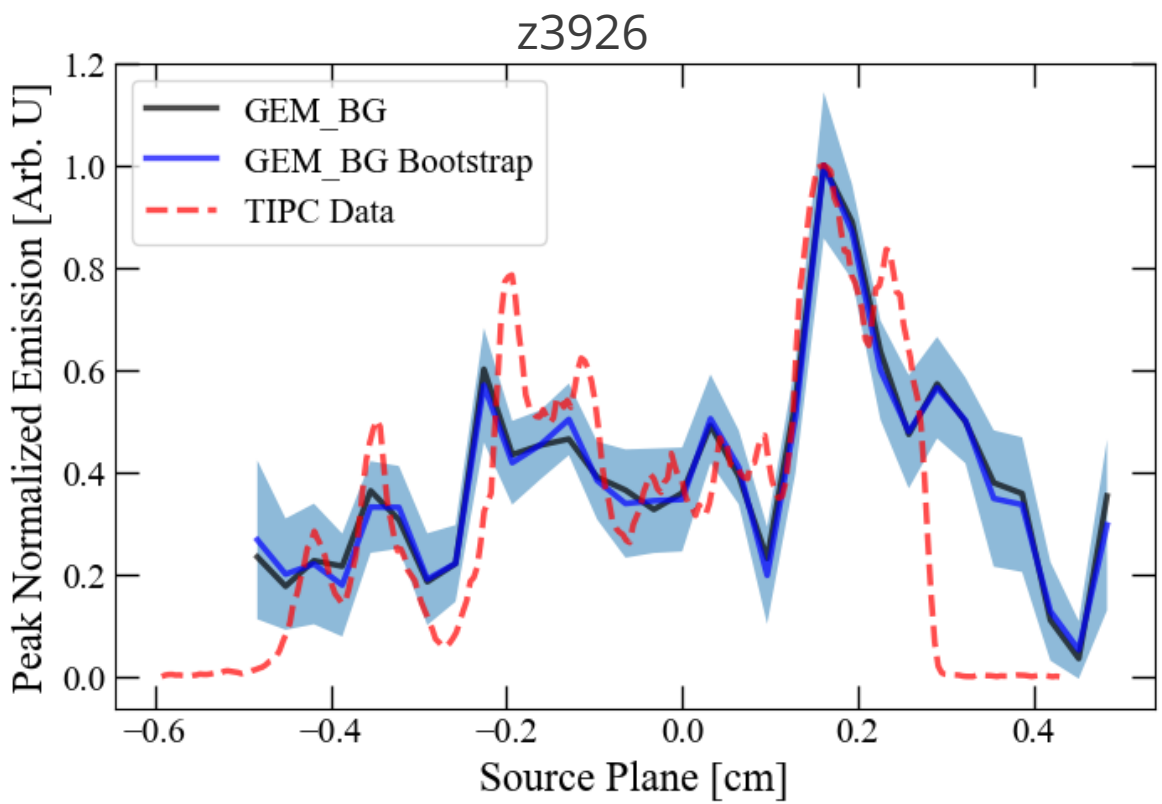

- We have developed a repeatable consistent reconstruction method for ODIN data
- This includes an error estimation via CLT bootstrapping

Final Thoughts and Conclusions

Future Image Reconstruction Improvements

- Use multiple CR-39 scans
  - Summation of 2-D data (increases SNR)
  - Simultaneous data reconstruction (increases number of fitted points)
- Data processing improvements
  - Optimize discrimination settings (front vs back and intrinsic noise tracks)
  - Change detector image resolution (increases number of points, lowers SNR)
  - Change source resolution (“super-resolution”)
- β optimization
  - Bayesian inference (β becomes a hyperparameter solved in the iteration steps)

Fielding Recommendations

- Alignment measurements
  - Taking measurements in-chamber would allow for specific IRF matrix development
- Monolithic structure
  - Would reduce possibility of misalignments between source, aperture, and detector package
- Magnification change
  - Changing the magnification could reduce edge areas difficult to fit to
  - Find an “optimal” magnification for ODIN

Conclusions

- MagLIF experiments produce an ~1cm tall neutron emitting plasma region
- There is a backlog of ODIN data needed to be analyzed
- A forward model of ODIN has been developed to create IRF matrices needed for image reconstruction
- A forward model sensitivity analysis was conducted to understand and quantify the effects of fielding parameter sensitivity on multiple image reconstruction methods
- The GEM algorithm was modified to account for an unknown background and CR-39 source reconstructions were successfully performed on two experimental data sets
- Improvements were to GEM_BG algorithm methodology generated neutron emission profiles from z3289 and z3926 which showed quantitative agreement with TIPC x-ray data

Acknowledgements

- Thank you to my committee members for their help during this research
  - Dr. Jim Morel[1], Dr. Sunil Chirayath[1], Dr. Craig Marianno[1], Dr. Peter Kuchment[1], Dr. Michael Mangan[2], Dr. Marvin Adams[1]
- Thank you to my many colleagues and collaborators who supported this research
  - P. Volegov[3], D. N. Fittinghoff[4], O. M. Mannion[2], W. E. Lewis[2], A. J. Harvey-Thompson[2], J. R. Fein[2], D. J. Ampleford[2]

[1]Texas A&M University, College Station, TX
[2]Sandia National Laboratories, Albuquerque, NM
[3]Los Alamos National Laboratory, Los Alamos, NM
[4]Lawrence Livermore National Laboratory, Livermore, CA

Questions